Crural Indices in Neandertals and Modern Humans: Implications for Limb Proportions, Environment, and Body Size Variation

Miguel Ochoa

A dissertation
submitted in partial fulfillment of the
requirements for the degree of

Doctor of Philosophy

University of Washington

2025

Reading Committee:
Patricia Ann Kramer, Chair
Steven M. Goodreau
Steven G. Lautzenheiser

Program Authorized to Offer Degree:

Anthropology

University of Washington

Abstract

Crural Indices in Neandertals and Modern Humans: Implications for Limb Proportions, Environment, and Body Size Variation

Miguel Ochoa

Chair of the Supervisory Committee:

Patricia Ann Kramer

Department of Anthropology

This dissertation investigates the functional and adaptive significance of Neandertal limb morphology by integrating comparative anatomy, biomechanical modeling, and methodological validation. The crural index (CI)— a ratio of tibial to femoral length— served as a key metric for exploring thermoregulatory and terrain-related adaptations.

In Chapter 3, CI values were analyzed across 21 modern human populations and multiple Neandertal individuals. Neandertals exhibited lower average CIs than modern humans, consistent with cold-adapted body forms, but fell within the observed range of modern variation. Chapter 4 modeled center of mass (CoM) shifts on sloped terrain and found that Neandertal limb proportions and trunk morphology produced a lower and more posterior CoM than in modern humans. These differences became more pronounced on inclines, suggesting biomechanical advantages for locomotion in rugged environments. Chapter 5 validated the use of external anatomical landmarks to estimate skeletal limb lengths using CT data from over 100 individuals. While femoral and tibial lengths showed strong agreement between external and skeletal

measurements ($R^2 > 0.97$), crural index values derived from external landmarks exhibited only moderate correlation ($R^2 = 0.60$), highlighting limitations in ratio-based proxies.

Together, these findings support a multifactorial model of Neandertal adaptation involving both climatic and biomechanical selective pressures. They also emphasize the importance of methodological rigor when using external measurements in evolutionary analyses. This work contributes a refined framework for interpreting postcranial morphology in both fossil and modern human populations.

Table of Contents

List of Figures

List of Tables

Acknowledgements

It is with deep gratitude that I thank those who have supported, mentored, and inspired me throughout this dissertation and my graduate journey. Foremost is my advisor, Dr. Patricia Ann Kramer, whose guidance, honesty, and commitment to her students have shaped not only this project, but who I am as a scholar, teacher, and person. I have been incredibly fortunate to work with someone who leads with clarity, high standards, and a deep respect for both the science and the people who do it.

Dr. Kramer took a chance on me when I was still figuring out how to merge my interests in human biology, evolution, and biomechanics— and she never let me lose sight of the big picture. Thank you for your mentorship, for expecting the best from me, and for helping me find my way forward even when I doubted myself. I hope to carry that same clarity and care into my own work with students someday.

Thank you to Dr. Steven Goodreau and Dr. Casey Self for your mentorship, collaboration, and kindness. You each played a role in helping me navigate not just this dissertation, but also the broader world of academia. Your guidance has shaped me into a more thoughtful teacher, researcher, and mentor.

To my friends from PEBL: Thank you for the camaraderie, laughter, and shared brainpower. Abigil, Yarinid, Isabella, Amanda, Alex, Elen, Emily, Rob, thank you for your friendship and keeping me afloat. Cristina and Hannah, thank you for your friendship, love, feedback, and unrelenting support. You helped me stay grounded and motivated through it all and I couldn't have made it without you and our shared chaos.

To my partner, Joseph— thank you for enduring the full force of grad school stress and loving me through it all. You've seen every version of this journey— the sleepless nights, the meltdown drafts, the little wins— and never once stopped believing in me even when I couldn't believe in myself.

To my sisters and my brother— thank you for everything you did to support not just me, but our whole family. I know you each put your own dreams on hold at times to help the rest of us get ahead. Your sacrifices live in every page of this work.

And to the younger version of myself— who never thought this was possible, but kept going anyway, through the hard days, the uncertainty, the exhaustion, and the doubt— this is for you, too.

DEDICATION

This dissertation is dedicated to my parents, who always encouraged us to learn, to keep going, and to work hard for what we wanted. I've taken your lessons to heart: to go through life with kindness, compassion, and respect, and to teach and help others who need it. You have sacrificed so much for us, and I want you to know that it was not in vain. Your love and strength will be forever appreciated. I love you both.

Este trabajo está dedicado a mis padres, quienes siempre nos animaron a aprender, a seguir adelante y a esforzarnos por lo que queríamos. He llevado sus enseñanzas en el corazón: vivir con amabilidad, compasión, y respeto, y enseñar y ayudar a quienes lo necesiten. Ustedes han sacrificado tanto por nosotros, y quiero que sepan que no fue en vano. Su amor y fortaleza siempre serán profundamente apreciados. Los quiero mucho.

Chapter 1: Introduction

Reconstructing the anatomy, behavior, and adaptations of extinct hominins is a central goal in paleoanthropology. Among these groups, Neandertals (*Homo neanderthalensis*) remain one of the most intensively studied and debated species (Stringer, 2022). As our closest extinct relatives, their morphology offers critical insight into the evolutionary pathways that shaped the human lineage (Trinkaus & Shipman, 1993; Green et al., 2010). Neandertals persisted in harsh glacial climates and occupied diverse, often rugged environments across Pleistocene Europe and western Asia (Van Andel & Davies, 2003; Hublin & Roebroeks, 2009). Understanding how their distinctive anatomy supported their survival in these conditions is essential for interpreting their evolutionary history and the broader biomechanical and physiological constraints that influence hominin locomotion and thermoregulation (Holliday, 1997; Roebroeks & Soressi, 2016).

Despite decades of research on Neandertal anatomy, key questions remain about the functional significance of their postcranial morphology. Traditional interpretations emphasize cold-climate adaptation, particularly their relatively short distal limbs, robust skeletal frames, and broad torsos—morphologies consistent with Bergmann's and Allen's ecogeographic rules (Trinkaus, 1981; Ruff, 1994; Holliday, 1997). Bergmann's rule predicts that larger body masses are advantageous in colder climates due to reduced surface area-to-volume ratios (Bergmann, 1847, as cited in Ruff, 1994), while Allen's rule states that shorter appendages help conserve heat (Allen, 1877). Neandertal body proportions generally follow these expectations, reinforcing the cold-adaptation hypothesis.

However, recent perspectives have highlighted the potential role of biomechanical demands, especially locomotor efficiency in environments with varied topography, in shaping these morphological features (Gruss, 2007; Higgins, 2011; Kramer & Eck, 2000). These overlapping hypotheses reflect a broader question in human evolution: to what extent do skeletal morphologies reflect environmental pressures, behavioral adaptations, or neutral processes such as genetic drift? (Weaver, 2009; Harvati et al., 2021). Answering this question requires an integrative approach, one that combines comparative data, biomechanical modeling, and standardized measurement protocols that reduce error and enhance reproducibility, particularly when working with fragmentary fossils or external landmarks.

One challenge in resolving these debates lies in the limited availability of fossil material. Neandertal remains are often fragmentary, making it difficult to accurately reconstruct body proportions or estimate biomechanical parameters with precision. This limitation is particularly salient for comparative studies involving modern humans, who exhibit considerable intra- and inter-population variation in limb proportions and body size (Holliday, 1997; Sylvester et al., 2008). Interpreting Neandertal morphology against this backdrop requires careful sampling and methodological consistency (e.g., using standardized imaging protocols and measurement software) in how measurements, such as the crural index (CI), are calculated. The crural index is a ratio of tibial length to femoral length (tibia/femur × 100), and provides a metric for evaluating limb proportions (Davenport, 1933). Lower crural index values are often associated with cold-climate adaptation, as shorter distal limb segments help conserve body heat (Higgins, 2011).

In addition to questions about morphology and adaptation, relatively few studies have quantitatively assessed the biomechanical implications of Neandertal anatomy. For instance, while it has been proposed that shortened distal limbs may offer energetic advantages on sloped

terrain by reducing the energy required to lift and swing the limb during uphill walking (Gruss, 2007; Higgins, 2011), few models explicitly examine how mass distribution and limb proportions affect whole-body center of mass (CoM) under realistic environmental conditions, which is important because shifts in CoM can influence the energy cost of locomotion (Whitcome et al., 2007; Buurke et al., 2023). Yet such modeling is crucial for understanding how Neandertals might have moved through and interacted with their landscapes (Kramer & Eck, 2000; Whitcome et al., 2007).

A further complication arises from the reliance on external anatomical landmarks—rather than direct skeletal measurements—when assessing limb proportions in both living humans, whereas fossil specimens only preserve skeletal elements, making direct measurement the standard approach. Although widely used in anthropological and clinical contexts, the validity of externally derived measurements for calculating functional indices like CI has received limited empirical testing (Steudel-Numbers & Tilkens, 2004; Higgins, 2011). Without this testing and validation, any interpretations of morphological function risk being biased; until the predictive relationship between external and internal measurements is confirmed, externally derived values should not be relied upon for comparative study.

These gaps highlight the need for an integrative, data-driven approach that combines fossil analysis, comparative anatomy, biomechanical modeling, and methodological validation. This dissertation addresses these challenges by investigating how Neandertal limb proportions and mass distribution influence biomechanical function, using a comparative framework grounded in both empirical and modeled data.

Research Questions and Hypotheses

This dissertation investigates whether Neandertal postcranial morphology reflects specific functional adaptations related to climate and terrain. It asks whether differences in limb proportions and mass distribution between Neandertals and modern humans can be linked to biomechanical performance and environmental pressures. Three overarching research questions guide this work:

1. Do Neandertal limb proportions, particularly the CI, reflect biomechanical adaptations, such as locomotion on rugged terrain, rather than (or in addition to) cold-climate adaptation?
2. How do Neandertal limb proportions and trunk morphology influence center of mass position, and what are the implications for balance and energetic cost—especially during locomotion on sloped terrain?
3. Can externally measured limb segment lengths serve as reliable proxies for skeletal dimensions in studies of lower limb proportions, or do externally measured values introduce meaningful error that could bias interpretations?

These questions are addressed through a series of empirical and modeling analyses presented in Chapters 3 through 5. Collectively, these chapters document the examination of the hypothesis that Neandertal morphology was not only shaped by thermoregulatory demands but also by the biomechanical requirements of traversing sloped landscapes. Additionally, I evaluate whether the commonly used external landmarks in anthropological research accurately represent the underlying skeletal structure, which is especially relevant in living humans, as fossil studies rely exclusively on direct skeletal measurements.

By integrating fossil data, modern human comparative datasets, and biomechanical modeling, this research aims to refine interpretations of Neandertal functional anatomy and improve methodological practices in the study of hominin postcranial variation.

Based on prior research and theoretical models, the following hypotheses guide the analyses presented in this dissertation:

- H1: Neandertals will exhibit significantly lower crural index (CI) values than modern humans. This hypothesis is consistent with both cold-climate adaptations as predicted by ecogeographical rules and biomechanical adaptations to rugged terrain, such as increased locomotor efficiency on slopes.
- H2: Neandertals will show a more medially and posteriorly located center of mass (CoM) compared to modern humans, particularly under inclined terrain conditions, reflecting biomechanical adaptations to rugged environments.
- H3: External limb segment measurements, such as external estimates of femur and tibia length based on anatomical landmarks, will strongly correlate with skeletal lengths for femur and tibia.

Structure of the Dissertation

This dissertation is organized into four core chapters, each addressing a different aspect of Neandertal postcranial morphology, functional adaptation, and improved methods for data collection and analysis. Together, these chapters contribute to a more integrated understanding of how Neandertal anatomy reflects both environmental pressures and biomechanical constraints.

Chapter 2 provides the evolutionary and anatomical background necessary to interpret Neandertal limb proportions and functional morphology. In this chapter, I review the fossil record, postcranial traits, and environmental contexts in which Neandertals lived, with a focus on features linked to thermoregulation and locomotor efficiency. This chapter also introduces interpretive debates regarding cold adaptation, terrain navigation, and the potential influence of genetic drift and developmental plasticity.

In Chapter 3 I investigate variation in the CI, often used to assess climatic adaptation and biomechanical variation, in Neandertals and modern human populations. Drawing on pooled comparative datasets, I examine whether Neandertal CI values fall within the observed range for cold-adapted modern human populations and evaluate whether Neandertal limb proportions may also reflect biomechanical adaptations to rugged terrain. This chapter also addresses methodological issues related to sample size, measurement consistency, and sex-based classification biases in fossil samples.

In Chapter 4 I use reconstructed body proportions and estimated segment masses to predict the center of mass (CoM) for Neandertals and modern humans across flat and inclined terrain. By applying segmental mass distribution equations (De Leva, 1996), this chapter documents how limb proportions and trunk morphology affect locomotor stability and energetic cost. The analysis examines whether Neandertal body form may have conferred functional advantages in sloped or rugged environments, building on hypotheses of terrain-specific locomotor adaptation. Rugged environments are defined here as sloped, uneven, elevated, or obstacle-rich landscapes such as inclines, rocky hillsides, or mountainous regions.

In Chapter 5 I evaluate the accuracy of external anatomical landmarks for estimating femoral and tibial lengths, with a particular focus on their use in calculating the crural index.

Using CT data from human cadavers, I compare externally measured anatomical segment lengths to internal skeletal dimensions and evaluate the level of agreement between external anatomical landmarks and internal skeletal measurements. The results inform the reliability of external-based measurements used throughout the dissertation and have broader implications for fossil analysis, clinical biomechanics, and anthropometry.

Collectively, I address whether Neandertal limb proportions and mass distribution reflect functional adaptations to cold environments, complex terrain, or both. I also assess the methodological tools used to reconstruct these traits, contributing to a more accurate and nuanced interpretation of Neandertal anatomy and behavior.

The dissertation concludes with Chapter 6, which synthesizes the main findings, reflects on their broader implications for paleoanthropology and functional morphology, and outlines potential directions for future research in hominin biomechanics and comparative anatomy.

Significance

Understanding how skeletal morphology may reflect functional and environmental pressures is fundamental to interpreting the fossil record. My work contributes to that goal by combining comparative analysis, biomechanical modeling, and methodological validation to explore how Neandertal limb proportions and mass distribution relate to thermoregulation, locomotion, and terrain adaptation. In doing so, I address key gaps in the paleoanthropological literature and offers new perspectives on longstanding hypotheses about Neandertal anatomy.

Beyond Neandertal-specific questions, the results presented here have broader implications for how we study extinct hominins. By quantifying how limb proportions influence center of mass and locomotor stability, this research highlights the importance of incorporating

biomechanical principles into evolutionary interpretations. I also demonstrate the need for methodological transparency when estimating body proportions from fragmentary or externally measured data, reinforcing the value of validation studies in anthropological research.

Additionally, this work underscores the significance of integrating fossil data with modern comparative datasets and modeling techniques. As digital reconstructions and biomechanical simulations become increasingly central to paleoanthropology, efforts to standardize and verify measurement protocols will be critical. The methods and results developed here are applicable not only to studies of Neandertals, but also to broader investigations of locomotion, adaptation, and body form across the hominin lineage.

Ultimately, I seek to bridge morphological description with functional interpretation, helping to clarify the adaptive significance of Neandertal anatomy while contributing to more rigorous, data-driven approaches in the study of human evolution.

REFERENCES

Allen, J. A. (1877). The influence of physical conditions in the genesis of species. *Radical Review*, 1, 108–140.

Bergström, A., Stringer, C., Hajdinjak, M., Scerri, E. M. L., & Skoglund, P. (2021). Origins of modern human ancestry. *Nature*, *590*(December 2020), 40–43. https://doi.org/10.1038/s41586-021-03244-5

Davenport, C. B. (1933). Body length and proportion of leg to trunk in man. *American Journal of Physical Anthropology, 17*(3), 289–317. https://doi.org/10.1002/ajpa.1330170316

de Leva, P. (1996). Adjustments to Zatsiorsky-Seluyanov's segment inertia parameters. *Journal of Biomechanics*, *29*(9), 1223–1230.

Froehle, A. W., & Churchill, S. E. (2009). Energetic Competition Between Neandertals and Anatomically Modern Humans. *PaleoAnthropology*, 96–116.

Green, R. E., Krause, J., Briggs, A. W., Maricic, T., Stenzel, U., Kircher, M., Patterson, N., Li, H., Zhai, W., Fritz, M. H. Y., Hansen, N. F., Durand, E. Y., Malaspinas, A. S., Jensen, J. D., Marques-Bonet, T., Alkan, C., Prüfer, K., Meyer, M., Burbano, H. A., … Pääbo, S. (2010). A draft sequence of the neandertal genome. *Science*, *328*(5979), 710–722. https://doi.org/10.1126/science.1188021

Gruss, L. T. (2007). Limb length and locomotor biomechanics in the genus Homo: An experimental study. *American Journal of Physical Anthropology*, *134*(1), 106–116. https://doi.org/10.1002/ajpa.20642

Harvati, K., & Ackermann, R. R. (2022). Merging morphological and genetic evidence to assess hybridization in Western Eurasian late Pleistocene hominins. *Nature Ecology and Evolution*, *6*(10), 1573–1585. https://doi.org/10.1038/s41559-022-01875-z

Higgins, R. W., & Ruff, C. B. (2011). The effects of distal limb segment shortening on locomotor efficiency in sloped terrain: Implications for Neandertal locomotor behavior. *American Journal of Physical Anthropology*, *146*(3), 336–345. https://doi.org/10.1002/ajpa.21575

Holliday, T. W. (1997). Postcranial Evidence of Cold Adaptation in European Neandertals. *American Journal of Physical Anthropology*, *104*, 245–258.

Hublin, J.-J., & Roebroeks, W. (2009). *Ebb and flow or regional extinctions? On the character of Neandertal occupation of northern environments.* Comptes Rendus Palevol, 8(5), 503–509. https://doi.org/10.1016/j.crpv.2009.04.001

Kramer, P. A., & Eck, G. G. (2000). Locomotor energetics and leg length in hominid bipedality. *Journal of Human Evolution*, *38*(5), 651–666. https://doi.org/10.1006/jhev.1999.0375

Roebroeks, W., & Soressi, M. (2016). Neandertals revised. *PNAS*, *113*(23), 6372–6379. https://doi.org/10.1073/pnas.1521269113

Ruff, C. B. (1994). Morphological adaptation to climate in modern and fossil hominids. *American Journal of Physical Anthropology*, *37*(19 S), 65–107. https://doi.org/10.1002/ajpa.1330370605

Steudel-Numbers, K. L., & Tilkens, M. J. (2004). The effect of lower limb length on the energetic cost of locomotion: implications for fossil hominins. *Journal of Human Evolution*, *47*, 95–109. https://doi.org/10.1016/j.jhevol.2004.06.002

Stringer, C., & Crete, L. (2022). Mapping Interactions of Homo neanderthalensis and Homo sapiens From the Fossil and Genetic Records. *PaleAnthropology*, 2, 1-15.

Sylvester, A. D., Kramer, P. A., & Jungers, W. L. (2008). Modern humans are not (quite) isometric. *American Journal of Physical Anthropology*, *137*(4), 371–383. https://doi.org/10.1002/ajpa.20880

Trinkaus, E. (1981). Neanderthal limb proportions and cold adaptation. *Aspects of Human Evolution*, *February*, 187–224. http://ci.nii.ac.jp/naid/10018145328/

Trinkaus, E., & Shipman, P. (1993). Neandertals: Images of Ourselves. *Evolutionary Anthropology*, *1*(6), 194–201. https://doi.org/10.2307/4612796

Weaver, T. D. (2009). The meaning of Neandertal skeletal morphology. *PNAS*, *106*(38), 16028–16033. www.pnas.orgcgidoi10.1073pnas.0903864106

Weaver, T. D., & Steudel-Numbers, K. (2005). Does Climate or Mobility Explain the Differences in Body Proportions Between Neandertals and Their Upper Paleolithic Successors? *Evolutionary Anthropology*, *14*, 218–223. https://doi.org/10.1002/evan.20069

Whitcome, K. K., Shapiro, L. J., & Lieberman, D. E. (2007). Fetal load and the evolution of lumbar lordosis in bipedal hominins. *Nature*, *450*, 1075–1077. https://doi.org/10.1038/nature06342

Chapter 2: Neandertals

Introduction

Homo neanderthalensis, or Neandertals, are our closest extinct relatives, based on genetic, anatomical, and behavioral similarities, and have intrigued scientists since their initial discovery in the mid-19th century. Genetic studies have confirmed their close relationship to modern humans, with Neandertals contributing between 1–4% of the genome of present-day non-African populations (Green et al., 2010; Sankararaman et al., 2012). The first recognized specimen, a partial cranium known as Feldhofer 1, was uncovered in 1856 in the Neander Valley of western Germany (Trinkaus & Shipman, 1993). This discovery sparked widespread scientific debate and marked the beginning of paleoanthropology as a discipline.

Early interpretations of Neandertals were heavily shaped by 19th- and early 20th-century biases. Marcellin Boule's influential reconstruction of La Chapelle-aux-Saints portrayed Neandertals as hunched, brutish, and cognitively inferior (Trinkaus & Shipman, 1993; Tattersall & Schwartz, 1998). Later reassessments corrected for the specimen's pathological features and revealed a more upright, modern-like posture, but Boule's depiction entrenched a legacy of misrepresentation that lingered for decades.

Today, Neandertals are understood as a highly adaptable and capable hominin group. They exhibited complex behaviors including symbolic expression, sophisticated tool manufacture and use, and social cooperation (e.g. Zilhão et al., 2010; Roebroeks & Soressi, 2016). Genetic evidence further demonstrates that Neandertals interbred with early *Homo sapiens*, contributing to the genomes of modern non-African human populations (e.g. Green et al., 2010; Sankararaman et al., 2012).

Understanding Neandertals offers crucial insight into our own evolutionary trajectory and the selective pressures that shaped human morphology and behavior. This chapter provides a comprehensive overview of Neandertal evolutionary history, environmental context, and postcranial morphology. Special attention is given to body form and limb proportions—key traits linked to hypotheses of cold-climate adaptation and biomechanical efficacy. This background lays the foundation for the quantitative comparisons explored in Chapters 3–5.

Taxonomy and Evolutionary History

Neandertals are generally classified as *Homo neanderthalensis*, a distinct sister species to anatomically modern humans (*Homo sapiens*). While some researchers have used the Biological Species Concept to argue that Neandertals should be considered a subspecies (*H. sapiens neanderthalensis*) due to evidence of interbreeding (Mayr, 1970) , the majority of recent studies support their designation as a separate species based on morphological and genetic distinctions (Tattersall & Schwartz, 1998; Trinkaus, 2007; Green et al., 2010; Sankararaman et al., 2012).

The Neandertal lineage likely diverged from the lineage leading to modern humans sometime between 550,000 and 765,000 years ago (Liu et al., 2015; Meyer et al., 2016; Prüfer et al., 2014). Genetic data indicate that Neandertals and modern humans share a common ancestor, likely *Homo heidelbergensis* or a closely related species (Rightmire, 1996; Stringer, 2012). Fossil evidence suggests a gradual accumulation of Neandertal morphological traits in the fossil record over time, with transitional forms appearing in Europe and western Asia during the Middle Pleistocene (Hublin, 2009; Harvati et al., 2022).

Fully derived Neandertals appeared in the fossil record approximately 200,000 years ago and persisted until around 40,000 years ago, when they disappeared from the fossil record (Higham et al., 2014). Their extinction roughly coincides with the expansion of anatomically

modern humans into Europe, and although the causes of their disappearance remain debated, hypotheses include climate fluctuations, resource competition, and assimilation through interbreeding (Stringer, 2012; Higham et al., 2014; Hublin, 2017).

Neandertals occupied a wide range of geographical landscapes across Europe and parts of western and central Asia, with attributed fossil sites extending from the Iberian Peninsula to the Altai Mountains (Harvati & Ackermann, 2022; see also Figure 1). Despite this 8,000km spread, their morphology remains relatively consistent, though some regional and temporal variation has been noted (Holliday, 1997; Weaver, 2009; Harvati & Ackermann, 2022). Understanding their evolutionary placement —both taxonomically and temporally— and distribution is critical for interpreting patterns of morphological variation and ecological adaptation discussed in the remainder of this chapter.

Environmental and Geographic Context

Neandertals evolved and thrived during the Middle (roughly 781,000-126,000 years ago) and Late Pleistocene (126,000-11,700 years ago), a period marked by pronounced climatic fluctuations and recurrent glacial cycles. These environmental conditions are thought to have had a profound impact on their morphology, behavior, and geographic distribution (Holliday, 1997; Gamble et al., 2004; Shea, 2008). Neandertals occupied a wide range of habitats across Europe and western Asia, from the Atlantic coasts of Iberia to the central plains of Russia and the mountainous regions of the Caucasus and Altai (Harvati & Ackermann, 2022). Their capacity to adapt to and thrive in such diverse environments is reflected in both their material culture and biological adaptations (Roebroeks & Soressi, 2016; Zilhão et al., 2010).

Neandertals not only occupied a wide geographical range, but they often settled and moved through regions characterized by rugged, sloped, and topographically varied terrain.

Archaeological and environmental data indicate that many of their campsites were situated in river valleys, uplands, and mountainous zones—landscapes that required frequent mobility over uneven ground and elevation changes (Gruss, 2007; Higgins & Ruff, 2011). These challenging environments likely exerted selective pressures favoring body forms that improved balance, stability, and energetic efficiency. For instance, shortened distal limb segments may reduce the moment arms at the knee and ankle, minimizing muscular effort during incline locomotion (Gruss, 2007; Higgins & Ruff, 2011). Chapter 3 evaluates these possibilities through an analysis of crural index variation, while Chapter 4 models how Neandertal mass distribution affects center of mass across slopes, revealing potential energetic advantages for locomotion in such environments (see Chapter 3; Chapter 4). These insights underscore the importance of terrain in interpreting Neandertal morphology and provide a biomechanical framework for the adaptations discussed in this chapter.

Throughout their existence, Neandertals experienced multiple glacial and interglacial cycles. During glacial periods, much of northern Europe was covered by ice or periglacial tundra, forcing Neandertals to retreat southward into more temperate refugia. In contrast, interglacial phases allowed for a broader expansion into northern latitudes (Gamble et al., 2004; J. J. Hublin, 2009). Their persistence across these fluctuating habitats demonstrates a high degree of ecological resilience and behavioral flexibility, including the ability to exploit large game, make fire, and construct shelters in cold climates (Roebroeks & Soressi, 2016; Zilhão et al., 2010).

Faunal remains from Neandertal-associated archaeological sites suggest that they often targeted large-bodied herbivores such as mammoths, woolly rhinoceroses, reindeer, and red deer, species that were themselves adapted to cold environments and open, rugged terrain —meaning

rocky, uneven, and topographically complex landscapes (Gaudzinski-Windheuser & Roebroeks, 2011; Stewart, 2005). These animals exhibit traits such as thick insulating fur, compact limbs, and robust builds—features paralleling the thermoregulatory adaptations observed in Neandertals. The recurring association between Neandertals and cold-adapted megafauna hints at ecological tracking and the potential co-evolution of morphological traits suited to glacial ecosystems.

These environmental pressures likely contributed to the development of their characteristic postcranial anatomy. Neandertals display morphological traits typically associated with thermoregulation in cold climates, such as short distal limb segments, increased body mass, and a barrel-shaped thorax (Trinkaus, 1981; Ruff, 1994; Holliday, 1997). These features have traditionally been interpreted through the lens of Bergmann's and Allen's rules, which link body shape and limb proportions to ambient temperature. However, previous research has also emphasized the potential role of locomotor biomechanics and terrain variability in shaping Neandertal anatomy (Gruss, 2007; Higgins, 2011; Kramer & Eck, 2000). Neandertal's extensive geographical distribution, combined with their repeated exposure to harsh glacial climates and rugged landscapes, provides critical environmental context for evaluating the selective pressures acting on their limb proportion and locomotor adaptations discussed in the following sections.

Postcranial Morphology and Functional Implications

Neandertals exhibit a distinctive postcranial anatomy characterized by high robusticity (Trinkaus, 1981), relatively short distal limb segments (Higgins & Ruff, 2011), and a broad, deep torso (Gómez-Olivencia et al., 2018). These traits have long been recognized as distinctly different from the morphology of most modern human populations (Figure 2), and they are

commonly interpreted as adaptative traits in cold climates requiring high-energy locomotion (Trinkaus, 1981; Ruff, 1994; Holliday, 1997; Gruss, 2007).

The thorax of Neandertals is notably barrel-shaped, with increased anteroposterior depth relative to modern humans. This expanded ribcage is often associated with increased lung volume, potentially supporting high oxygen demands during active foraging or thermoregulatory efficiency in cold environments, or physiological demands similar to those observed in high-altitude populations (Gómez-Olivencia et al., 2009; García-Martínez et al., 2020; Beall, 2001). Combined with a wide pelvis and large articular surfaces at the hip and knee, this morphology suggests a powerful, muscular build suited to challenging terrain and frequent load bearing (Trinkaus, 1983; Ruff, 2002). These traits likely enhanced locomotor stability, shock absorption, and mechanical leverage — factors particularly advantageous in environments requiring frequent mobility over uneven ground or while transporting heavy loads (Rue & Kramer, 2017). Rue & Kramer (2017) demonstrate that burden, gradient, and velocity meaningfully affect energy expenditure in modern human walkers, offering a functional context for interpreting the adaptive value of Neandertal morphology in similarly demanding environments.

One of the most salient features of Neandertal postcranial morphology is their relatively low crural index—the ratio of tibial to femoral length. Numerous studies have demonstrated that Neandertals possess lower CI values compared to modern human populations, particularly those from temperate or tropical climates (Trinkaus, 1981; Holliday, 1997; Weaver, 2009). This limb proportion pattern aligns with predictions from Allen's rule, in which shortened distal limbs reduce surface area and conserve body heat. However, alternative interpretations suggest that these proportions may also reflect biomechanical advantages in rugged or sloped environments (Higgins, 2011; Kramer & Eck, 2000), including reduced energy expenditure during incline

locomotion (Gruss, 2007). The detailed exploration of CI patterns in Neandertals is presented in Chapter 3.

Neandertals also show differences in spinal morphology that may have affected locomotor function. Vertebral column reconstructions suggest a reduced degree of lumbar lordosis compared to modern humans, potentially resulting in a more linear or kyphotic lumbar spine (Figure 3) (Been et al., 2012, 2014; Gómez-Olivencia et al., 2013). Lumbar lordosis plays a critical role in positioning the upper body mass over the pelvis, which in turn influences posture, balance, and energetic cost during walking (Whitcome et al., 2007). A reduced spinal curvature in Neandertals may have shifted their center of mass slightly forward, increasing muscular demands during upright locomotion, particularly on uneven terrain. These implications are explored in greater depth in Chapter 4, which models center of mass position across different slope conditions.

Overall, Neandertal postcranial morphology reflects a complex interplay of thermoregulation, biomechanical demands, and environmental pressures. Their robust frames, short distal limbs, and modified spinal structure suggest that Neandertals were not only adapted to cold climates, but also to physically demanding landscapes. These features set the stage for the more quantitative analyses that follow, which examine how specific limb proportions and mass distributions affected Neandertal mobility and functional efficacy.

Anatomical Variation Within Neandertals

Although Neandertals are often described as a relatively anatomically consistent population (Trinkaus, 1981; Hublin, 2009), closer examination reveals important variation in morphology. Differences in limb proportions, body size, and skeletal robusticity have been observed across

individuals from different regions and time periods, though the magnitude and interpretation of these differences remain debated (Holliday, 1997; Weaver, 2009; Harvati & Ackermann, 2022).

Many comparative studies have attempted to separate Neandertals by sex or inferred body size when analyzing limb proportions, often assuming that patterns of sexual dimorphism mirror those found in modern humans (e.g., robusticity and overall body size dimorphism observed in European and North American populations) (Trinkaus, 1981; Ruff, 1994; Gruss, 2007). These assumptions typically rely on estimated stature or limb lengths as proxies for biological sex. However, this approach may overstate the degree of sexual dimorphism in Neandertals and introduces circular reasoning when interpreting variation. Modern human populations exhibit considerable overlap in body size and height between sexes (Ruff, 2002; Auerbach & Ruff, 2006), and it is unclear whether Neandertals followed similar patterns (Weaver, 2009; Harvati & Ackermann, 2022). Additionally, many Neandertal fossils are incomplete, complicating both sex estimation and the reconstruction of limb proportions.

For these reasons, the analyses in this dissertation avoid separating Neandertal individuals into sex-based or body size-based categories. Instead, all specimens with sufficiently complete limb measurements are pooled for comparative analysis. This approach minimizes classification bias and reflects the limitations of the fossil record while still allowing for robust interspecific comparisons with modern humans.

Some regional and temporal variation in Neandertal morphology has been observed—for example, specimens from southern or eastern sites (e.g., Amud and Shanidar) sometimes show slightly more elongated limb proportions compared to those from colder northern climates (e.g., La Ferrassie and La Chapelle-aux-Saints) (Holliday, 1997; Weaver, 2009). However, such variation is subtle and typically falls within the broader range of Neandertal morphological

diversity. Recognizing this diversity is essential for interpreting patterns of adaptation and for understanding the evolutionary significance of the morphological trends explored in the following chapters.

Interpretive Debates: Cold Adaptation, Biomechanics, and Evolutionary Processes

The distinctive morphology of Neandertals has sparked decades of debate over the evolutionary and environmental forces responsible for shaping their anatomy. Multiple hypotheses have been proposed to explain traits such as their robust build, low crural indices, and broad thorax. These include climatic adaptation (Holliday, 1997; Ruff, 1994), biomechanical function (Gruss, 2007; Kramer & Eck, 2000), genetic drift (Weaver, 2009), and developmental plasticity (Harvati & Ackermann, 2022). Rather than representing mutually exclusive explanations, these hypotheses likely reflect overlapping influences acting at different biological and temporal scales.

The traditional interpretation of Neandertal limb proportions is grounded in ecogeographic principles, particularly Bergmann's and Allen's rules. According to this view, Neandertals' short distal limbs and large body mass minimized surface area relative to volume, reducing heat loss in glacial environments (Trinkaus, 1981; Holliday, 1997). This cold-climate adaptation model has been supported by the geographic distribution of Neandertal fossils and their frequent association with cold or variable Pleistocene habitats (Holliday, 1997; Weaver, 2009). However, some Neandertal populations, such as those from southern Spain and Italy, inhabited relatively temperate environments. These exceptions highlight that thermoregulation may not fully account for Neandertal morphology, prompting consideration of additional selective pressures such as locomotor efficiency and terrain navigation.

Therefore, thermoregulation alone may not fully explain the functional morphology of Neandertals. Recent research has emphasized the importance of biomechanical and locomotor

demands, particularly in rugged or sloped terrain. For instance, shorter tibiae may reduce the moment arm at the knee during uphill locomotion, thereby lowering muscular effort and energy expenditure (Gruss, 2007; Higgins, 2011). Other anatomical features—such as wide pelves, large joint surfaces, and altered spinal curvature—may likewise reflect adaptations to navigating complex landscapes with frequent elevation changes (Kramer & Eck, 2000; Gómez-Olivencia et al., 2009; Been et al., 2014).

Additional perspectives suggest that aspects of Neandertal anatomy may be the result of non-adaptive processes, including genetic drift or developmental constraints. Given the relatively small effective population sizes and prolonged regional isolation of Neandertals, driven in part by climatic fluctuations and topographic barriers that fragmented populations across Europe and western Asia, some morphological traits, such as variation in limb robusticity or vertebral shape, could have arisen or persisted due to random genetic changes rather than direct selection (Weaver, 2009; Harvati & Ackermann, 2022). Others argue that body proportions may be shaped during growth and development through environmentally responsive plasticity, especially in limb lengths, which are sensitive to both temperature and activity levels (Ruff, 1994; Bogin, 1999).

Each of these explanations offers a plausible account for Neandertals' distinct morphology, but disentangling their relative contributions remains challenging. Many traits likely reflect a combination of selective and non-selective pressures, compounded by the difficulty of reconstructing soft tissue, behavior, and environmental exposure from fossil remains.

This dissertation builds on these interpretive frameworks by testing whether specific morphological traits—namely limb proportions and mass distribution—can be linked to biomechanical function and environmental conditions. Chapters 3 and 4 quantitatively assess

whether crural index and center of mass differences between Neandertals and modern humans correspond to functional adaptations. Chapter 5 further evaluates the reliability of measurement methods used in these comparisons. Together, these analyses contribute to a more integrated understanding of the evolutionary processes shaping Neandertal postcranial anatomy.

Summary

Neandertals represent a distinctive and morphologically complex hominin population shaped by a combination of environmental pressures, biomechanical demands, and evolutionary processes. Their robust anatomy, short distal limbs, broad thorax, and modified spinal curvature have traditionally been interpreted as cold-climate adaptations, though more recent perspectives emphasize the potential influence of terrain navigation and locomotor efficiency. Ongoing debates regarding the relative roles of thermoregulation, biomechanics, and non-adaptive forces such as genetic drift or developmental constraints. However, it is important to distinguish these from developmental plasticity, which is itself an adaptive response to environmental variation despite not resulting from genetic change, highlighting the need for integrative, quantitative approaches to Neandertal functional morphology.

This chapter has outlined the evolutionary context, environmental setting, and key anatomical traits of Neandertals, providing a foundation for the analyses that follow. The next chapter investigates variation in crural index—a metric central to hypotheses of thermoregulation and terrain adaptation—using pooled Neandertal and modern human data. Chapter 4 builds on these findings by modeling how differences in limb proportions and mass distribution affect whole-body center of mass across varying terrain conditions. Chapter 5 evaluates the accuracy of external limb measurements used in these analyses, addressing methodological concerns relevant to both fossil and clinical research.

Together, these chapters aim to refine our understanding of Neandertal locomotor adaptation and the evolutionary forces that shaped their unique anatomy.

Figure 1: Neandertal fossil distribution across Eurasia

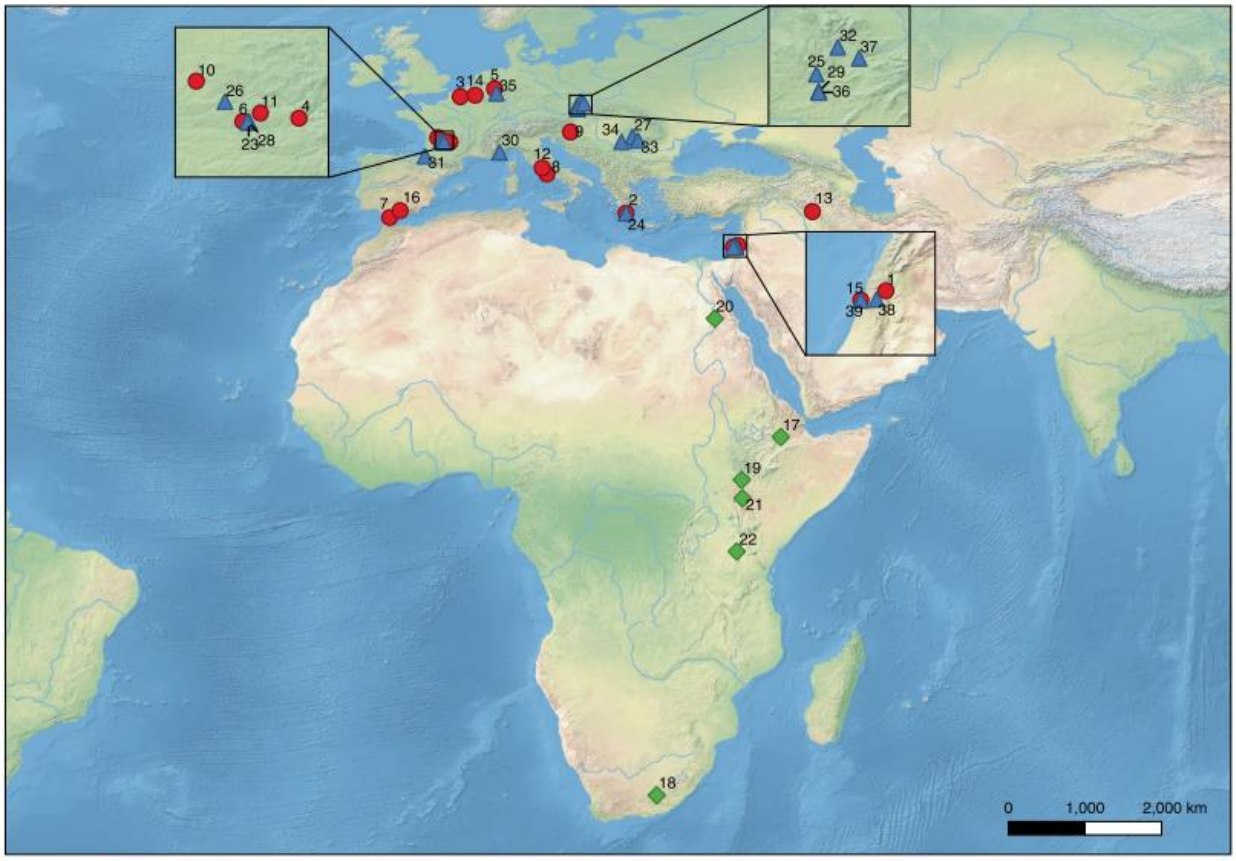

1 Amud 1
2 Apidima 2
3 Biache-Saint-Vaast
4 La Chapelle-aux-Saints
5 Feldhofer
6 La Ferrassie 1
7 Gibraltar 1
8 Guattari 1
9 Krapina J
10 La Quina 5
11 Régourdou
12 Saccopastore 1
13 Shanidar 1,5
14 Spy 1,2
15 Tabun C1
16 Zafarraya
17 Aduma 3
18 Hofmeyr
19 Omo 1
20 Wadi Kubbaniya
21 Eliye Springs
22 LH18
23 Abri Pataud
24 Apidima 1
25 Brno 2
26 Chancelade
27 Cioclovina
28 Cro Magnon 1,2,3
29 Dolní Věstonice 3,13,14,15,16
30 Grimaldi
31 Isturitz III
32 Mladeč 1,5
33 Muierii 1
34 Oase 1,2
35 Oberkassel 1,2
36 Pavlov 1
37 Predmost 3,4
38 Qafzeh 6,9
39 Skhul 5

Figure 1: Neandertal fossil distribution across Western Eurasia, with overlap zones where interactions with Homo sapiens likely occurred. Adapted from (Harvati & Ackermann (2022).

Figure 2: Comparative anatomy of modern human postcranial skeletons.

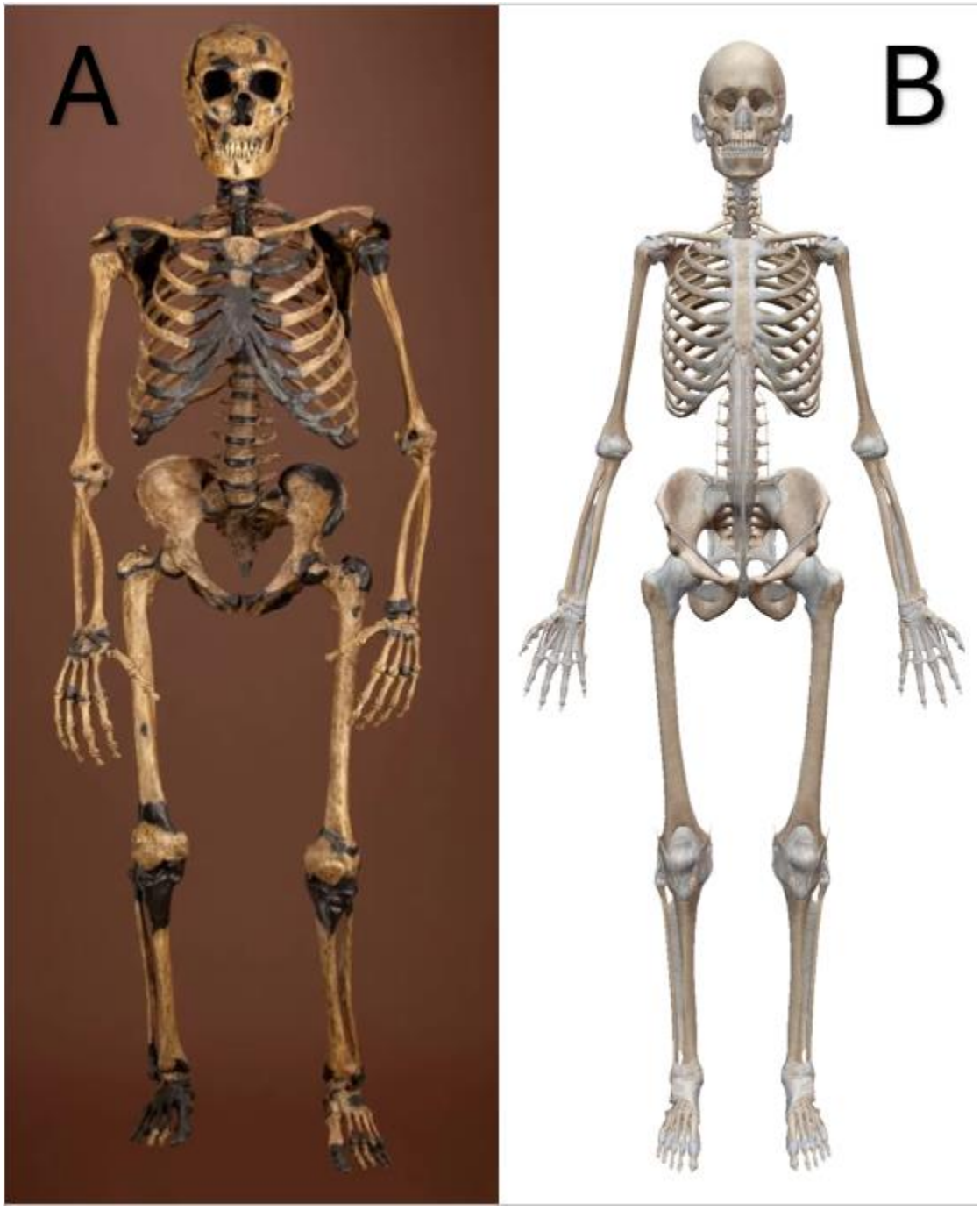

Figure 2: Comparative anatomy of modern human postcranial skeletons. The Neandertal image (A) is from the Smithsonian Institution's Human Origins Program. The modern human image (B) is from the Visible Body Human Anatomy Atlas app.

Figure 3: Comparison of the Kebara 2 Neandertal spine.

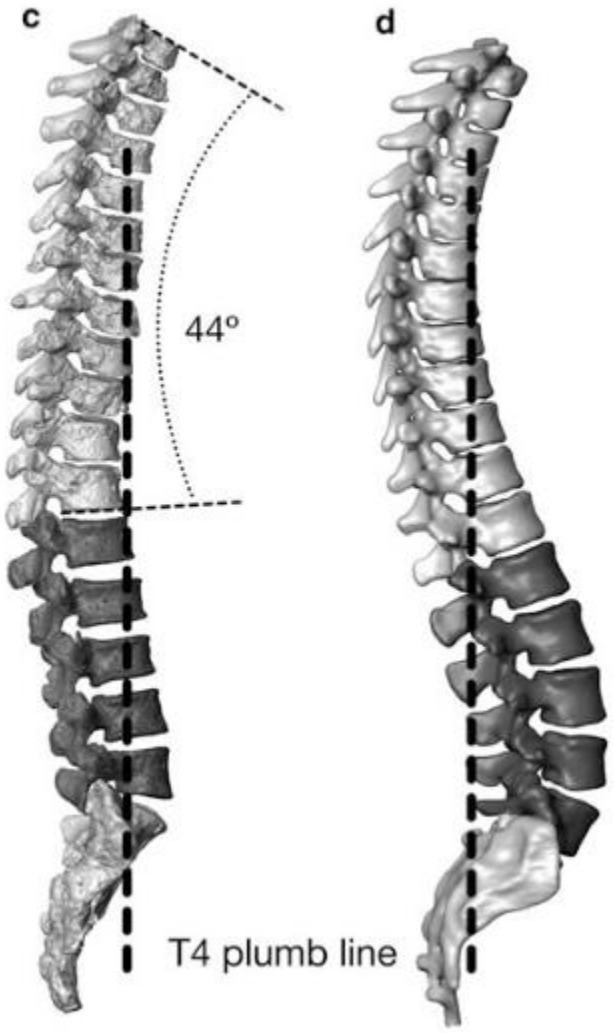

Figure 3: Comparison of the Kebara 2 Neandertal spine (left) with a modern human spine (right) showing the differences in spinal posture. Adapted from (Been et al., 2017) Fig. 18.6

REFERENCES

Auerbach, B. M., & Ruff, C. B. (2006). Limb bone bilateral asymmetry: Variability and commonality among modern humans. Journal of Human Evolution, 50(2), 203–218.

Beall, C. M. (2001). Adaptations to altitude: A current assessment. *Annual Review of Anthropology, 30*, 423–456. https://doi.org/10.1146/annurev.anthro.30.1.423

Been, E., Gómez-Olivencia, A., & Kramer, P. A. (2012). Lumbar lordosis of Extinct Hominins. *AMERICAN JOURNAL OF PHYSICAL ANTHROPOLOGY*, *147*, 64–77. https://doi.org/10.1002/ajpa.21633

Been, E., Gómez-Olivencia, A., & Kramer, P. A. (2014). Brief Communication: Lumbar Lordosis in Extinct Hominins: Implications of the Pelvic Incidence. *American Journal of Physical Anthropology*, *154*, 307–314. https://doi.org/10.1002/ajpa.22507

Been, E., Gómez-Olivencia, A., Kramer, P. A., & Barash, A. (2017). 3D Reconstruction of Spinal Posture of the Kebara 2 Neanderthal. In A. Marom & E. Hovers (Eds.), *Human Paleontology and Prehistory: Contributions in Honor of Yoel Rak* (Issue January, pp. 239–251). Springer. https://doi.org/10.1007/978-3-319-46646-0

Bogin, B. (1999). Patterns of human growth (2nd ed.). Cambridge University Press.

Gamble, C., Davies, W., Pettitt, P., & Richards, M. (2004). Climate change and evolving human diversity in Europe during the last glacial. *Philosophical Transactions of the Royal Society B: Biological Sciences*, *359*, 243–254. https://doi.org/10.1098/rstb.2003.1396

García-Martínez, D., Bastir, M., Gómez-Olivencia, A., Maureille, B., Golovanova, L., Doronichev, V., Akazawa, T., Kondo, O., Ishida, H., Gascho, D., Zollikofer, C. P. E., de León, M. P., & Heuzé, Y. (2020). Early development of the neanderthal ribcage reveals a different body shape at birth compared to modern humans. *Science Advances*, *6*(41), 1–10.

Gaudzinski-Windheuser, S., Roebroeks, W. (2011). On Neanderthal Subsistence in Last Interglacial Forested Environments in Northern Europe. In: Conard, N.J., Richter, J. (eds) Neanderthal Lifeways, Subsistence and Technology. Vertebrate Paleobiology and Paleoanthropology Series. Springer, Dordrecht. https://doi-org.offcampus.lib.washington.edu/10.1007/978-94-007-0415-2_7

Gómez-Olivencia, A., Couture-Veschambre, C., Madelaine, S., & Maureille, B. (2013). The vertebral column of the Regourdou 1 Neandertal. *Journal of Human Evolution*, *64*(6), 582–607. https://doi.org/10.1016/j.jhevol.2013.02.006

Gómez-Olivencia, A., Lindsay Eaves-Johnson, K., Franciscus, R. G., Carretero, M., & Luis Arsuaga, J. (2009). Kebara 2: new insights regarding the most complete Neandertal thorax. *Journal of Human Evolution*, *57*, 75–90. https://doi.org/10.1016/j.jhevol.2009.02.009

Gómez-Olivencia, A., Barash, A., García-Martínez, D., Arlegi, M., Kramer, P. A., Bastir, M., & Been, E. (2018). 3D virtual reconstruction of the Kebara 2 Neandertal thorax. *Nature Communications, 9*, 4387. https://doi.org/10.1038/s41467-018-06803-z

Green, R. E., Krause, J., Briggs, A. W., Maricic, T., Stenzel, U., Kircher, M., Patterson, N., Li, H., Zhai, W., Fritz, M. H. Y., Hansen, N. F., Durand, E. Y., Malaspinas, A. S., Jensen, J. D., Marques-Bonet, T., Alkan, C., Prüfer, K., Meyer, M., Burbano, H. A., … Pääbo, S. (2010). A draft sequence of the neandertal genome. *Science*, *328*(5979), 710–722. https://doi.org/10.1126/science.1188021

Gruss, L. T. (2007). Limb length and locomotor biomechanics in the genus Homo: An experimental study. *American Journal of Physical Anthropology*, *134*(1), 106–116. https://doi.org/10.1002/ajpa.20642

Harvati, K., & Ackermann, R. R. (2022). Merging morphological and genetic evidence to assess hybridization in Western Eurasian late Pleistocene hominins. *Nature Ecology and Evolution*, *6*(10), 1573–1585. https://doi.org/10.1038/s41559-022-01875-z

Higgins, R. W., & Ruff, C. B. (2011). The effects of distal limb segment shortening on locomotor efficiency in sloped terrain: Implications for Neandertal locomotor behavior. *American Journal of Physical Anthropology*, *146*(3), 336–345. https://doi.org/10.1002/ajpa.21575

Higham, T., Douka, K., Wood, R., Ramsey, C. B., Brock, F., Basell, L., Camps, M., Arrizabalaga, A., Baena, J., Barroso-Ruíz, C., Bergman, C., Boitard, C., Boscato, P., Caparrós, M., Conard, N. J., Draily, C., Froment, A., Galván, B., Gambassini, P., … Jacobi, R. (2014). The timing and spatiotemporal patterning of Neanderthal disappearance. *Nature*, *512*, 306–309. https://doi.org/10.1038/nature13621

Holliday, T. W. (1997a). Body proportions in Late Pleistocene Europe and modern human origins. *Journal of Human Evolution*, *32*, 423–447.

Holliday, T. W. (1997b). Postcranial Evidence of Cold Adaptation in European Neandertals. *American Journal of Physical Anthropology*, *104*, 245–258.

Hublin, J. J. (2009). The origin of Neandertals. *PNAS*, *106*(38), 16022–16027. www.pnas.orgcgidoi10.1073pnas.0904119106

Hublin, J.-J. (2015). The modern human colonization of western Eurasia: when and where? *Quaternary Science Reviews*, *118*, 194–210. https://doi.org/10.1016/j.quascirev.2014.08.011

Kramer, P. A. (1999). Hominid locomotor energetics. *Journal of Experimental Biology*, *202*, 2807–2818.

Kramer, P. A. (2010). The effect on energy expenditure of walking on gradients or carrying burdens. *American Journal of Human Biology*, *22*(4), 497–507. https://doi.org/10.1002/ajhb.21027

Kramer, P. A., & Eck, G. G. (2000). Locomotor energetics and leg length in hominid bipedality. *Journal of Human Evolution*, *38*(5), 651–666. https://doi.org/10.1006/jhev.1999.0375

Liu, W., Martinón-Torres, M., Cai, Y.-J., Xing, S., Tong, H.-W., Pei, S.-W., Sier, M. J., Wu, X.-H., Lawrence Edwards, R., Cheng, H., Li, Y.-Y., Yang, X.-X., María Bermúdez De Castro, J., & Wu, X.-J. (2015). The earliest unequivocally modern humans in southern China. *Nature*, *526*, 696–700. https://doi.org/10.1038/nature15696

Mayr, E. (1970). Populations, species, and evolution: an abridgment of animal species and evolution (Vol. 19). Harvard University Press.

Meyer, M., Arsuaga, J.-L., De Filippo, C., Nagel, S., Aximu-Petri, A., Nickel, B., Martínez, I., Gracia, A., María Bermúdez De Castro, J., Carbonell, E., Viola, B., Kelso, J., Prüfer, K., Pääbo, S., & Domingo, M. (2015). Nuclear DNA sequences from the Middle Pleistocene Sima de los Huesos hominins. *Nature*, *531*, 504–508. https://doi.org/10.1038/nature17405

Prüfer, K., Racimo, F., Patterson, N., Jay, F., Sankararaman, S., Sawyer, S., Heinze, A., Renaud, G., Sudmant, P. H., De Filippo, C., Li, H., Mallick, S., Dannemann, M., Fu, Q., Kircher, M., Kuhlwilm, M., Lachmann, M., Meyer, M., Ongyerth, M., … Pääbo, S. (2014). The complete genome sequence of a Neanderthal from the Altai Mountains. *Nature*, *505*(7481), 43–49. https://doi.org/10.1038/nature12886

Reich, D., Green, R. E., Kircher, M., Krause, J., Patterson, N., Durand, E. Y., Viola, B., Briggs, A. W., Stenzel, U., Johnson, P. L. F., Maricic, T., Good, J. M., Marques-Bonet, T., Alkan, C., Fu, Q., Mallick, S., Li, H., Meyer, M., Eichler, E. E., … Pääbo, S. (2010). Genetic history of an archaic hominin group from Denisova cave in Siberia. *Nature*, *468*(7327), 1053–1060. https://doi.org/10.1038/nature09710

Rightmire, P. G. (1996). The human cranium from Bodo, Ethiopia: Evidence for speciation in the Middle Pleistocene? *Journal of Human Evolution*, *31*, 21–39.

Roebroeks, W., & Soressi, M. (2016). Neandertals revised. *PNAS*, *113*(23), 6372–6379. https://doi.org/10.1073/pnas.1521269113

Ruff, C. (2002). VARIATION IN HUMAN BODY SIZE AND SHAPE. *Annu. Rev. Anthropol*, *29*, 211–243. https://doi.org/10.1146/annurev.anthro.31.040402.085407

Ruff, C. B. (1994). Morphological adaptation to climate in modern and fossil hominids. *American Journal of Physical Anthropology*, *37*(19 S), 65–107. https://doi.org/10.1002/ajpa.1330370605

Sankararaman, S., Mallick, S., Dannemann, M., Prüfer, K., Kelso, J., Pääbo, S., Patterson, N., & Reich, D. (2014). The genomic landscape of Neanderthal ancestry in present-day humans. *Nature*, *507*(7492), 354–357. https://doi.org/10.1038/nature12961

Shea, J. J. (2008). Transitions or turnovers? Climatically-forced extinctions of Homo sapiens and Neanderthals in the east Mediterranean Levant. *Quaternary Science Reviews*, *27*, 2253–2270. https://doi.org/10.1016/j.quascirev.2008.08.015

Smithsonian Institution. (n.d.). Neanderthal Composite Skeleton. https://humanorigins.si.edu/evidence/human-fossils/fossils/neanderthal-composite-skeleton

Stewart, J. R. (2005). The ecology and adaptation of Neanderthals during the non-analogue environment of Oxygen Isotope Stage 3. *Quaternary International, 137*(1), 35–46. https://doi.org/10.1016/j.quaint.2004.11.018

Stringer, C. (2012). The status of Homo heidelbergensis (Schoetensack 1908). *Evolutionary Anthropology*, *21*(3), 101–107. https://doi.org/10.1002/EVAN.21311

Stringer, C., & Crété, L. (2022). Mapping Interactions of Homo neanderthalensis and Homo sapiens From the Fossil and Genetic Records. *PaleoAnthropology*, *2*, 1–15. https://doi.org/10.48738/2022.iss2.130

Tattersall, I., & Schwartz, J. H. (1999). Commentary Hominids and hybrids: The place of Neanderthals in human evolution. *PNAS*, *96*, 7117–7119. www.pnas.org.

Trinkaus, E. (1981). Neanderthal limb proportions and cold adaptation. *Aspects of Human Evolution*, *February*, 187–224. http://ci.nii.ac.jp/naid/10018145328/

Trinkaus, E. (1986). The Neandertals and Modern Human Origins. *Source: Annual Review of Anthropology*, *15*, 193–218. https://www.jstor.org/stable/2155760?seq=1&cid=pdf-

Trinkaus, E. (2007). European early modern humans and the fate of the Neandertals. *PNAS*, *104*(18), 7367–7372. www.pnas.orgcgidoi10.1073pnas.0702214104

Trinkaus, E., & Shipman, P. (1993). Neandertals: Images of Ourselves. *Evolutionary Anthropology*, *1*(6), 194–201. https://doi.org/10.2307/4612796

Visible Body. (2025). *Human Anatomy Atlas* [Mobile application software). Argosy Publishing. https://www.visiblebody.com

Weaver, T. D. (2009). The meaning of Neandertal skeletal morphology. *PNAS*, *106*(38), 16028–16033. www.pnas.orgcgidoi10.1073pnas.0903864106

Whitcome, K. K., Shapiro, L. J., & Lieberman, D. E. (2007). Fetal load and the evolution of lumbar lordosis in bipedal hominins. *Nature*, *450*, 1075–1077. https://doi.org/10.1038/nature06342

Zilhão, J. (2006). Neandertals and moderns mixed, and it matters. *Evolutionary Anthropology*, *15*(5), 183–195. https://doi.org/10.1002/evan.20110

Zilhão, J., Angelucci, D. E., Badal-García, E., D'Errico, F., Daniel, F., Dayet, L., Douka, K., Higham, T. F. G., Martínez-Sánchez, M. J., Montes-Bernárdez, R., Murcia-Mascarós, S., Pérez-Sirvent, C., Roldán-García, C., Vanhaeren, M., Villaverde, V., Wood, R., & Zapata, J. (2010). Symbolic use of marine shells and mineral pigments by Iberian Neandertals. *Proceedings of the National Academy of Sciences of the United States of America*, *107*(3), 1023–1028. https://doi.org/10.1073/pnas.0914088107

Chapter 3: The Crural Index

Introduction

The crural index (CI), defined as the ratio of tibial length to femoral length, is a widely used metric in anthropology for assessing limb proportions in hominin evolution (e.g., Trinkaus, 1981; Holliday, 1997). It has been applied to investigate thermoregulatory adaptations, biomechanical efficacy, and morphological variation among past and present human populations (e.g. Higgins & Ruff, 2011; Holliday, 1997, 1999; Holliday & Ruff, 2001; Trinkaus, 1981, 2005, 2007, 2011). CI is particularly relevant to Bergmann's and Allen's rules, which associate body proportions with climatic adaptations (Bergmann, 1847, as cited in Ruff, 1994; Allen, 1877). Cold-adapted populations typically have shorter distal limb segments, resulting in a lower CI that reflects relatively short tibiae compared to femora.

Although CI trends align with ecogeographic expectations, some inconsistencies remain, particularly in populations adapted to rugged terrain where limb proportions may reflect biomechanical demands rather than thermoregulation alone. This raises the possibility that CI could also serve as a functional index for locomotor adaptation. The sections that follow evaluate CI in Neandertals considering both hypotheses: thermoregulatory adaptation and locomotor efficacy.

Neandertals consistently exhibit lower CI values than modern humans (e.g., Holliday, 1997, 1999; Holliday & Ruff, 2001; Trinkaus, 1981, 2005, 2007), a pattern that has traditionally been interpreted as an adaptation to cold climates. This chapter builds on that established pattern to ask whether these limb proportions may also reflect biomechanical adaptations to rugged terrain, where shorter distal limbs could enhance stability or reduce energy costs during locomotion on slopes (Gruss, 2007; Higgins & Ruff, 2011).

Modern humans occupy a much broader ecogeographical range, including both cold and mountainous environments, defined here as regions with elevation changes, including high-altitude plateaus and steep, uneven terrain, which can influence locomotor demands (Gruss, 2007; Higgins & Ruff, 2011). This ecological breadth enables meaningful comparison: by analyzing whether Neandertal CI values overlap with those of modern populations in similar climates or terrain types, we can gain insight into whether thermoregulation, locomotion, or both better explain their morphology.

Yet, interpreting CI patterns is complicated by methodological inconsistencies. Higgins & Ruff, 2011 emphasizes the importance of standardized measurement techniques, as differences in anatomical landmarks or measurement tools can affect CI values. These inconsistencies have led to conflicting conclusions about how Neandertals differ from anatomically modern humans. A more detailed assessment of how measurement technique influences CI values— particularly when using external versus internal (skeletal) landmarks— is presented in Chapter 5. Nevertheless, studies by (Porter, 1999a, 1999b) and (Minetti, 1993; Minetti et al., 2006) demonstrate that CI plays a role in locomotor efficacy and energy expenditure, reinforcing its relevance as a tool for interpreting hominin adaptation. Neandertals consistently exhibit lower CI values than modern humans, a characteristic linked to cold-climate adaptation. Their shortened tibiae relative to femora have been posited to reflect a physiological response to glacial environments, minimizing heat loss while maintaining biomechanical efficacy (Holliday, 1997, 1999; Holliday & Ruff, 2001). In contrast, modern human populations demonstrate a broader range of CI values.

Despite its utility, assessing Neandertal CI presents several methodological challenges. Although prior research has proposed small sex-based differences in crural index, the dataset

used in this analysis does not include sex-specific femoral and tibial lengths. Sylvester et al. (2008) provide separate allometry coefficients for males and females, but do not report average bone lengths by sex, preventing direct calculation of sex-based CI differences. Earlier research suggests that any sex-based differences in CI are likely small and not biologically meaningful most comparative contexts (Trinkaus, 1981; Auerbach, 2007). However, applying sex-based comparisons to Neandertal fossils is problematic: skeletal remains are often fragmentary and lack sufficient morphological or contextual data for reliable sex estimation. This complicates efforts to categorize individuals and compare limb proportions meaningfully across populations (Trinkaus, 2007). Further, the broad variation in CI among modern humans— shaped by genetic, developmental, and environmental factors— complicates direct comparisons with Neandertals (Higgins & Ruff, 2011; Kramer & Sylvester, 2023). Discrepancies in how femoral and tibial lengths are measured also affect CI values; some studies (summarized in (Higgins & Ruff, 2011)) rely on maximum bone lengths, while others use specific anatomical landmarks, affecting comparability (Higgins & Ruff, 2011).

In this study, I compare CI variation between Neandertals and modern human populational averages to evaluate differences in limb proportions and their potential evolutionary significance. Further, I examine the implications of CI for mass distribution and locomotion, particularly in the context of Neandertal mobility and biomechanical adaptations. By addressing these objectives, this study contributes to existing knowledge on hominin limb morphology by refining methodological consistency in assessing CI. This research expands on prior findings (Higgins & Ruff, 2011; Sylvester et al., 2008) by incorporating additional datasets and refining comparative frameworks.

Materials and Methods

The goal of this chapter is to assess whether meaningful differences in CI exist between Neandertals and modern human populational averages and to elucidate the evolutionary and environmental implications of these differences. This approach involved a meta-analysis of published measurement data, supplemented by original calculations and quantitative analyses. Given the challenges of sex estimation in Neandertals and supported by prior findings from Kramer (2012) and the Goldman dataset (Auerbach & Ruff, 2004, 2006; Auerbach, n.d.), individuals were not categorized by sex. Instead of dividing the human sample by sex, modern human data were population averages that include all individual Neandertal specimens were treated as individual data points, a Neandertal population average was calculated, and both were compared against the human population averages to avoid classification bias.

The central variables of interest in this analysis include tibial length, femoral length, and the CI, previously defined as the ratio of tibial length to femoral length (Davenport, 1933). These measurements serve as proxies for evaluating limb proportion variation across groups and their potential relevance to thermoregulation and locomotion. Stature is also considered as a contextual variable in this analysis, particularly for Neandertal individuals, where estimated stature values complement CI data by providing a broader picture of body size. Although not directly compared across populations in this chapter, stature is relevant to understanding the relationship between limb segment proportions, overall size, and ecological adaptation (Carretero et al., 2012; Feldesman et al., 1990; Trotter & Gleser, 1958), and I will use stature in Chapter 4. Some studies (Kramer, 2008, 2012) suggest a modest positive relationship between total leg length and CI (i.e., longer-legged populations may exhibit higher CIs), though this relationship is not universal or strictly linear (Holliday & Ruff, 2001; Kramer, 2012). In some cases, such as

with skeletal remains like those of Neandertals, total leg length is not possible to obtain, so an effective lower limb length (tibial + femoral length) is used as a proxy (Kramer 2012) to relate limb length and CI across populations.

I estimated modern human population average statures using the Trotter and Gleser equations, which predict stature from long bone lengths, based on reported population average femoral lengths. For this study, I used the combined femur + tibia formula: Stature = 1.26 × (Femur + Tibia) + 67.09 (Trotter & Gleser, 1958) Average effective leg length was calculated by summing femoral and tibial lengths for each specimen, following the approach described in Kramer (2012).

CI values for Neandertals and modern humans were compared descriptively to evaluate general trends in limb proportions. Modern human population data (from Sylvester et al., 2008) were treated as discrete population averages for comparative purposes. While this approach does not follow classical parametric testing based on individual-level data, it allows for a broad descriptive comparison between Neandertal and modern populations. While modern humans are represented by population-level averages, Neandertals were treated as individual data points due to the limited sample size. This asymmetrical comparison introduces interpretive limitations. While population averages smooth out individual variation in modern humans, each Neandertal specimen is represented as a single data point, potentially exaggerating perceived differences or underrepresenting Neandertal variability. This approach is best suited for identifying broad group-level patterns rather than making fine-grained statistical comparisons between individuals. I also calculate a Neandertal population average.

Neandertal Data

Limb measurements for Neandertals were compiled from established datasets and primary sources (Trinkaus, 1981, 1983 Carretero et al., 2012; Feldesman et al., 1990). These datasets provided femoral and tibial lengths, estimated statures, and CIs, supplemented by new calculations. Measurements were aggregated into a master dataset (Table 1) for comparative analyses. Table 1 presents the full dataset of Neandertal lower limb measurements compiled from published sources. This includes femoral and tibial lengths, CI values, and related estimates across all available Neandertal fossils, including those ultimately excluded from the final comparative analysis due to their fragmentary nature.

Stature values for 18 Neandertal fossils were compiled from Carretero et al. (2012) and Feldesman et al. (1990), both of whom applied regression equations based on modern human data, including the Trotter and Gleser (1958) formulas. Although CI is the primary focus of this study, stature is included here as a contextual variable that reflects overall body size and complements interpretations of limb proportion. These estimates were derived from various long bones, including humeri, radii, ulnae, and femora (Tables 2 and 3). Table 2 presents stature estimates reported by Carretero et al. (2012), while Table 3 includes estimates from Feldesman et al. (1990) based on both femur length and the Trotter and Gleser method. For fossils with multiple estimates from different elements, I averaged the values. For instance, Kebara 2 had reported statures of 168.7 cm (humerus), 171.5 cm (radius), and 175.9 cm (ulna), yielding an average of 172.0 cm.

Trunk lengths, which are needed for the next chapter, are derived for Neandertals with reconstructed complete lower limb measurements, meaning both femoral and tibial lengths were available, regardless of whether minor reconstruction was necessary, using the formula:

$TL = S - (MH + TL_{tibia} + FL_{femur})$,

where S represents stature, MH is malleolar height (the vertical distance from the ground to the lateral malleolus of the fibula and is a proxy for the location of the ankle joint), TL_{tibia} is tibial length, and FL_{femur} is femoral length. For consistency, a constant malleolar height of 12.7 cm was assumed (de Leva, 1996)) and applied across all individuals and human populations.

Table 4 summarizes the nine Neandertal specimens with reconstructed complete lower limb measurements that were included in the final comparative dataset. CIs were calculated using the formula:

$$CI = \frac{Tibial\ length}{Femoral\ length}$$

as described by (Davenport, 1933). For example, for the La Chapelle-aux-Saints Neandertal, with a tibial length of 34.0 cm and a femoral length of 43.0 cm, the CI is $\left(\frac{34.0\ cm}{43.0\ cm}\right) = 0.79$.

Averaging overlapping measurements, such as multiple reported lengths for the same bone from different sources or estimates adjusted through reconstruction, mitigated methodological inconsistencies.

Modern Human Data

Reference data for modern human measurements were obtained from a published dataset (Sylvester et al., 2008), which provided skeletal limb segment population averages from groups with variable body size and broad geographical distribution (Table 5). The work emphasized pooled human variation (n=2705) rather than population-specific comparisons. Crural indices were calculated by me based on the femoral and tibial length means in the dataset, as CI values

were not reported in the original publication. These population CI values reflect overall human variability rather than specific ancestral or cultural differences.

Results

The calculation of CIs revealed distinct patterns between Neandertals and modern human population means. Modern human populational average CIs (mean CI = 0.821, SD = 0.020, range: 0.773 to 0.849, N=21) appear to be different from individual Neandertal values (mean CI of 0.783, SD = 0.023, range: 0.748 to 0.817, n=9). These values were used to generate a comparative scatterplot (Figure 5) displaying CI relative to total leg length for Neandertal individuals and modern human populations means.

The cold adapted modern human populations (Arctic Native Americans, Inuit, and Sami (CIs: 0.77–0.80)) overlap with the Neandertal population mean and most of the individual Neandertal CI values, supporting the hypothesis that Neandertal limb proportions may reflect cold adaptation consistent with Allen's rule. This overlap is summarized in Table 6, which compares CI values for Neandertals and Arctic-adapted modern human populations. This pattern is also visualized in Figure 4, which illustrates the distribution of CI values and the extent of overlap between the two groups.

One noteworthy exception to the cold adapted relationship with CI is one modern human population average (WWII), which falls below the Neandertal population mean, yet this group is not typically associated with cold adaptation. This highlights that lower CI values may emerge under different ecological or physiological contexts, and not exclusively a thermoregulatory adaptation. The low CI values observed in this group may instead reflect demographic or physiological factors unrelated to climate. The WWII sample consists of male soldiers from a

demographic group with potentially unique nutritional, developmental, and stress-related backgrounds, which could have influenced growth patterns. The sample consisted of American male miliary personnel whose remains were repatriated through the American Graves Registration Service during the United States Repatriation Program (Trotter & Gleser, 1952). These individuals were casualties in the Pacific theater during World War II. Their statures were recorded at induction, and long bone measurements were taken postmortem from clean, dry skeletons after natural decomposition during temporary burial. From an osteological perspective, the tibia and femur fuse between approximately ages 16–20 in males, with the distal tibia beginning to fuse slightly earlier than the proximal tibia and distal femur (Christensen et al., 2019). If growth was disrupted during this critical period, due to factors such as war-time nutrition or early enlistment for example, it is possible that the tibia experienced reduced growth relative to the femur, potentially resulting in a lower crural index. It is also possible that these recruits came from lower socioeconomic situations that had limited childhood nutrition during the great depression when their tibia were growing longer. These speculations illustrate the role of nutritional environment on CI and that it may reflect more than ecogeographic adaptation alone. Future work in limb proportions should consider the importance of developmental biology when interpreting limb proportions.

Discussion

Neandertal individual CI values exhibit a broad range, which may reflect biomechanical adaptations to diverse environments, ranging from cold glacial zones in Western Europe to more temperate and mountainous regions in the Levant, including sloped terrain and rugged habitats (Higgins & Ruff, 2011). This range underscores the interplay of environmental and biomechanical factors in shaping their morphology. The observed overlap in CI values between

Neandertals and cold-adapted modern humans reinforces the role of climatic pressures in shaping limb proportions, consistent with Bergmann's and Allen's rules.

The limb proportions observed in modern humans reflect adaptations for diverse climates and efficient locomotion. Cold-adapted modern populations such as the Inuit and Sami exhibited narrow CI ranges (0.77-0.80), aligning with adaptations to minimize heat loss (Holliday, 1997; Trinkaus, 1981). Neandertals fall well within that range, with a mean CI of 0.783 and range from 0.75- 0.82, as do the WWII population (CI of 0.78) which has no (known) adaptation to cold climates. Unfortunately, no data are available from modern human populations adapted to moving in mountainous environments, although other mountain-adapted mammals do exhibit shorter tibiae relative to femora than their closest lowland counterparts (Higgins & Ruff 2011).

The observed range in Neandertal CI values may, therefore, reflect energetic adaptations to locomotion in sloped or rugged terrain, as suggested by Higgins & Ruff, 2011, in addition to thermoregulatory influences. Beyond cold climates, environmental factors such as topography and childhood nutritional patterns may have influenced Neandertal morphology. These results warrant further exploration of geographical and biomechanical influences on Neandertal adaptations. While some of the regions represented in this analysis were later occupied by *Homo sapiens*, Neandertals experienced these environments over a much longer evolutionary timeframe (e.g., Hublin & Roebroeks, 2009). However, data on contemporaneous *Homo sapiens* from these same regions are limited, making it difficult to assess whether similar CI adaptations also emerged in those populations. This distinction is important, as adaptations—particularly to climate and terrain—are shaped not only by geography, but by the duration and context of occupation (Potts, 1998). The pronounced shift in CI values seen in Neandertals, relative to other

fossil hominins, may therefore reflect long-term pressures unique to populations evolving outside of Africa.

Comparative studies of other mammals support this interpretation. For example, bovids that inhabit mountainous environments consistently exhibit shorter distal limb segments, regardless of climate, mirroring the same pattern seen in Neandertals (Higgins & Ruff, 2011). Similar trends have also been observed in nonhuman primates. Mountain gorillas, which inhabit high-altitude, forested environments in central Africa, display significantly lower crural indices compared to lowland gorillas— approximately 0.797-0.804 in mountain gorillas versus 0.829-0.831 in lowland gorillas— reflecting both thermoregulatory adaptations and biomechanical demands associated with steep, uneven terrain (Ruff et al., 2022; Table S6). In addition, mountain gorillas exhibit more robust lower limb bones with thicker cortical structure, likely due to increased loading during vertical climbing and support-intensive locomotion (Ruff et al., 2018). These combined proportional and structural differences reinforce the idea that environmental topography— independent of phylogenetic lineage— can shape limb morphology through consistent selective pressures. Together, these cross-species comparisons strengthen the hypothesis that Neandertal limb proportions may reflect similar adaptations to long-term movement in rugged landscapes, acting in concert with cold climate pressures.

Limitations and Future Directions

The small sample size of Neandertal fossils limits the statistical power of this study's conclusions. Methodological inconsistencies in measurement techniques across published sources also introduce potential bias. While standard deviations for tibial and femoral lengths were available for modern human populations, individual-level data were not, preventing direct calculation of within-population CI variability.

Future research should prioritize expanding Neandertal datasets through additional fossil discoveries and incorporating advanced imaging technologies like 3D morphometrics. Comparative studies across a wider range of hominin species, including both extinct and extant populations, could provide a broader evolutionary context for interpreting CI variation. These efforts will improve our understanding of the complex relationships among morphology, climate, terrain, and locomotor demands in hominin evolution. New populational datasets, collected ethically with informed consent, from areas with different environmental conditions would greatly facilitate understanding functional morphological adaptation.

Table 1: Neandertal Lower Limb Measurements

Table 3. Neandertal Lower Limb Measurements from Literature Sources

Specimen	Femur (cm)	Tibia (cm)	Stature (cm)	Trunk (cm)	Mass (kg)	CI
Amud 1	24.1	38.6	176.75	79.45	75.3	0.80
Kebara 2	-	-	172.03	-	75.6	-
Kiik-Koba 1	-	34.6	161.20	-	78.1	-
La Chapelle 1	43	34	168.05	73.5	77.3	0.79
La Ferrassie 1	45.8	37	172.28	76.15	85	0.81
La Ferrassie 2	40.9	30.6	170.63	79.45	67	0.75
La Quina 5	-	-	164.55	-	71.2	-
Lezetxiki	-	-	167.30	-	73.9	-
Neanderthal 1	44.05	-	165.73	-	78.9	-
Regourdou 1	-	-	162.30	-	72.1	-
Shanidar 1	45.95	35.5	171.14	77.65	80.5	0.78
Shanidar 2	-	32.5	154.30	-	75.2	-
Shanidar 3	-	-	-	-	79.9	-
Shanidar 4	42.2	-	162.65	-	72	-
Shanidar 5	44.7	36.5	164.95	74.4	68.5	0.82
Shanidar 6	38.4	30	-	-	59.4	0.78
Sidron	-	-	164.75	-	-	-
Spy 2	42.425	32.05	159.90	72.725	83.6	0.76
Tabun 1	41.3	31.7	154.30	77.65	63.2	0.77

Table 1: Femoral and tibial lengths, crural indices (CI), and related estimates compiled from published sources including Trinkaus (1981), Carretero et al. (2012), and Feldesman et al. (1990). This table includes all available Neandertal fossils evaluated in this study, including those not used in the final comparative analysis.

Table 2: Stature Estimates from Carretero et al (2012)

Table 3: Stature Estimates from Carretero et al. (2012)

Specimen	Humerus (cm)	Radius (cm)	Ulna (cm)	Femur (cm)	Tibia (cm)	Average Stature (cm)
Kebara 2	168.7	171.5	175.9	-	-	172.03
La Chapelle	163.6	-	-	-	-	163.60
Neandertal 1	164.5	165.5	-	165.8	-	165.27
Lezetxiki	167.3	-	-	-	-	167.30
Regourdou 1	162.2	162.4	-	-	-	162.30
Shanidar 1	-	168.6	172.5	170.8	-	170.63
Shanidar 2	-	-	-	-	154.3	154.30
Shanidar 4	-	164.7	164.4	-	-	164.55
Shanidar 5	-	-	161.6	-	-	161.60
La Ferrassie 1	-	-	172.9	-	-	172.90
Sidron	-	-	167.2	-	-	167.20
Amud 1	-	-	-	176.75	-	176.75
Spy 2	-	-	-	161	156.2	158.60
Kiik-Koba 1	-	-	-	-	161.2	161.20
Sidron	159.9	-	-	-	-	159.90
La Ferrassie 2	151.1	150.3	149.6	157.2	146.4	150.92
Tabun 1	151.6	158.6	158.9	158.6	151	155.74
La Quina 5	-	-	158.9	-	-	158.90

Table 2**:** Stature estimates from Carretero et al. (2012). Estimated statures for 18 Neandertal fossils, derived from various long bones using population-specific regression equations. These values were used in this study as part of stature reconstruction.

Table 3: Stature Estimates from Feldesman et al. (1990)

Table 3: Stature Estimates from Feldesman et al. 1990

Specimen	Femur Stature (cm)	Trotter-Gleser (cm)	Average Stature (cm)
La Chapelle 1	161.1	165.3	163.2
La Ferrassie 1 R	171.5	171.8	171.65
Neanderthal 1	164.8	167.6	166.2
Spy 2	158.6	163.8	161.2
Amud 1	180.5	177.4	178.95
Shanidar 1	171.5	171.8	171.65
Shanidar 4	158.1	163.4	160.75
Shanidar 5	167.4	169.2	168.3
La Ferrassie 2	152.4	157.9	155.15
Shanidar 6	143.8	152.6	148.2
Tabun C1	153.6	158.6	156.1

Table 3: Stature Estimates from Feldesman et al. 1990. Stature estimates for Neandertal fossils based on femur length and the Trotter and Gleser method. These values were averaged and incorporated into this study's stature estimates.

Table 4: Neandertal Crural Indices and Lower Limb Measurements

Table 4. Neandertal Crural Indices and Lower Limb Measurements

Specimen	Femur (cm)	Tibia (cm)	Stature (cm)	Trunk (cm)	Leg Length (mm)	Mass (kg)	CI
Amud 1	48.2	38.6	176.75	79.45	434.2	75.3	0.80
La Chapelle 1	43	34	168.05	73.5	383	77.3	0.79
La Ferrassie 1	45.8	37	172.28	76.15	415.8	85	0.81
La Ferrassie 2	40.9	30.6	170.63	79.45	346.9	67	0.75
Shanidar 1	45.95	35.5	171.14	77.65	400.95	80.5	0.78
Shanidar 5	44.7	36.5	164.95	74.4	409.7	68.5	0.82
Shanidar 6	38.4	30	148.20	67.1	338.4	59.4	0.78
Spy 2	42.425	32.05	159.90	72.73	362.93	83.6	0.76
Tabun 1	41.3	31.7	154.30	77.65	358.3	63.2	0.77
Mean	43.41	33.99	165.13	75.34	383.35	73.3	0.78
SD	2.86	2.89	8.77	3.71	31.69	8.65	0.02

Table 4: Neandertal Crural Indices and Lower Limb Measurements. Femoral and tibial lengths, stature, trunk length, leg length, body mass estimates, and crural indices (CI) for nine Neandertal specimens with reconstructed complete lower limbs used in the final comparative dataset.

Table 5: Modern Human Lower Limb Measurements, Stature, and CI

Table 5: Modern Human Lower Limb Measurements, Stature, and CI

Population	Femur		Tibia		Leg Length	Stature	Crural Index
	Mean (mm)	SD	Mean (mm)	SD	(mm)	(cm)	
Pooled	448.03	35.02	364.90	31.30	812.93	169.52	0.81
African American	467.42	27.94	383.31	25.35	850.73	174.28	0.82
Andaman	385.03	17.24	323.19	14.05	708.22	156.33	0.84
Anglo-Saxon	450.39	27.37	367.73	25.63	818.12	170.17	0.82
Arctic Native American *	416.14	24.43	334.69	23.67	750.83	161.69	0.80
Arikara	434.55	24.27	367.47	23.52	802.02	168.14	0.85
Bosnian	474.12	24.93	392.99	22.58	867.11	176.35	0.83
Cobb	456.54	30.16	381.30	27.52	837.84	172.66	0.84
Egyptian	437.27	23.29	367.20	23.69	804.47	168.45	0.84
Forensic	460.80	30.79	381.64	28.89	842.44	173.24	0.83
Inuit *	420.88	28.38	331.23	25.12	752.11	161.86	0.79
Khoesan	415.50	23.51	345.74	21.93	761.24	163.01	0.83
Mokapu	420.12	23.66	344.84	21.13	764.96	163.47	0.82
Northern Chinese	439.39	18.07	362.16	15.51	801.55	168.09	0.82
Poundbury	432.82	24.72	356.06	25.77	788.88	166.49	0.82
Pygmy	379.83	21.51	322.46	21.68	702.29	155.58	0.85
Sami *	400.49	25.43	309.60	21.84	710.09	156.56	0.77
Southern Chinese	431.92	23.32	355.46	21.40	787.38	166.30	0.82
Spitalfields	421.20	29.96	344.60	26.37	765.80	163.58	0.82
WWII	472.02	23.48	367.87	21.15	839.89	172.92	0.78
Zulu	441.20	27.10	368.07	27.84	809.27	169.06	0.83

Table 5: Modern Human Long Bone Measurements and Crural Indices. Mean and standard deviation of femur and tibia lengths, leg length, and calculated crural indices for 20 modern human populations, compiled from Sylvester, Kramer, and Jungers (2008). Populations marked with an asterisk (*) are considered cold-adapted. A pooled human sample is included.

Table 6: Crural Index of Neandertals and Arctic Region Modern Humans

Table 6: Crural Index of Neandertals and Arctic Region Modern Humans

Specimen	CI	Population	CI
Amud 1	0.80	Arctic Native American	0.80
La Chapelle 1	0.79	Inuit	0.79
La Ferrassie 1	0.81	Sami	0.77
La Ferrassie 2	0.75		
Shanidar 1	0.78		
Shanidar 5	0.82		
Shanidar 6	0.78		
Spy 2	0.76		
Tabun 1	0.77		

Table 6: Comparison of Crural Indices Between Neandertals and Arctic-Adapted Modern Human Populations. CI values for nine Neandertal specimens compared to Arctic-adapted modern human populations (Arctic Native Americans, Inuit, Sami). Highlights the extent of overlap in CI and possible cold-adaptive convergence.

Figure 4: Box Plot Comparing Crural Indices of Neandertals and Arctic-Adapted Modern Humans

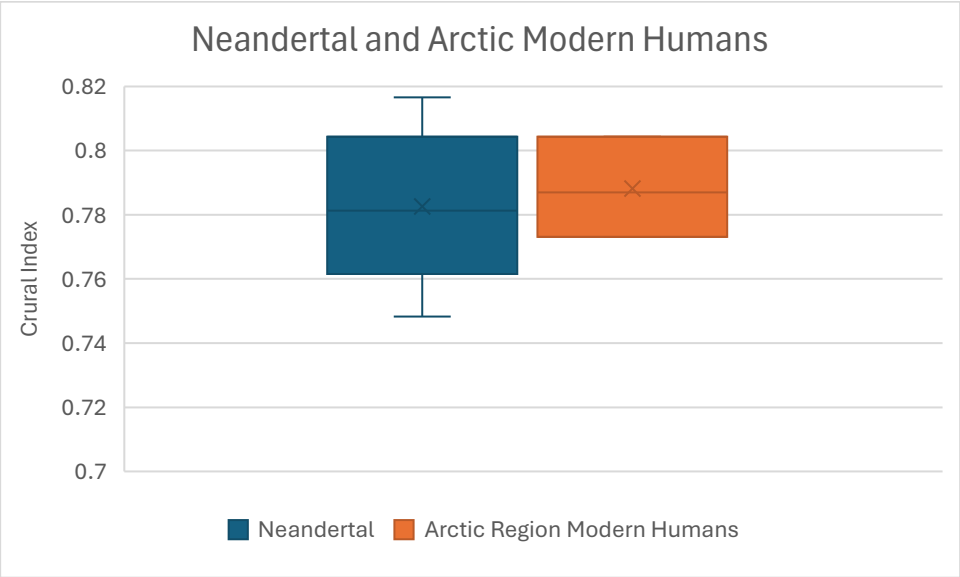

Figure 4: Box Plot Comparing Crural Indices of Neandertals and Arctic-Adapted Modern Humans. Box plot illustrating CI distributions in nine Neandertal specimens and Arctic-adapted modern human populations (Arctic Native Americans, Inuit, Sami). Highlights overlap and variability, with implications for cold-climate adaptation.

Figure 5: Scatterplot of CI vs Leg Length

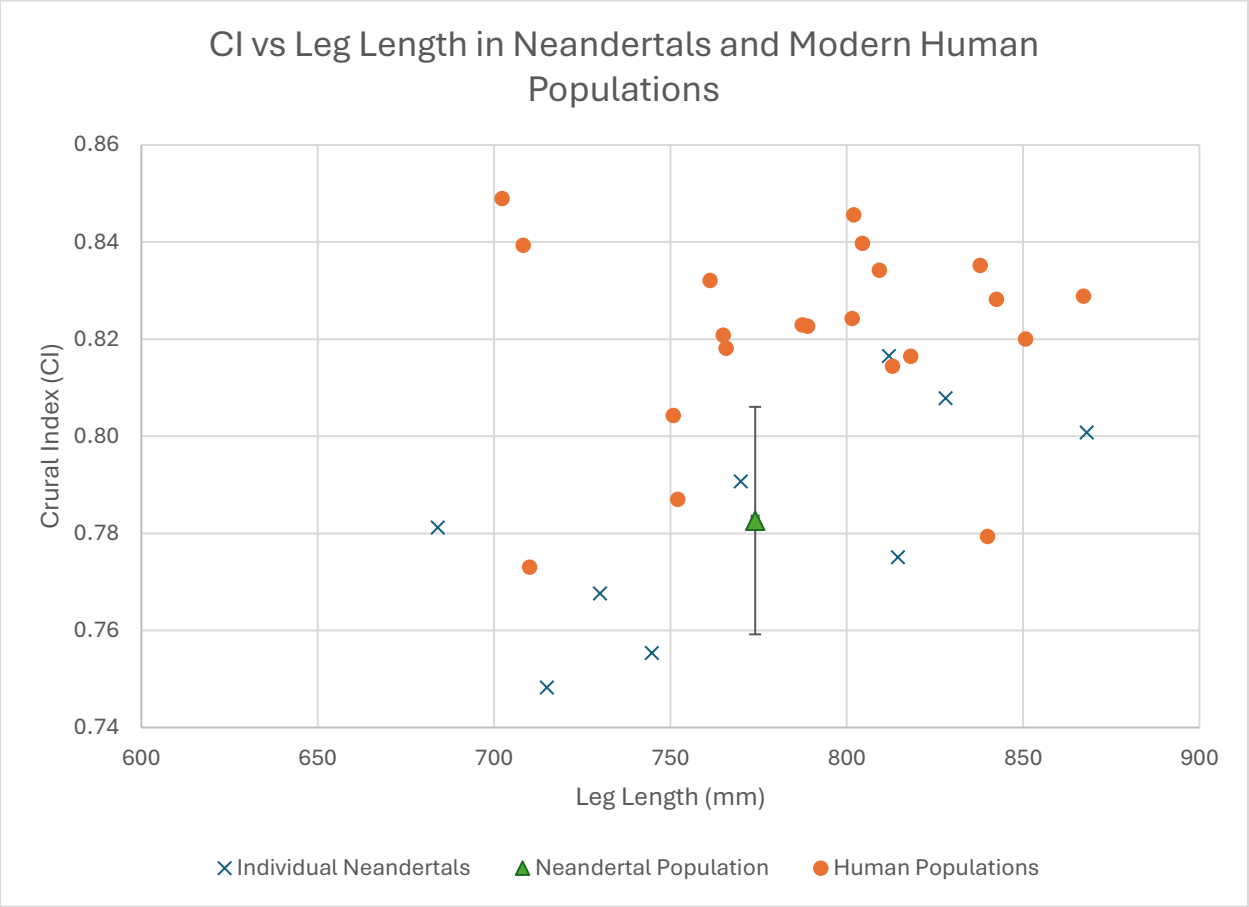

Figure 5: Scatterplot of CI vs. leg length (femur + tibia) for Neandertals (individuals), modern human population means, and the Neandertal population mean. Error bars reflect ±1 standard deviation for CI and leg length. Visualizes variability and overlap relevant to environmental and biomechanical adaptation.

REFERENCES

Allen, J. A. (1877). The influence of physical conditions in the genesis of species. *Radical Review*, 1, 108–140.

Auerbach BM, & Ruff CB. 2004. Human body mass estimation: a comparison of "morphometric" and "mechanical" methods. American Journal of Physical Anthropology 125:331-342.

Auerbach, B. M., & Ruff, C. B. (2006). Limb bone bilateral asymmetry: Variability and commonality among modern humans. Journal of Human Evolution, 50(2), 203–218.

Auerbach, B. M. (n.d.). *The Goldman Osteometric Data Set.* University of Tennessee. Retrieved November 27, 2024, from https://web.utk.edu/~auerbach/GOLD.htm

Carretero, J. M., Rodríguez, L., García-González, R., Arsuaga, J. L., Gómez-Olivencia, A., Lorenzo, C., Bonmatí, A., Gracia, A., Martínez, I., & Quam, R. (2012). Stature estimation from complete long bones in the Middle Pleistocene humans from the Sima de los Huesos, Sierra de Atapuerca (Spain). *Journal of Human Evolution*, *62*(2), 242–255. https://doi.org/10.1016/j.jhevol.2011.11.004

Christensen, A. M., Passalacqua, N. V., & Bartelink, E. J. (2019). *Forensic anthropology: Current methods and practice* (2nd ed.). Academic Press.

Davenport, C. B. (1933). The Crural Index. *American Journal of Physical Anthropology*, *17*(8).

de Leva, P. (1996). Adjustments to Zatsiorsky-Seluyanov's segment inertia parameters. *Journal of Biomechanics*, *29*(9), 1223–1230.

Feldesman, M. R., Kleckner, J. G., & Lundy, J. K. (1990). Femur/stature ratio and estimates of stature in mid- and late-pleistocene fossil hominids. *American Journal of Physical Anthropology*, *83*(3), 359–372. https://doi.org/10.1002/ajpa.1330830309

Gruss, L. T. (2007). Limb length and locomotor biomechanics in the genus Homo: An experimental study. *American Journal of Physical Anthropology*, *134*(1), 106–116. https://doi.org/10.1002/ajpa.20642

Higgins, R. W., & Ruff, C. B. (2011). The effects of distal limb segment shortening on locomotor efficiency in sloped terrain: Implications for Neandertal locomotor behavior. *American Journal of Physical Anthropology*, *146*(3), 336–345. https://doi.org/10.1002/ajpa.21575

Holliday, T. W. (1997). Postcranial Evidence of Cold Adaptation in European Neandertals. *American Journal of Physical Anthropology*, *104*, 245–258.

Holliday, T. W. (1999). Brachial and crural indices of European Late Upper Paleolithic and Mesolithic humans. *Journal of Human Evolution*, *36*, 549–566. http://www.idealibrary.com

Holliday, T. W., & Ruff, C. B. (2001). Relative variation in human proximal and distal limb segment lengths. *American Journal of Physical Anthropology*, *116*(1), 26–33. https://doi.org/10.1002/ajpa.1098

Hublin, J.-J., & Roebroeks, W. (2009). *Ebb and flow or regional extinctions? On the character of Neandertal occupation of northern environments.* Comptes Rendus Palevol, 8(5), 503–509. https://doi.org/10.1016/j.crpv.2009.04.001

Kramer, P.A., Sarton-Miller, I. (2008). The energetics of human walking: is Froude number (*Fr)* useful for metabolic comparisons? *Gait & Posture*, 27, (209-2015). 10.1016/j.gaitpost.2007.03.009

Kramer, P.A. (2012). Brief Communication: Could Kadanuumuu (KSD-VP-1/1) and Lucy (AL 288-1) Have Walked Together Comfortably? *American Journal of Physical Anthropology*, 149, 616-621. 10.1002/ajpa.22169

Kramer, P. A., & Sylvester, A. D. (2023). Hip width and metabolic energy expenditure of abductor muscles. *PLoS ONE*, *18*(4). https://doi.org/10.1371/journal.pone.0284450

Minetti, A. E. (1993). MECHANICAL DETERMINANTS OF GRADIENT WALKING ENERGETICS IN MAN BY. *Journal of Physiology*, *471*, 725–735.

Minetti, A. E., Formenti, F., & Ardigò, L. P. (2006). Himalayan porter's specialization: Metabolic power, economy, efficiency and skill. *Proceedings of the Royal Society B: Biological Sciences*, *273*(1602), 2791–2797. https://doi.org/10.1098/rspb.2006.3653

Ocobock, C., Lacy, S., & Niclou, A. (2021). Between a Rock and a Cold Place: Neanderthal Biocultural Cold Adaptations. *Evolutionary Anthropology*, 1–18. https://doi.org/10.1002/evan.21894

Porter, A. M. W. (1999a). Modern human, early modern human and Neanderthal limb proportions. *International Journal of Osteoarchaeology*, *9*(1), 54–67. https://doi.org/10.1002/(SICI)1099-1212(199901/02)9:1<54::AID-OA459>3.0.CO;2-R

Porter, A. M. W. (1999b). The prediction of physique from the skeleton. *International Journal of Osteoarchaeology*, *9*(2), 102–115. https://doi.org/10.1002/(SICI)1099-1212(199903/04)9:2<102::AID-OA460>3.0.CO;2-2

Potts, R. (1998). *Environmental Hypotheses of Hominin Evolution.* Yearbook of Physical Anthropology, 41, 93–136.

Ruff, C. B., Burgess, M. L., Junno, J.-A., Mudakikwa, A., Zollikofer, C. P. E., Ponce de Leon, M. S., & McFarlin, S. C. (2018). Phylogenetic and environmental effects on limb bone structure in gorillas. *American Journal of Physical Anthropology*, 166, 353–372. https://doi.org/10.1002/ajpa.23457

Ruff, C. B., Junno, J.-A., Burgess, M. L., Canington, S. L., Harper, C., Mudakikwa, A., & McFarlin, S. C. (2022). Body proportions and environmental adaptation in gorillas. *American Journal of Biological Anthropology*, 177, 501–529. https://doi.org/10.1002/ajpa.24628

Sylvester, A. D., Kramer, P. A., & Jungers, W. L. (2008). Modern humans are not (quite) isometric. *American Journal of Physical Anthropology*, *137*(4), 371–383. https://doi.org/10.1002/ajpa.20880

Trinkaus, E. (1981). Neanderthal limb proportions and cold adaptation. *Aspects of Human Evolution*, *February*, 187–224. http://ci.nii.ac.jp/naid/10018145328/

Trinkaus, E., 1983. The Shanidar Neandertals. Academic Press, New York.

Trinkaus, E. (2005). Early Modern Humans. *Annual Review of Anthropology*, *34*, 207–230. https://doi.org/10.1146/annurev.anthro.34.030905.154913

Trinkaus, E. (2007). European early modern humans and the fate of the Neandertals. *PNAS*, *104*(18), 7367–7372. www.pnas.orgcgidoi10.1073pnas.0702214104

Trinkaus, E. (2011). The Postcranial Dimensions of the La Chapelle-aux-Saints 1 Neandertal. *American Journal of Physical Anthropology*, *145*, 461–468. https://doi.org/10.1002/ajpa.21528

Trotter, M., & Gleser, G.C. (1952). Estimation of stature from long bones of American Whites and Negroes. *American Journal of Physical Anthropology, 10*(4), 463-514. https://doi.org/10.1002/ajpa.1330100407

Trotter, M., & Gleser, G. C. (1958). A RE-EVALUATION OF ESTIMATION OF STATURE BASED ON MEASUREMENTS OF STATURE TAKEN DURING LIFE AND OF LONG BONES AFTER DEATH. *American Journal of Physical Anthropology*, *16*(1), 79–123.

Weaver, T. D. (2009). The meaning of Neandertal skeletal morphology. *PNAS*, *106*(38), 16028–16033. www.pnas.orgcgidoi10.1073pnas.0903864106

Weaver, T. D., Coqueugniot, H., Golovanova, L. V, Doronichev, V. B., Maureille, B., & Hublin, J.-J. (2016). Neonatal postcrania from Mezmaiskaya, Russia, and Le Moustier, France, and the development of Neandertal body form. *PNAS*, *113*(23), 6472–6477. https://doi.org/10.1073/pnas.1523677113

Weaver, T. D., & Steudel-Numbers, K. (2005). Does Climate or Mobility Explain the Differences in Body Proportions Between Neandertals and Their Upper Paleolithic Successors? *Evolutionary Anthropology*, *14*, 218–223. https://doi.org/10.1002/evan.20069

Chapter 4 – Mass Distribution and Center of Mass in Neandertals and Modern Humans

Introduction

The center of mass (CoM) is a critical component of hominin biomechanics because it influences balance, posture, and locomotor efficiency—especially in bipedal organisms. In bipeds, the position of the CoM affects how forces are distributed across the body during movement, and it plays a central role in maintaining stability and minimizing energetic costs on varied terrains. The CoM can be determined mathematically through analysis of the individual body segments (e.g., thigh, calf, trunk), based on their mass and dimensions. Segment-specific differences in mass and length affect the mechanical demands placed on the musculoskeletal system, particularly during gait and balance recovery (Franz & Kram, 2012; Hamner & Delp, 2013). In bipeds, the CoM typically lies just anterior to the sacrum, though its position varies depending on segment mass distribution and limb proportions (Chou et al., 2001; de Leva, 1996). In modern humans, these parameters have been extensively studied, but their application to extinct hominins—particularly Neandertals—remains underdeveloped.

Neandertals exhibit distinct postcranial morphology relative to modern humans, including reduced crural indices, shorter distal limbs, a wide pelvis, and a barrel-shaped thorax (Gómez-Olivencia et al., 2009; Sylvester et al., 2008; Trinkaus, 1981). Vertebral morphology suggests reduced lumbar lordosis, possibly indicating a more kyphotic or straighter spinal column (Been et al., 2012; Been & Kalichman, 2014; Gómez-Olivencia et al., 2013). These structural differences likely alter trunk mass distribution and shift the CoM position relative to that of modern humans. Modern human lumbar lordosis helps align the upper body mass over the hips, improving stability and reducing energetic demands during bipedal locomotion (Whitcome et al.,

2007). A reduction in lumbar curvature could increase the energetic cost of balance and forward propulsion in Neandertals.

While previous studies have modeled Neandertal posture and gait (e.g., Been et al., 2014; Gómez-Olivencia et al., 2017; Trinkaus, 2011), few have directly examined how differences in segment proportions and spinal curvature affect whole-body CoM positioning. Kramer and Eck (2000) provided foundational models for understanding Neandertal biomechanics and acknowledged the inherent limitations of relying on modern human data for soft tissue and mass distribution estimates. Many comparative studies continue to face these challenges, as reconstructions are constrained by incomplete fossil evidence and assumptions that may not fully capture Neandertal movement dynamics (Haeusler et al., 2019). These issues underscore the need for approaches that can better approximate Neandertal CoM and mass distribution using species-specific morphology.

In this chapter, I investigate whether differences in mass distribution between Neandertals and modern humans result in shifts in CoM, both in static posture and on inclined surfaces. Building on the dimensional data presented in the previous chapter, this analysis applies De Leva's (1996) segment parameter values to both groups. Comparisons will assess whether these CoM differences could have influenced locomotor stability and energetic cost, particularly in the context of sloped terrain. This approach provides a biomechanical foundation for interpreting Neandertal movement and sets the stage for future virtual modeling of hominin locomotor behavior.

Theoretical Framework

This analysis is grounded in three interrelated biomechanical assumptions regarding mass distribution and its influence on force distribution, stability, and energy expenditure. These assumptions are derived from prior research on locomotion, posture, and anatomical variation in both modern humans and extinct hominins.

Assumption 1: Mass distribution affects force application.

Variations in body segment proportions shift the way forces are distributed during standing and movement. For example, an increase in proximal limb mass or trunk mass alters mechanical loading on the pelvis and lower limbs, influencing joint stress and postural control (Chou et al., 2001; Franz & Kram, 2012). In neandertals, reduced crural indices and a broader thorax suggest difference in segmental mass that may affect force transmission during locomotion.

Assumption 2: Mass influences stability

More superiorly located CoMs reduce stability in environments that introduce instability such as rugged terrain or incline compared to more inferiorly located CoMs. Stability is partially determined by the body's ability to maintain its CoM within the base of support (i.e., the area between the soles of the feet and the substrate) (Winter, 1995; Granata & Lockhart, 2008). Neandertals' more anteriorly displaced trunk mass, paired with shorter distal limbs, may alter this balance relationship (Hamner & Delp, 2013; Higgins & Ruff, 2011).

Assumption 3: Center of mass position affects energetic cost.

A more superior or anterior located CoM requires greater muscular effort to maintain balance because the body must counteract a larger sagittal plane rotational moment to prevent the CoM

from moving beyond the base of support, particularly when moving or carrying loads (Buurke et al., 2023; Whitcome et al., 2007). This increase occurs because anterior displacement of the trunk requires compensatory posterior muscle forces (e.g. gluteus maximus) to stabilize the body (Zajac et al., 2003; Wall-Scheffler et al., 2010). Muscles use metabolic energy to generate and maintain force, especially under conditions that require sustained posture or movement against gravitational or external loads (Zajac et al., 2002; Kramer et al., 2023; Vidal-Cordasco et al., 2017) Neandertals, with differences in spinal curvature and limb proportions, may have experienced different energetic demands than modern humans.

Of note is that these assumptions have only been evaluate for standing or walking on level surfaces. Moderate incline walking potentially disrupts the geometric relationships, altering the location of the base of support and the segments.

Nonetheless, these assumptions suggest that mass distribution plays a critical role in shaping the biomechanical and energetic consequences of posture and movement. The following sections assess whether these theoretical expectations are borne out by comparisons of modern humans and neandertals using modeled CoM Data.

Comparative Analysis: Neandertals vs. Modern Humans in Standing Posture

This section documents the evaluation of the center of mass (CoM) differences between Neandertals and modern humans in a static standing posture, using segmental mass estimates and limb proportion data derived from previous chapters. The analysis examines whether differences in crural index and trunk morphology result in meaningful shifts in whole-body CoM location, and whether those shifts could have biomechanical or energetic consequences.

CoM estimates were calculated using the methodology outlined by De Leva (1996), which assigns relative mass and CoM location to each body segment based on modern human anatomical data. This method was applied to modern human population average data from Sylvester et al. (2018), as well as to Neandertal reconstructions using average segment lengths and mass assumptions informed by fossil measurements and previous work (Carretero et al., 2012; Feldesman et al., 1990; Sylvester et al., 2008; Trinkaus, 1981). Neandertal segment proportions were derived from the same dataset used for crural index analysis, with trunk length and body mass estimated from long bone-based stature reconstructions.

The standing posture analysis models both groups in anatomical position on level ground. For each population, the X and Z coordinates of the CoM were calculated using a spreadsheet-based implementation of the theory of forces and moments equations. Segment masses (derived from De Leva 1996) were weighted and summed to determine the overall body CoM. To improve interpretability, results are reported as both raw values and as a percentage of total body height. These values were then compared between Neandertals and modern human population averages to assess the degree of positional shift.

Locomotion on Inclined Terrain: Impact of Mass Distribution

Neandertal mobility must be understood within the environmental context they inhabited. Paleogeographic and archaeological evidence suggests that Neandertals frequently occupied rugged, sloped, and mountainous regions across Europe and western Asia (Higgins & Ruff, 2011). These topographic conditions introduce additional challenges for locomotion that go beyond the biomechanical demands of level-ground walking. On inclines, both CoM location and mass distribution affect stability, stride efficiency, and the energy required for forward motion (e.g., Hamner & Delp, 2013; Higgins & Ruff, 2011). As slope increases, small

differences in limb proportions and trunk mass may result in disproportionately larger effects on balance and therefore energetic cost.

Previous models of Neandertal locomotion have largely focused on level-ground scenarios and have relied on modern human analogs, potentially underestimating the effects of topography. Higgins (2011) proposed that Neandertals' shortened distal limb segments — reflected in their low crural indices —may have conferred energetic advantages on sloped terrain. Specifically, shorter tibiae may reduce the moment arm at the knee and ankle, thereby minimizing the muscular effort required to stabilize the limb during uphill locomotion. This would suggest that Neandertal anatomy, while potentially disadvantageous on level ground, may have been well suited to environments with frequent elevation changes.

These terrain-based locomotor challenges are particularly relevant in the context of Neandertal anatomy, which exhibits traits potentially adaptive for rugged environments. (Gruss, 2007) suggests that Neandertal morphology reflects not only climatic adaptation, but also mechanical demands related to variable topography. Similarly, Kramer and Eck (2000) emphasize that limb proportions and segmental mass significantly influence locomotor energetics, especially when navigating slopes. Steudel (1994) further notes that body mass, rather than just limb length, may be the primary determinant of energy expenditure in terrestrial locomotion.

To test these hypotheses, I calculated center of mass coordinates for Neandertals and modern human populations at multiple incline conditions: 0° (flat), 30°, and 45°. These angles approximate common natural terrain gradients encountered in Neandertal habitats. Using body segment parameters and proportional limb data (as described in the following sections), both X (anteroposterior) and Z (vertical) positions of the CoM were calculated for each slope. These

shifts between level and sloped terrain were then assessed to determine how much mass is displaced anteriorly or superiorly during slope walking. If Neandertals show minimized CoM shifts or energetically favorable displacement, this would support the idea that their morphology reflects biomechanical adaptations to complex terrain.

Materials and Methods

This analysis uses De Leva's (1996) segment parameter masses and dimensions to estimate the location of the whole-body center of mass (CoM) for Neandertals and modern humans under various terrain conditions. CoM estimates were calculated using spreadsheet-based models that incorporate segment lengths, segmental mass proportions, and relative CoM locations for each body region. Calculations were conducted in both static (0° incline) and inclined (30° and 45°) standing postures.

Modern human segment parameters were derived from De Leva (1996), who provides normalized mass and CoM locations for 14 body segments based on samples of adult modern human males and females. These segment proportions were applied to population-level long bone data from Sylvester et al. (2008). To estimate stature for each population, the Trotter and Gleser (1958) regression equation was used: Stature = 1.26 x (Femur + Tibia) + 67.09. Body mass was estimated using Ruff's (2023) formula based on femoral head supero-inferior diameter (FHSI): Mass = 2.262 x FHSI – 38.7. These methods were consistent with those used in Chapter 3, which explored variation in crural indices and lower limb proportions across Neandertals and modern humans populations. In that chapter, stature was estimated to contextualize differences in body size and limb segment proportions, which were later applied to this chapter's CoM analysis. Neandertals consistently exhibited lower crural indices, reflecting shorter tibiae relative

to femora compared to modern humans. These limb proportions likely influence trunk length and segment mass distribution, both of which directly affect CoM estimates presented here.

Due to limitations in the availability of femoral head measurements for all skeletal samples in the Sylvester et al (2008). dataset, body mass could only be estimated for five populations: Arikara, Forensic, Poundbury, Southern Chinese, and Spitalfields. These population averages were used in the final CoM modeling for modern humans.

Neandertal segment lengths were reconstructed from fossil long bone measurements using specimens with complete or near-complete lower limbs. The following individuals were included: Amud 1, La Chapelle-aux-Saints 1, La Ferrassie 1, La Ferrassie 2, Shanidar 1, Shanidar 5, Spy 2, and Tabun 1. Stature and body mass estimates were taken from published sources, including Trinkaus (1981), Carretero et al. (2012), and Feldesman et al. (1990). Trunk lengths and shoulder height were calculated by me using long bone-based estimates of total stature and standard anatomical assumptions (e.g., constant malleolar height of 10 cm based on De Leva, 1996).

To calculate CoM in anatomical position, segment coordinates were used to compute the X and Z moment contributions for each body segment. The X-axis represents the anteroposterior (horizontal) direction and the Z-axis the superior-inferior (vertical) direction. These moments were summed and divided by total body mass to determine the full-body CoM location in two dimensions. This process was repeated under simulated incline conditions for 30° and 45°, adjusting segment orientation relative to the slope. To reflect realistic uphill locomotion, trunk angle was modified to simulate the natural forward lean humans use to maintain balance and center of mass while ascending. CoM estimates for Neandertals were calculated across three

slope conditions: flat ground (0°), moderate incline (30°), and steep incline (45°). Eight Neandertal individuals with sufficiently complete lower limb data were included in the analysis.

All calculations were conducted with Microsoft Excel. Specimen-specific spreadsheets were created for each Neandertal individual and for each modern human population with complete data. Each sheet included segment mass estimates, segment CoM position, and the resulting whole-body CoM. Summary tables of calculated CoM coordinates by slope conditions are provided in the Results section. Representative spreadsheets and calculation examples are included in Appendix A (Neandertals) and Appendix B (modern human populations). Figure 6 illustrates the Neandertal model used for these calculations, including limb segment lengths, trunk slope, terrain incline, and step lengths.

Results

On level ground, Neandertals exhibited a mean horizontal CoM (X) of 0.11 m and a vertical CoM (Z) of 1.07 m. As the slope increased, the horizontal CoM shifted anteriorly to 0.21 m at 30° and 0.25 m at 45°, while the vertical CoM showed modest increases to 1.09 m and 1.08 m, respectively. These results are summarized in Table 7.

At 0°, Neandertals' average CoM was located at approximately 64% of body height vertically (Z = 0.638) and 6.4% forward from the baseline (X = 0.064), compared to 68% vertically and 8.8% horizontally in modern humans (Table 8 and Table 10). As slope increased, both groups demonstrated anterior shifts in CoM, but Neandertals consistently maintained lower vertical positions (Z = 0.647 vs. 0.665 at 45°) and slightly smaller horizontal displacements. The normalized differences between groups are presented in Table 12.

CoM estimates for modern humans were calculated using the same three slope conditions. On level ground, modern humans exhibited a mean horizontal CoM (X) of 0.15 m and a vertical CoM (Z) of 1.14 m. At 30° incline, the horizontal CoM shifted anteriorly to 0.21m, with the vertical CoM increasing slightly to 1.13 m. At 45° incline, the horizontal CoM further increased to 0.25 m, and the vertical CoM was 1.11 m. These results are summarized in Table 9.

Preliminary results suggest that while modern humans and neandertals exhibit similar overall CoM positions in standing posture, Neandertals tend to have a slightly lower and more anterior CoM due to their shorter distal limbs and broader trunk mass distribution. However, the magnitude of differences is modest, and the implications for standing balance appear minimal under level-ground conditions. These results support the interpretation that static posture alone may not reveal major functional consequences of Neandertal mass distribution, necessitating further analysis under dynamic or uneven terrain conditions.

The increase in CoM X position with slope reflects the body's forward lean necessary to maintain balance on an incline. The relatively small increase in Z position suggests that vertical displacement of the CoM remains minimal across slope conditions. This limited vertical shift may reduce energetic penalties associated with elevating the body's mass during uphill locomotion. The low variability in CoM X and Z across individuals (standard deviations < 0.05 m) supports the interpretation that these shifts are consistent across the sampled Neandertal population.

When compared to modern humans, Neandertals exhibit consistently lower and more posterior CoM positions across all slope conditions. At 0°, the average Neandertal CoM was located at 0.11 m (X) and 1.07 m (Z), whereas modern humans averaged 0.15 m (X) and 1.14 m (Z). Similar differences were observed at 30° and 45°, with Neandertals showing smaller anterior

shifts and less vertical elevation than their modern counterparts (Table 9). For example, at 45°, the horizontal CoM for Neandertals averaged 0.25 m compared to 0.25 m in modern humans, while vertical CoM values were 1.08 m and 1.11 m, respectively.

Discussion

Although the numerical differences are modest, they may reflect meaningful biomechanical variation. Descriptive statistics summarizing these values for each group are presented in (Table 11). The slightly lower and more centralized CoM in Neandertals could contribute to increased stability, particularly in inclined environments. Conversely, the more elevated CoM in modern humans may impose greater postural demands, potentially requiring more muscular effort to maintain balance. These patterns suggest that Neandertal mass distribution may have conferred advantages in rugged terrain, supporting hypotheses of terrain-adapted locomotor strategies (Gruss, 2007; Higgins & Ruff, 2011). These calculated differences in CoM position between the two groups are presented in (Table 13).

To account for body size, CoM values were also normalized by stature. This approach also ensured methodological consistency when comparing the Neandertal sample—composed of individual reconstructions—with modern human data derived from population-level averages. By converting CoM positions into proportions of total body height, direct comparisons could be made across groups with differing absolute statures while reducing potential bias from size-based variability. When normalized, Neandertals exhibited a lower and more posterior CoM relative to modern humans across all slope conditions. These results, summarized in Table 12, suggest that Neandertals carried their mass relatively lower and more centered within the body, a configuration that may enhance stability and reduce muscular demand on inclined terrain.

The anterior displacement of CoM during incline walking could also carry implications for muscle recruitment and postural control. A more forward-placed CoM may reduce the moment required at the ankle and knee joints, particularly in individuals with shorter distal limb segments. These results align with the idea that Neandertal body proportions represent not just cold-climate adaptations but may also reflect locomotor strategies optimized for variable topography. Further biomechanical modeling and the inclusion of a broader comparative sample will help clarify the functional implications of these CoM shifts.

Conclusion and Future Directions

This chapter explored differences in CoM location between Neandertal and modern humans across three slope conditions, using reconstructed segment parameters and empirical data from fossil and skeletal conditions. Results indicate that Neandertals exhibit a slightly lower and more posterior CoM in static posture, with modest shifts anteriorly and vertically as slope increases. Compared to modern humans, Neandertals showed less vertical CoM elevation and slightly more centralized mass distribution across all slope angles.

These results build on the results of the previous chapter, which demonstrated differences in lower limb proportions between Neandertals and modern humans. The CoM patterns observed here suggest that Neandertal mass distribution may have offered biomechanical advantages in rugged or sloped environments. The reduced CoM elevation with incline could lower the energetic cost of uphill locomotion, while the posterior placement may enhance stability by keeping the CoM closer to the base of support. This interpretation aligns with previous hypotheses that Neandertal morphology reflects not only climatic adaptation but also terrain-specific locomotor strategies. Although the differences observed are modest, they are consistent

and biomechanically meaningful when viewed in the context of Neandertal behavior and landscape use.

This raises an important point about how to interpret these results in light of the two main hypotheses explored in this dissertation— cold climate adaptations versus adaptations to rugged terrain. While the CoM results presented here suggest a potential advantage for locomotion on slopes, it is possible that this pattern could also reflect a secondary effect of cold-adapted limb proportions. However, changes in CI do not necessarily correspond to changes in total leg length or stature; rather, they reflect the proportional relationship between the femur and the tibia, which can shift the body's mass distribution even when overall limb length remains the same. This distinction is key, as it suggests that CoM patterns may be influenced by segment proportions independently of cold-adapted short limbs. Additionally, many Neandertal sites— such as those in Israel and Iraq— do not represent glacial climates, but still present rugged topographies, suggesting terrain may have been a more consistent selective pressure than temperature. While direct CoM data from cold-adapted modern populations like the Inuit or Sami are lacking, the consistent differences presented here that are seen in Neandertal CoM positions across slope conditions —and broader comparative evidence from terrain-adapted mammals (Higgins & Ruff, 2011)— support the interpretation that Neandertal morphology may reflect adaptations to the landscape they evolved in, with cold-adaptive benefits as a possible secondary outcome. This interpretation is further supported by studies of mountain and lowland gorillas, which show that even within a single genus, limb segment proportions differ in relation to environmental topography: mountain gorillas exhibit shorter distal limb segments and more robust bones than their lowland counterparts, consistent with the demands of climbing and navigating steep terrain (Ruff et al., 2018; Ruff et al., 2022).

Future research should incorporate comparative data from a broader range of modern human populations, including highland or terrain-adapted groups. Data from Himalayan porters, for instance, suggest biomechanical adaptations to steep terrain, including lower limb joint power redistribution and efficient posture during incline load carriage (Minetti et al., 2006). Similarly, research on Andean populations has documented morphological variation, such as relatively shorter limbs and larger chest volumes, potentially linked to both high-altitude hypoxia and terrestrial mobility demands (Beall, 2001). These populations provide useful comparative contexts for testing whether similar CoM patterns are associated with environmental and physiological factors. Digital modeling platforms, such as OpenSim or AnyBody, could be used to simulate joint loading and muscle activity across incline conditions, providing a more dynamic assessment of the biomechanical implications of mass distribution. Additionally, integrating pelvic and spinal curvature reconstructions into full-body models may improve estimates of trunk mass and refine whole-body CoM projections.

Ultimately, this study contributes to a growing body of work that seeks to understand extinct hominin locomotion not only through isolated anatomical traits but through holistic biomechanical modeling. By grounding interpretations in functional principles such as balance and energy optimization, we can better reconstruct the lived experience of past hominins and the selective pressures that shaped their anatomy.

Figure 6: Neandertal Model (Hand Drawn)

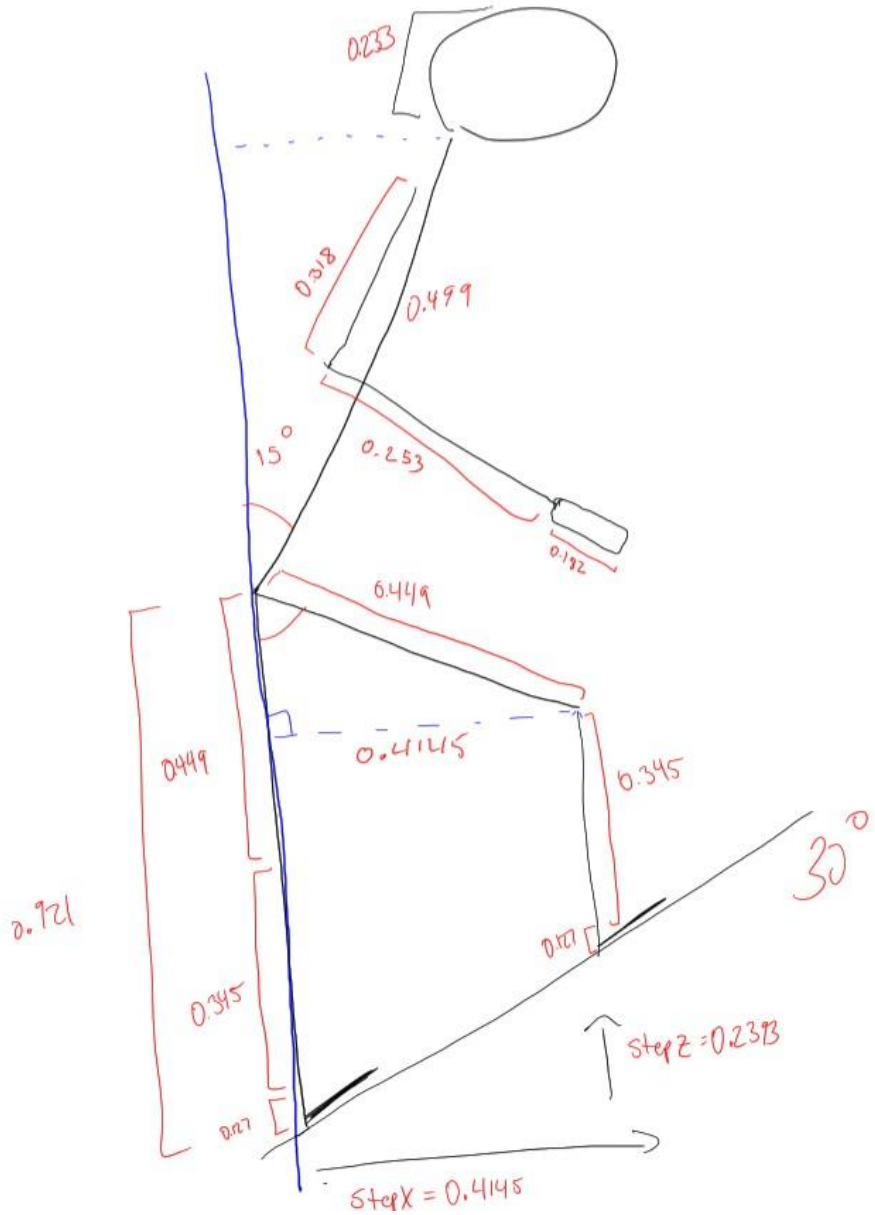

Figure 6: Hand drawn Neandertal model with limb segment lengths, trunk slope, terrain incline, and step lengths.

Table 7: Neandertal Specimen CoM Estimates

Table 7: Neandertal Specimen Center of Mass Estimates

Specimen	Stature (m)	Mass (kg)	CG X (0°)	CG Z (0°)	CG X (30°)	CG Z (30°)	CG X (45°)	CG Z (45°)
Amud 1	1.77	75.3	0.12	1.15	0.23	1.17	0.26	1.17
La Chapelle 1	1.68	77.3	0.1	1.04	0.21	1.06	0.24	1.06
La Ferrassie 1	1.72	85	0.11	1.1	0.22	1.13	0.25	1.12
La Ferrassie 2	1.71	67	0.1	1.02	0.2	1.03	0.24	1.02
Shanidar 1	1.71	80.5	0.11	1.1	0.22	1.12	0.25	1.11
Shanidar 5	1.65	68.5	0.11	1.08	0.21	1.1	0.25	1.1
Spy 2	1.6	83.6	0.1	1.01	0.2	1.03	0.24	1.03
Tabun 1	1.54	63.2	0.1	1.03	0.2	1.04	0.24	1.04

Table 7: Descriptive statistics for Neandertal individuals used in the analysis. Includes estimated stature, body mass, and center of mass (CoM) posititions in the horizontal (X) and the vertical (Z) planes across flat (0°), moderate (30°), and steep (45°) slope conditions.

Table 8: Normalized CoM Positions for Neandertals

Table 8: Normalized Center of Mass Positions for Neandertal Individuals

Specimen	Stature (m)	Mass (kg)	CG X (0°)	CG Z (0°)	CG X (30°)	CG Z (30°)	CG X (45°)	CG Z (45°)
Amud 1	1.77	75.3	0.07	0.65	0.13	0.66	0.15	0.66
La Chapelle 1	1.68	77.3	0.06	0.62	0.13	0.63	0.14	0.63
La Ferrassie 1	1.72	85	0.06	0.64	0.13	0.66	0.15	0.65
La Ferrassie 2	1.71	67	0.06	0.60	0.12	0.60	0.14	0.60
Shanidar 1	1.71	80.5	0.06	0.64	0.13	0.65	0.15	0.65
Shanidar 5	1.65	68.5	0.07	0.65	0.13	0.67	0.15	0.67
Spy 2	1.6	83.6	0.06	0.63	0.13	0.64	0.15	0.64
Tabun 1	1.54	63.2	0.06	0.67	0.13	0.68	0.16	0.68

Table 8. Normalized center of mass (CoM) positions for Neandertal individuals across three slope conditions (0°, 30°, 45°). Raw CoM X and Z coordinates are expressed as proportions of total body stature to account for individual size differences. This allows for comparison of CoM positioning across specimens with different statures and highlights the relative vertical (Z) and horizontal (X) location of body mass in standing posture and on inclined terrain.

Table 9: Modern Human Group Means for CoM Estimates

Table 9: Modern Human Group Means for CoM Estimates

Specimen	Stature (m)	Mass (kg)	CG X (0°)	CG Z (0°)	CG X (30°)	CG Z (30°)	CG X (45°)	CG Z (45°)
Arikara	1.68	62.33	0.15	1.14	0.22	1.13	0.25	1.12
Forensic	1.73	66.21	0.15	1.17	0.22	1.16	0.26	1.15
Poundbury	1.66	63.75	0.15	1.13	0.21	1.12	0.25	1.11
Southern Chinese	1.66	58.59	0.15	1.13	0.21	1.12	0.25	1.1
Spitalfields	1.64	57.91	0.14	1.11	0.21	1.1	0.24	1.09

Table 9: Average stature, mass, and CoM posititions for five modern human populations modeled in this study. Data represents group means for each slope condition.

Table 10: Normalized Center of Mass Positions for Modern Human Populations

Table 10: Normalized Center of Mass Positions for Modern Human Populations

Specimen	Stature (m)	Mass (kg)	CG X (0°)	CG Z (0°)	CG X (30°)	CG Z (30°)	CG X (45°)	CG Z (45°)
Arikara	1.68	62.33	0.09	0.68	0.13	0.67	0.15	0.67
Forensic	1.73	66.21	0.09	0.68	0.13	0.67	0.15	0.66
Poundbury	1.66	63.75	0.09	0.68	0.13	0.67	0.15	0.67
Southern Chinese	1.66	58.59	0.09	0.68	0.13	0.67	0.15	0.66
Spitalfields	1.64	57.91	0.09	0.68	0.13	0.67	0.15	0.66

Table 10. Normalized center of mass (CoM) positions for modern human populations across three slope conditions (0°, 30°, 45°). CoM positions in the horizontal (X) and vertical (Z) dimensions are expressed as proportions of total stature. Normalizing these values allows for meaningful comparison of mass distribution patterns across populations of varying body size, and helps identify relative CoM displacement across terrain conditions.

Table 11: Summary Statistics for Neandertals and Modern Humans

Table 11: Summary Statistics for Neandertals and Modern Humans

Group	CG X (0°)	CG Z (0°)	CG X (30°)	CG Z (30°)	CG X (45°)	CG Z (45°)
Neandertals	0.11 (0.01)	1.07 (0.05)	0.21 (0.01)	1.09 (0.01)	0.25 (0.01)	1.08 (0.05)
Modern Humans	0.15 (0.00)	1.14 (0.02)	0.21 (0.01)	1.13 (0.02)	0.25 (0.01)	1.11 (0.02)

Table 11: Group Means and standard deviations of CoM X and Z posititions for Neandertals and modern humans across terrain conditions. Mean (SD).

Table 12: Comparative Normalized CoM Position Means: Neandertals vs Modern Human Populations

Table 12: Comparative Normalized CoM Position Means: Neandertals vs Modern Human Populations

Group	CG X (0°)	CG Z (0°)	CG X (30°)	CG Z (30°)	CG X (45°)	CG Z (45°)
Neandertals	0.06	0.64	0.13	0.65	0.15	0.65
Modern Humans	0.09	0.68	0.13	0.67	0.15	0.67

Table 12: Group mean comparisons of normalized center of mass (CoM) positions for Neandertals and modern humans across three slope conditions. Values are expressed as proportions of total body stature and summarize relative anterior (X) and vertical (Z) displacement of the CoM between groups.

Table 13: CoM Differences Between Groups

Table 13: CoM Differences Between Groups

Slope	Δ CG X (Modern − Neandertal)	Δ CG Z (Modern − Neandertal)
0°	0.04	0.07
30°	0.00	0.04
45°	0.00	0.03

Table 13: Differences in average center of mass positions between modern humans and Neandertals by slope angle.

Table 14: Normalized CoM Differences Between Groups

Slope	Δ CG X (Modern − Neandertal)	Δ CG Z (Modern − Neandertal)
0°	0.02	0.04
30°	0.00	0.02
45°	0.00	0.02
Table 14: Differences in normalized center of mass (CoM) positions between modern humans and Neandertals across slope conditions. Values		

REFERENCES

Beall, C. M. (2001). Adaptations to altitude: A current assessment. *Annual Review of Anthropology, 30*, 423–456. https://doi.org/10.1146/annurev.anthro.30.1.423

Been, E., Gómez-Olivencia, A., & Kramer, P. A. (2012). Lumbar lordosis of Extinct Hominins. *AMERICAN JOURNAL OF PHYSICAL ANTHROPOLOGY*, *147*, 64–77. https://doi.org/10.1002/ajpa.21633

Been, E., & Kalichman, L. (2014). Lumbar lordosis. *The Spine Journal*, *14*, 87–97. https://doi.org/10.1016/j.spinee.2013.07.464

Buurke, T. J. W., van de Venis, L., den Otter, R., Nonnekes, J., & Keijsers, N. (2023). Comparison of ground reaction force and marker-based methods to estimate mediolateral center of mass displacement and margins of stability during walking. *Journal of Biomechanics*, *146*. https://doi.org/10.1016/J.JBIOMECH.2022.111415

Carretero, J. M., Rodríguez, L., García-González, R., Arsuaga, J. L., Gómez-Olivencia, A., Lorenzo, C., Bonmatí, A., Gracia, A., Martínez, I., & Quam, R. (2012). Stature estimation from complete long bones in the Middle Pleistocene humans from the Sima de los Huesos, Sierra de Atapuerca (Spain). *Journal of Human Evolution*, *62*(2), 242–255. https://doi.org/10.1016/j.jhevol.2011.11.004

Chou, L. S., Kaufman, K. R., Brey, R. H., & Draganich, L. F. (2001). Motion of the whole body's center of mass when stepping over obstacles of different heights. *Gait and Posture*, *13*(1), 17–26. https://doi.org/10.1016/S0966-6362(00)00087-4

de Leva, P. (1996). Adjustments to Zatsiorsky-Seluyanov's segment inertia parameters. *Journal of Biomechanics*, *29*(9), 1223–1230.

Feldesman, M. R., Kleckner, J. G., & Lundy, J. K. (1990). Femur/stature ratio and estimates of stature in mid- and late-pleistocene fossil hominids. *American Journal of Physical Anthropology*, *83*(3), 359–372. https://doi.org/10.1002/ajpa.1330830309

Franz, J. R., & Kram, R. (2012). The effects of grade and speed on leg muscle activations during walking. *Gait and Posture*, *35*(1), 143–147. https://doi.org/10.1016/J.GAITPOST.2011.08.025

Gómez-Olivencia, A., Couture-Veschambre, C., Madelaine, S., & Maureille, B. (2013). The vertebral column of the Regourdou 1 Neandertal. *Journal of Human Evolution*, *64*(6), 582–607. https://doi.org/10.1016/j.jhevol.2013.02.006

Gómez-Olivencia, A., Lindsay Eaves-Johnson, K., Franciscus, R. G., Carretero, M., & Luis Arsuaga, J. (2009). Kebara 2: new insights regarding the most complete Neandertal thorax. *Journal of Human Evolution*, *57*, 75–90. https://doi.org/10.1016/j.jhevol.2009.02.009

Granata, K. P., & Lockhart, T. E. (2008). Dynamic stability differences in fall-prone and healthy adults. *Journal of Electromyography and Kinesiology*, 18(2), 172–178. https://doi.org/10.1016/j.jelekin.2007.06.008

Gruss, L. T. (2007). Limb length and locomotor biomechanics in the genus Homo: An experimental study. *American Journal of Physical Anthropology*, *134*(1), 106–116. https://doi.org/10.1002/ajpa.20642

Haeusler, M., Trinkaus, E., Fornai, C., Müller, J., Bonneau, N., Boeni, T., Frater, N., Rosenberg, K., & Rothschild, B. M. (2019). Morphology, pathology, and the vertebral posture of the La Chapelle-aux-Saints Neandertal. *PNAS*, *116*(11), 4923–4927. https://doi.org/10.1073/pnas.1820745116

Hamner, S. R., & Delp, S. L. (2013). Muscle contributions to fore-aft and vertical body mass center accelerations over a range of running speeds. *Journal of Biomechanics*, *46*, 780–787. https://doi.org/10.1016/J.JBIOMECH.2012.11.024

Higgins, R. W., & Ruff, C. B. (2011). The effects of distal limb segment shortening on locomotor efficiency in sloped terrain: Implications for Neandertal locomotor behavior. *American Journal of Physical Anthropology*, *146*(3), 336–345. https://doi.org/10.1002/ajpa.21575

Kramer, P. A., & Eck, G. G. (2000). Locomotor energetics and leg length in hominid bipedality. *Journal of Human Evolution*, *38*(5), 651–666. https://doi.org/10.1006/jhev.1999.0375

Kramer, P. A., & Sylvester, A. D. (2023). Hip width and metabolic energy expenditure of abductor muscles. *PLoS ONE*, *18*(4). https://doi.org/10.1371/journal.pone.0284450

Minetti, A. E., Formenti, F., & Ardigò, L. P. (2006). Himalayan porter's specialization: Metabolic power, economy, efficiency and skill. *Proceedings of the Royal Society B: Biological Sciences*, *273*(1602), 2791–2797. https://doi.org/10.1098/rspb.2006.3653

Sylvester, A. D., Kramer, P. A., & Jungers, W. L. (2008). Modern humans are not (quite) isometric. *American Journal of Physical Anthropology*, *137*(4), 371–383. https://doi.org/10.1002/ajpa.20880

Ruff, C.B., Wood, B.A. (2023). The estimation and evolution of hominin body mass. *Evolutionary Anthropology,* 32, 223-237. DOI: 10.1002/evan.21988

Ruff, C. B., Burgess, M. L., Junno, J.-A., Mudakikwa, A., Zollikofer, C. P. E., Ponce de Leon, M. S., & McFarlin, S. C. (2018). Phylogenetic and environmental effects on limb bone structure in gorillas. *American Journal of Physical Anthropology*, 166, 353–372. https://doi.org/10.1002/ajpa.23457

Ruff, C. B., Junno, J.-A., Burgess, M. L., Canington, S. L., Harper, C., Mudakikwa, A., & McFarlin, S. C. (2022). Body proportions and environmental adaptation in gorillas. *American Journal of Biological Anthropology*, 177, 501–529. https://doi.org/10.1002/ajpa.24628

Trinkaus, E. (1981). Neanderthal limb proportions and cold adaptation. *Aspects of Human Evolution*, *February*, 187–224. http://ci.nii.ac.jp/naid/10018145328/

Vidal-Cordasco, M., Mateos, A., Zorrilla-Revilla, G., Prado-Nóvoa, O., & Rodríguez, J. (2017). Energetic cost of walking in fossil hominins. *American Journal of Physical Anthropology*, *164*(3), 609-622 https://doi.org/ 10.1002/ajpa.23301

Wall-Scheffler, C. M., Chumanov, E., Steudel-Numbers, K., & Heiderscheit, B. (2010). Electromyography activity across gait and incline: The impact of muscular activity on human morphology. *American Journal of Physical Anthropology*, *143*(4), 601–611. https://doi.org/10.1002/ajpa.21356

Whitcome, K. K., Shapiro, L. J., & Lieberman, D. E. (2007). Fetal load and the evolution of lumbar lordosis in bipedal hominins. *Nature*, *450*, 1075–1077. https://doi.org/10.1038/nature06342

Winter, D. A. (1995). *Human balance and posture control during standing and walking*. *Gait & Posture*, 3(4), 193–214. https://doi.org/10.1016/0966-6362(96)82849-9

Zajac, F. E., Neptune, R. R., & Kautz, S. A. (2002). Biomechanics and muscle coordination of human walking: Part I: Introduction to concepts, power transfer, dynamics and simulations. *Gait & Posture*, 16(3), 215–232. https://doi.org/10.1016/S0966-6362(02)00068-1

Zajac, F. E., Neptune, R. R., & Kautz, S. A. (2003). Biomechanics and muscle coordination of human walking: Part II: Lessons from dynamical simulations and clinical implications. *Gait & Posture*, 17(1), 1–17. https://doi.org/10.1016/S0966-6362(02)00069-3

Chapter 5: Validating External Landmark Measurements for Skeletal Proportions in the Lower Limb

Introduction

Accurate estimation of skeletal dimensions is critical for research in biological anthropology, biomechanics, and clinical science. As detailed in Chapter 3, most analyses of limb bone dimensions have relied on skeletal remains but working with skeletal remains entails ethical and logistical difficulties. Consequently, external anatomical landmarks, such as the trochanterion or lateral malleolus, are frequently used as non-invasive proxies for underlying skeletal dimensions. Despite their widespread application, few studies have evaluated the relationship between external (skin surface) and internal (skeletal) measurements.

This chapter examines the relationship between external and skeletal measurements of the femur and tibia using computed tomography (CT) data from human cadavers. The primary focus is on the crural index (CI), the ratio of tibial to femoral length, which is a foundational metric in studies of thermoregulatory adaptation, locomotor energetics, and morphological variation in hominin populations (Higgins & Ruff, 2011; Holliday, 1997a, 1997b; Porter, 1999; Trinkaus, 1981). CI has been employed extensively in anthropological and biomechanical contexts to infer environmental adaptations and functional morphology, particularly in Neandertals, whose shortened distal limb segments are thought to reflect cold-climate or terrain-based adaptations (Gruss, 2007; Higgins & Ruff, 2011; Kramer & Eck, 2000).

The present study uses CT imaging to compare internal skeletal landmarks with external surface (skin) landmarks in the same individuals, offering a rare opportunity to quantify the accuracy of external measurements under controlled conditions. The dataset includes over 100 decedents from the New Mexico Decedent Image Database (NMDID), with no lower limb

trauma, and includes male and female individuals. Femoral and tibial lengths were measured using both skeletal landmarks (e.g., femoral head to medial condyle) and externally accessible references (e.g., trochanterion to tibiale laterale), following established anthropometric standards (Davenport, 1933; Norton & Easton, 2019).

This chapter plays a methodological role in the overall structure of the dissertation. Chapter 3 examined CI variation across modern and fossil populations, while Chapter 4 modeled how differences in limb proportions affect center of mass (CoM) and locomotor stability on inclined terrain. Both chapters rely on accurate limb length estimations, which may be affected by the source of measurement—external vs. skeletal. By validating external measurements, this chapter helps assess the reliability of CI values used in comparative, evolutionary, and functional studies throughout the dissertation.

In addition to its paleoanthropological applications, this study has broader relevance to biomechanics, kinesiology, and physical therapy, where external measurements are often used in assessing musculoskeletal health, mobility, and rehabilitation progress (Lautzenheiser et al., 2020; Steudel-Numbers & Tilkens, 2004). However, even small discrepancies in external segment lengths can compound when calculating ratios like CI, potentially skewing results or masking population-level trends. This study addresses whether these discrepancies are negligible or if they require caution when interpreting CI-based inferences.

By evaluating both raw lengths and calculated crural indices, this chapter provides a quantitative assessment of proxy validity. The results clarify whether surface-based measurements are sufficient for use in paleoanthropological models and comparative skeletal analyses or whether correction factors or methodological adjustments are needed. Ultimately, this chapter offers a foundational test of the accuracy, reliability, and limitations of external

landmark-based estimation methods and supports more confident interpretation of crural index patterns across both modern and extinct populations.

Materials and Methods

This study evaluates the reliability of external anatomical landmarks in estimating internal skeletal dimensions of the femur and tibia. Special attention is given to how these measurements affect the accuracy of crural index (CI) values, which are widely used in both anthropological and biomechanical studies.

Sample and Imaging Data

The analysis is based on computed tomography (CT) scans from 111 adult cadavers with no evidence of lower limb trauma. Data were obtained from the New Mexico Decedent Image Database (NMDID). To reduce variation caused by age-related pathology such as osteoarthritis, we restricted the sample to individuals below a mass cap of 115 kg for males and 100 kg for females, and selected individuals within a target age range of 20-40 years.

I initially aimed for a balanced sample of 50 males and 50 females based on a priori sample size calculations. Due to oversampling of males, the final dataset included 61 males and 50 females. After exploratory analysis suggested that the sample size exceeded what was necessary for initial model development, the dataset was divided into two groups:

- Training set: 50 males and 50 females
- Validation set: 11 additional males

The mean body mass of male decedents was 92.81 kg (SD= 16.56), and the mean body mass of females was 67.59 kg (SD=12.96).

Landmark Identification and Measurement Protocols

CT scans were analyzed using OsiriX (Pixmeo, Geneva), a DICOM viewer that allows for detailed 3D visualization and landmark placement (Lautzenheiser et al., 2020). We used Thin ST Lower Limb and Thin ST Torso scan protocols to ensure complete coverage of the lower limbs.

A total of 28 anatomical landmarks were identified for each individual (Table 15):

- 16 skeletal landmarks, following standards from *Data Collection Procedures for Forensic Skeletal Material 2.0* (Langley et al., 2016)
- 12 external landmarks, based on anthropometric guidelines from *Standards for Anthropometry Assessment in Kinanthropometry and Exercise Physiology* (Norton & Easton, 2019)

Landmark coordinates were collected in 3D Cartesian space, and both external and skeletal lengths were calculated from these coordinates. Inter- and intrarater reliability was confirmed by two independent researchers, with all intraclass correlation coefficients exceeding 0.90.

Figures 7 and 8 illustrate examples of landmark placement on CT images, highlighting the distinction between skeletal and external reference points.

Skeletal and External Length Definitions

Skeletal measurements:

- Femoral length: from the most superior point of the femoral head to the most distal point of the medial condyle
- Tibial length: from the superior articular surface of the lateral tibial condyle to the most inferior aspect of the medial malleolus
- Skeletal leg length: total length from femoral head to medial malleolus

External measurements:

- Thigh length: from the trochanterion to the lateral tibial condyle (tibiale laterale)
- Shank length: from the tibiale mediale to the inferior aspect of the medial malleolus
- External leg length: from the trochanterion to the external lateral malleolus

For landmarks not visible in 2D slices, the OsiriX 3D viewer was used for precise placement.

Crural Index Calculation

The crural index (CI) was calculated using standard formulas from Davenport (1933) and Porter (1999) (Davenport, 1933; Porter, 1999):

- Skeletal CI: tibial length ÷ femoral length
- External CI: external shank length ÷ external thigh length

Statistical Analysis

We applied linear regression to evaluate the relationship between external and skeletal femoral lengths, tibial lengths, and crural indices. Additionally, two methods for leg length estimation were compared:

1. Summed skeletal femoral and tibial lengths vs. summed external thigh and shank lengths
2. Direct measurement from femoral head to medial malleolus (skeletal) vs. trochanterion to lateral malleolus (external)

To assess prediction accuracy for crural index, we also applied reduced major axis (RMA) regression, which accounts for measurement error in both variables. Performance was evaluated using root mean squared error (RMSE) in the validation set. All analyses were conducted in Stata 17 (StataCorp, College Station, TX).

Results

Regression analyses were conducted using the training set of 50 males and 50 females to assess the degree of concordance between external and skeletal measurements.

Femoral and Tibial Length Agreement

The linear regression comparing external and skeletal femoral lengths produced an R^2 of 0.97 ($p < 0.001$; Figures 9 and 10) indicating a very strong relationship between these measurements. Similarly, the regression for external and skeletal tibial lengths yielded an R^2 of 0.98 ($p < 0.001$; Figures 11 and 12), also reflecting a high level of agreement. These results suggest that external landmarks provide a reliable approximation of skeletal segment lengths in the lower limb.

Leg Length Agreement Across Methods

To assess consistency across different methods of leg length estimation, two approaches were compared:

1. Summed segment lengths: Femoral + tibial (skeletal) vs. thigh + shank (external)
2. Total leg length: From femoral head to medial malleolus (skeletal) vs. trochanterion to lateral malleolus (external)

The regression comparing the summed segment lengths produced an R^2 of 0.99 ($p < 0.05$; Figures 13 and 14), and total leg lengths produced an R^2 of 0.98 ($p < 0.05$; Figures 15 and 16), demonstrating near-perfect agreement between the two methods.

Crural Index Agreement

When comparing skeletal and external CI values, the regression analysis resulted in an R^2 of 0.60 (Figures 17 and 18), indicating only moderate agreement. While still statistically significant ($p < 0.05$), this value reflects considerably more prediction error than observed in the femoral or tibial

length comparisons. This suggests that although individual segment lengths can be reliably estimated from external landmarks, combining these measures into a ratio (as in CI) may introduce compounding errors.

To further explore this issue, we tested whether using regression-predicted skeletal lengths — rather than raw external measurements— would improve agreement with actual skeletal CI values. Specifically, we applied the equations derived from external tibial and femoral lengths to predict their skeletal counterparts and then calculated the predicted CI as a ration of those two estimates. This approach yielded a higher R^2 of 0.60 compared to the original R^2 of 0.53 when directly regressing external CI against skeletal CI. However, since both femoral and tibial length estimates contain error, combining them into a ratio (CI) still results in error propagation. To better account for measurement error in both variables, we used a Reduced Major Axis (RMA) regression model trained on a subset of the data and evaluated using Root Mean Square Error (RMSE). This approach produced an RMSE of 0.01, reflecting more stable agreement than the raw external CI method, and was therefore used for subsequent analyses.

Validation Model Performance

To address this, we applied a reduced major axis (RMA) regression model to the training set. This method accounts for potential measurement error in both independent and dependent variables, which is especially appropriate for ratio-based comparisons where independence cannot be assumed.

The RMA model was then tested on the validation set of 11 males. Root Mean Squared Error (RMSE) was calculated to evaluate predictive performance of the model. The RMSE for predicted versus observed skeletal CI values was 0.01.

Discussion

The results of this study demonstrate a strong relationship between external anatomical landmarks and skeletal measurements for both femoral and tibial lengths. The high r^2 values for these comparisons (0.97 and 0.98, respectively) indicate that external measurements can serve as reliable proxies for skeletal segment lengths in the lower limb. These findings validate the widespread use of external anthropometric landmarks in clinical, biomechanical, and anthropological research when direct skeletal measurements are unavailable.

However, the moderate correlation between external and skeletal crural index (CI) values ($r^2 = 0.60$) highlights a potential limitation. While individual segment lengths can be accurately estimated from external landmarks, the use of these values to calculate a ratio introduces compounding error. Even minor discrepancies in external femoral or tibial length estimates can amplify when expressed as a ratio, resulting in moderate agreement between externally and skeletally derived CI values. This result is especially relevant for anthropological studies that rely on crural index to infer thermoregulatory adaptation, biomechanical efficiency, or evolutionary trends.

The reduced major axis (RMA) regression model produced a RMSE of 0.01 in the validation set. Still, caution is warranted in applying external CI values for fine-scale population comparisons or evolutionary reconstructions, particularly when differences between groups are subtle. This has direct relevance to the preceding chapters, where crural index was used to evaluate variation between modern humans and Neandertals and to assess the impact of limb proportions on center of mass and locomotor efficiency.

Chapter 3 demonstrated that Neandertals exhibit lower average crural indices and greater variation than modern humans, a pattern often interpreted as a cold-climate adaptation or terrain-

based functional response. Chapter 4 built on this by modeling how differences in limb proportions and mass distribution influence whole-body center of mass (CoM) and biomechanical efficiency, especially during inclined locomotion. Both analyses depend on the assumption that the CI values used are accurate representations of skeletal reality. This chapter provides a crucial methodological foundation for those interpretations by testing whether externally derived measurements—and by extension, CI values—are sufficiently reliable for use in comparative and biomechanical modeling studies.

Importantly, this study also contributes to broader methodological discussions in the field. Despite the common use of surface landmarks in anthropometry and clinical settings (Norton & Easton, 2019; Lautzenheiser et al., 2020), relatively few studies have validated these proxies against internal skeletal data using imaging-based approaches. By employing CT data and landmark-based measurements on the same individuals, this research offers a rare opportunity to quantify the magnitude of error introduced by using external reference points.

In summary, while external measurements of femoral and tibial lengths are highly reliable and can be used confidently in most applications, external CI values should be interpreted with caution. When possible, skeletal measurements remain the gold standard, especially for ratio-based analyses or when working with fossil data. However, in contexts where only external data are available—such as living populations, CT reconstructions without bone segmentation, or fragmentary fossil remains, this study supports the use of correction models to minimize error and enhance comparability.

Limitations

While this study provides important validation of external anatomical landmarks as proxies for skeletal dimensions, several limitations should be acknowledged.

First, the sample was drawn entirely from the New Mexico Decedent Image Database (NMDID). Although this dataset includes a broad range of body sizes, its geographic specificity may limit the generalizability of findings to other populations. Future studies should replicate this analysis using CT data from individuals across different ethnic, geographic, and temporal contexts to evaluate whether external-to-skeletal correspondence holds consistently across groups.

Second, the reliability of external measurements may vary in living humans due to factors such as soft tissue variability, posture, or movement. While this study used high-resolution CT imaging from cadavers to precisely locate landmarks, external measurement error could be greater in field or clinical settings (Steudel-Numbers & Tilkens, 2004). Nonetheless, the high degree of agreement observed here supports the idea that surface landmarks remain valid under controlled measurement conditions.

Third, the crural index discrepancy observed between skeletal and external measurements highlights a fundamental limitation of using ratios. CI is sensitive to small errors (Higgins & Ruff, 2011; Porter, 1999) in either femoral or tibial length, which can be magnified when expressed as a proportion. This reinforces the need for careful measurement and, when feasible, the use of skeletal data or corrected external estimates in anthropological and biomechanical applications.

Finally, some anatomical inconsistencies limited direct comparisons. For example, the medial malleolus landmark—used in both skeletal and external tibial length—could not be assessed at exactly the same point in both measurement contexts (Lautzenheiser et al., 2020). On skeletal measurements, the endpoint is the most inferior point on the bony malleolus, while on external CT scans, the visible contour of the soft tissue often obscures this precise location. As a result, the external tibial length may terminate slightly differently—typically at the visible skin surface near the malleolus—creating a consistent, if minor, offset. While 3D CT views were used to standardize landmark placement, this surface-to-skeleton mismatch introduces subtle but systematic measurement error that may contribute to the observed CI variation.

Despite these limitations, the present study provides robust evidence that external landmarks accurately reflect femoral and tibial lengths and offers guidance on the cautious interpretation of externally derived crural indices. Addressing these constraints in future work will further enhance our understanding of the relationship between external and skeletal measurements, especially in applied anthropological, clinical, and biomechanical contexts.

Conclusion

This study evaluated the accuracy of external anatomical landmarks as proxies for internal skeletal measurements of the femur and tibia, with a focus on their use in calculating the crural index (CI). Using CT imaging and 3D landmarking on a large sample of cadavers, we found high concordance between external and skeletal segment lengths ($r^2 = 0.97–0.98$), supporting the validity of external measurements for estimating lower limb dimensions. These findings are consistent with prior work demonstrating the utility of surface landmarks in biomechanical and anthropometric research (Lautzenheiser et al., 2020; Steudel-Numbers & Tilkens, 2004).

In contrast, the moderate agreement between external and skeletal CI values ($r^2 = 0.60$) highlights the challenge of using ratio-based indices, where minor errors in individual measurements can become amplified (Higgins & Ruff, 2011; Porter, 1999). This result is especially important in anthropological and evolutionary studies, where CI is often used to infer climatic adaptation, functional morphology, and locomotor energetics (Holliday, 1997a; Trinkaus, 1981).

The results presented here provide a methodological foundation for the broader analyses in this dissertation. In Chapter 3, we used CI to compare Neandertals and modern humans, and in Chapter 4, we modeled how limb proportions influence center of mass (CoM) and biomechanical efficiency across different terrains. The present findings validate the use of external measurements in contexts where skeletal data are unavailable, while also cautioning against uncritical application of external CI values without consideration of measurement error and population-specific variation.

Ultimately, this chapter demonstrates that external landmarks are highly effective for estimating femoral and tibial lengths, and that correction models can help mitigate the limitations of externally derived CI values. These findings enhance the interpretability of comparative data in evolutionary anthropology, biomechanics, and clinical applications, and support continued refinement of measurement methods across disciplines.

Table 15: Anatomical Landmarks Used

Skeletal Points
L/R Skeletal Superior Greater Trochanter
L/R Skeletal Greater Trochanter
L/R Superior Femoral Head
L/R Inferior Femoral Head
L/R Skeletal Lateral Femoral Condyle
L/R Skeletal Medial Femoral Condyle
L/R Skeletal Tibial Plateau
L/R Skeletal Inferior Medial Malleolus
External Points
L/R Trochanterion
L/R External Lateral Epicondyle
L/R External Lateral Tibial Condyle
L/R External Later Malleolus
L/R External Medial Tibial Condyle
L/R External Medial Malleolus

Table 15: List of the 28 anatomical landmarks used (16 skeletal, 12 external)

Figure 7: Rendered CT image of distal femur and proximal Tibia

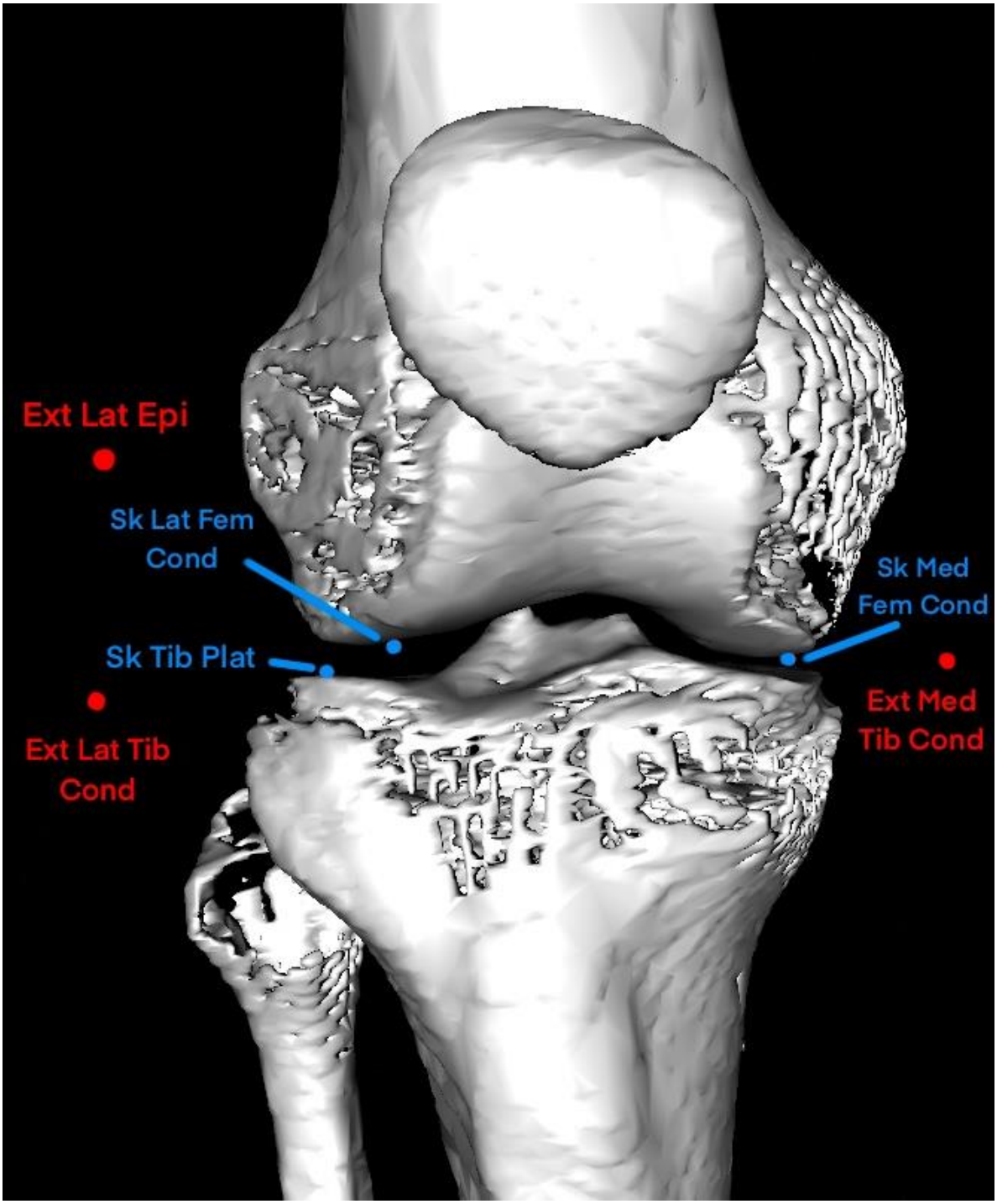

Figure 7: Rendered CT image of distal femur and proximal tibia with markers. Blue markers are skeletal markers, and the floating red markers are external. External CT image not shown.

Figure 8: CT image slice of distal femur

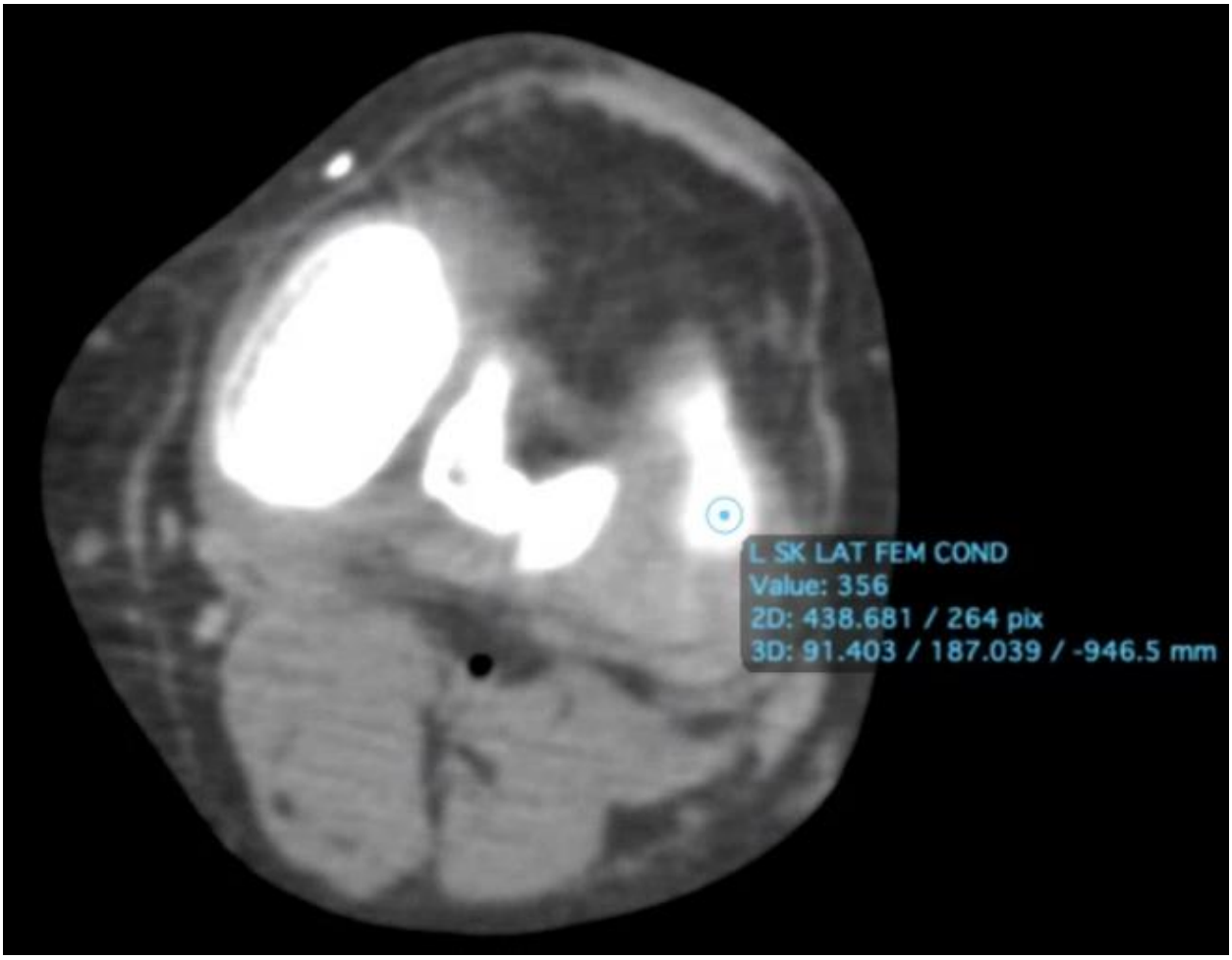

Figure 8: CT image slice of distal femur showing skeletal marker placement for the left skeletal lateral femoral condyle. This example illustrates precision in identifying distal femoral landmarks in the OsiriX 3D viewer.

Figure 9: Regression Summary: Skeletal vs. External Femoral Length (Left Leg)

Source	SS	df	MS	Number of obs	=	70
				F(1, 68)	=	2149.28
Model	69460.9007	1	69460.9007	Prob > F	=	0.0000
Residual	2197.63552	68	32.3181695	R-squared	=	0.9693
				Adj R-squared	=	0.9689
Total	71658.5363	69	1038.52951	Root MSE	=	5.6849

Lskfemlength	Coefficient	Std. err.	t	P>|t|	[95% conf.	interval]
Lextfemlength	1.075722	.0232035	46.36	0.000	1.02942	1.122024
_cons	-14.585	10.22835	-1.43	0.158	-34.99535	5.82535

Figure 9: Linear regression results comparing external and skeletal femoral lengths on the left side (training set; n = 70). The model produced an r^2 of 0.97 ($p < 0.001$), indicating a very strong relationship between externally measured femur length and skeletal femur length.

Figure 10: Femoral Leg Agreement

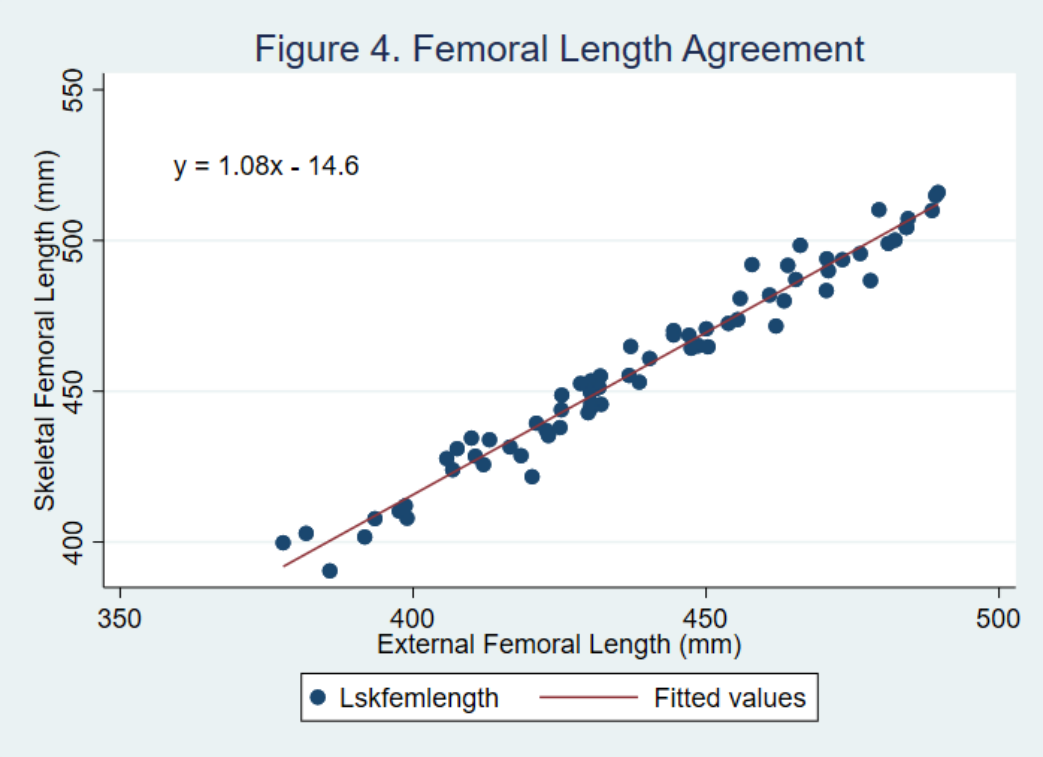

Figure 10: Scatterplot showing agreement between external and skeletal femoral lengths. A fitted regression line demonstrates strong concordance ($r^2 = 0.97$), supporting the validity of external measures in estimating skeletal femur length.

Figure 11: Regression Summary: Skeletal vs. External Tibial Length (Left Leg)

Source	SS	df	MS	Number of obs	=	70
				F(1, 68)	=	3616.27
Model	58050.7553	1	58050.7553	Prob > F	=	0.0000
Residual	1091.58017	68	16.0526496	R-squared	=	0.9815
				Adj R-squared	=	0.9813
Total	59142.3355	69	857.135296	Root MSE	=	4.0066

Lsktiblength	Coefficient	Std. err.	t	P>|t|	[95% conf.	interval]
Lexttiblength	.9924969	.0165044	60.14	0.000	.959563	1.025431
_cons	19.92916	6.041938	3.30	0.002	7.872661	31.98566

Figure 11: Regression results comparing left skeletal and external tibial lengths (n = 70). The analysis yielded an r^2 of 0.98 ($p < 0.001$), reflecting very strong predictive agreement between externally and skeletally measured tibial lengths.

Figure 12: Tibial Length Agreement

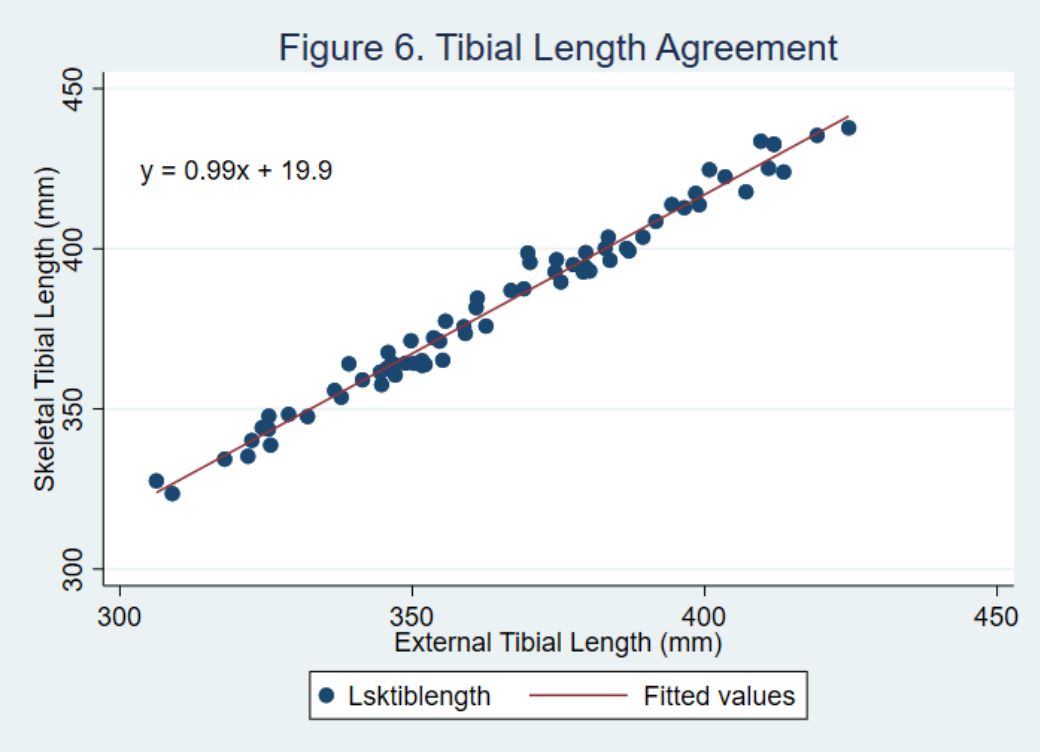

Figure 12: Scatterplot comparing external and skeletal tibial lengths on the left side, with a regression line illustrating high agreement ($r^2 = 0.98$). External tibial length accurately predicts skeletal tibial length with minimal variation.

Figure 13: Regression Summary: Skeletal vs. External Summed Leg Segment Lengths

Source	SS	df	MS	Number of obs	=	70
				F(1, 68)	=	7303.78
Model	250985.523	1	250985.523	Prob > F	=	0.0000
Residual	2336.73639	68	34.3637705	R-squared	=	0.9908
				Adj R-squared	=	0.9906
Total	253322.259	69	3671.33709	Root MSE	=	5.8621

Lskleglength	Coefficient	Std. err.	t	P>|t|	[95% conf.	interval]
Lextleglength	1.039703	.0121656	85.46	0.000	1.015426	1.063979
_cons	-16.05678	9.997542	-1.61	0.113	-36.00656	3.893003

Figure 13: Regression analysis comparing total skeletal and external leg lengths derived by summing femoral and tibial segments. The model showed strong agreement ($r^2 = 0.99$, $p < 0.05$), supporting this method as a reliable approximation of total leg length.

Figure 14: Summed Segment Leg Length Agreement

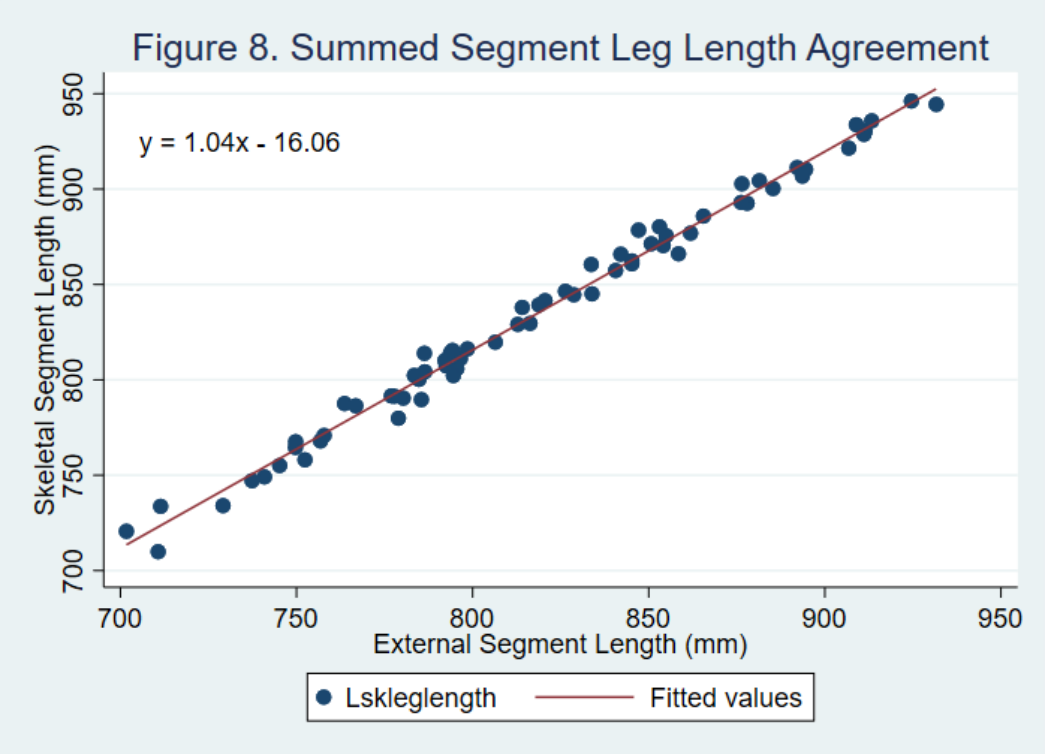

Figure 6.8: Scatterplot comparing summed external and skeletal segment lengths (femur + tibia). A fitted regression line illustrates the degree of agreement using this segment-based method of total leg length estimation.

Figure 15: Regression Summary: Total Leg Length Comparison (Skeletal vs. External)

Source	SS	df	MS		
Model	251277.648	1	251277.648	Number of obs	= 70
Residual	4026.73132	68	59.2166371	F(1, 68)	= 4243.36
				Prob > F	= 0.0000
Total	255304.379	69	3700.06347	R-squared	= 0.9842
				Adj R-squared	= 0.9840
				Root MSE	= 7.6952

Lskll	Coefficient	Std. err.	t	P>|t|	[95% conf.	interval]
Lexll	1.038134	.0159367	65.14	0.000	1.006333	1.069936
_cons	5.221893	12.85827	0.41	0.686	-20.43639	30.88018

Figure 15: Regression comparing continuous skeletal leg length (femoral head to medial malleolus) and external leg length (trochanterion to lateral malleolus). This method produced an r^2 of 0.99 ($p < 0.001$), indicating near-perfect agreement between total skeletal and external leg length estimates.

Figure 16: Total Leg Length Agreement

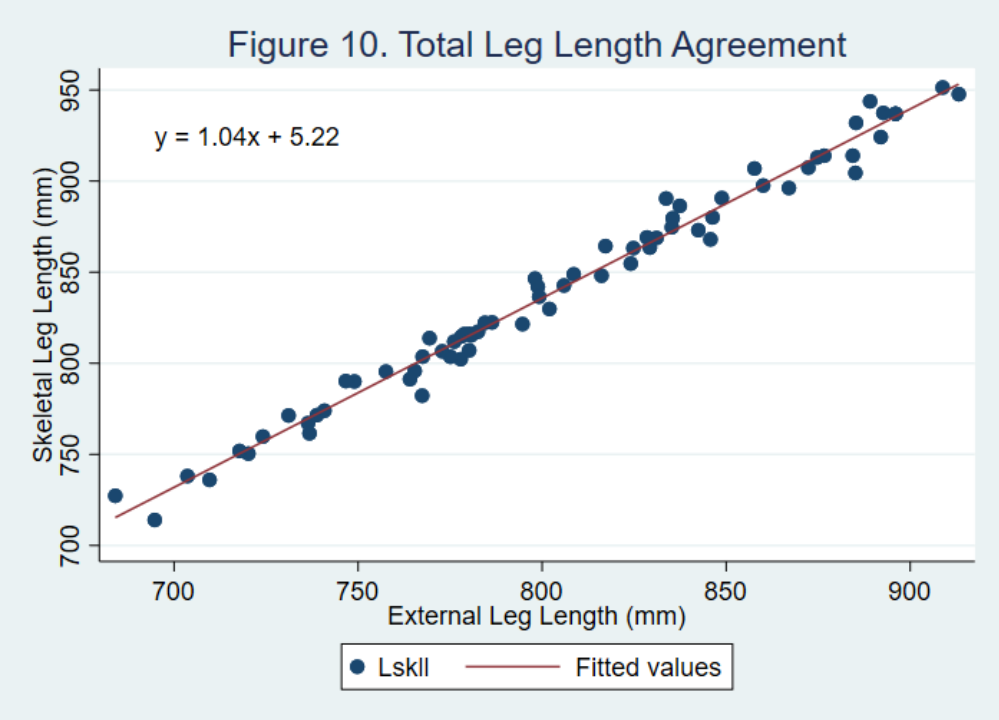

Figure 16: Scatterplot comparing continuous skeletal and external leg length measurements. A regression line indicates exceptionally strong concordance ($r^2 = 0.99$), validating this method as highly reliable for leg length estimation.

Figure 17: Regression Summary: Skeletal vs. External Crural Index

Source	SS	df	MS	Number of obs	=	70
				F(1, 68)	=	103.74
Model	.014705133	1	.014705133	Prob > F	=	0.0000
Residual	.009638729	68	.000141746	R-squared	=	0.6041
				Adj R-squared	=	0.5982
Total	.024343862	69	.00035281	Root MSE	=	.01191

Lskcrural	Coefficient	Std. err.	t	P>|t|	[95% conf.	interval]
Lextcrural	.727052	.0713816	10.19	0.000	.5846121	.8694918
_cons	.2303104	.0592039	3.89	0.000	.1121709	.3484498

Figure 17: Regression analysis comparing skeletal and external crural index values (tibia/femur ratios) on the left side. The model produced an r^2 of 0.60 ($p < 0.05$), indicating moderate agreement and highlighting the compounded error that arises when estimating ratios from external segment lengths.

Figure 18: Crural Index Agreement

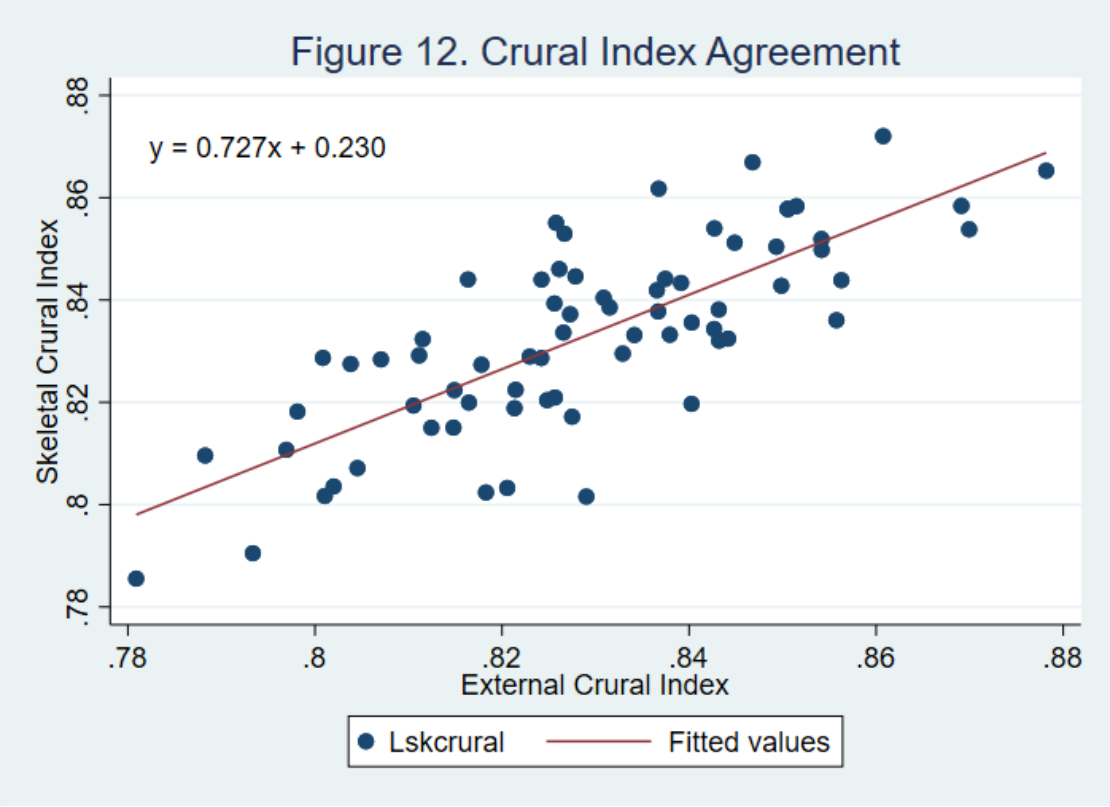

Figure 18: Scatterplot showing agreement between external and skeletal crural index values. The regression line indicates moderate concordance ($r^2 = 0.60$), with greater variability likely due to compounded error from combining two segment estimates into a ratio.

REFERENCES

Davenport, C. B. (1933). The Crural Index. *American Journal of Physical Anthropology*, *17*(8).

Gruss, L. T. (2007). Limb length and locomotor biomechanics in the genus Homo: An experimental study. *American Journal of Physical Anthropology*, *134*(1), 106–116. https://doi.org/10.1002/ajpa.20642

Higgins, R. W., & Ruff, C. B. (2011). The effects of distal limb segment shortening on locomotor efficiency in sloped terrain: Implications for Neandertal locomotor behavior. *American Journal of Physical Anthropology*, *146*(3), 336–345. https://doi.org/10.1002/ajpa.21575

Holliday, T. W. (1997a). Body proportions in Late Pleistocene Europe and modern human origins. *Journal of Human Evolution*, *32*, 423–447.

Holliday, T. W. (1997b). Postcranial Evidence of Cold Adaptation in European Neandertals. *American Journal of Physical Anthropology*, *104*, 245–258.

Kramer, P. A., & Eck, G. G. (2000). Locomotor energetics and leg length in hominid bipedality. *Journal of Human Evolution*, *38*(5), 651–666. https://doi.org/10.1006/jhev.1999.0375

Langley, N. R., Jantz, L. M., Ousley, S. D., Jantz, R. L., & Milner, G. (2016). *Data collection procedures for forensic skeletal material 2.0*. Forensic Anthropology Center, University of Tennessee. https://fac.utk.edu/wp-content/uploads/2016/03/DCP20_webversion.pdf

Lautzenheiser, S. G., Sylvester, A. D., & Kramer, P. A. (2020). Estimating the in vivo location of the talus from external surface landmarks. *American Journal of Physical Anthropology*, *171*, 354–360. https://doi.org/10.1002/ajpa.23957

Norton, K., & Eston, R. (Eds.). (2018). Kinanthropometry and Exercise Physiology (4th ed.). Routledge. https://doi.org/10.4324/9781315385662

Porter, A. M. W. (1999). Modern human, early modern human and Neanderthal limb proportions. *International Journal of Osteoarchaeology*, *9*(1), 54–67. https://doi.org/10.1002/(SICI)1099-1212(199901/02)9:1<54::AID-OA459>3.0.CO;2-R

Steudel-Numbers, K. L., & Tilkens, M. J. (2004). The effect of lower limb length on the energetic cost of locomotion: implications for fossil hominins. *Journal of Human Evolution*, *47*, 95–109. https://doi.org/10.1016/j.jhevol.2004.06.002

Trinkaus, E. (1981). Neanderthal limb proportions and cold adaptation. *Aspects of Human Evolution*, *February*, 187–224. http://ci.nii.ac.jp/naid/10018145328/

Chapter 6: Conclusion

I set out to examine the functional significance of Neandertal postcranial morphology by integrating comparative anatomy, biomechanical modeling, and methodological validation. By focusing on limb proportions, mass distribution, and measurement accuracy, I sought to determine whether Neandertal anatomy reflects adaptations to cold climates, rugged terrain, or both — and whether the tools used to study these traits yields reliable results.

Each chapter contributed to this overarching aim. Chapter 2 established the evolutionary and environmental context of Neandertal life, emphasizing the longstanding debate over the drivers of their distinctive anatomy. Chapter 3 analyzed crural index variation, demonstrating that while Neandertals exhibit values consistent with cold-adapted modern humans, their broader range of CI suggests additional selective pressures, potentially linked to locomotion in complex terrain. Chapter 4 expanded on this by modeling how limb proportions and trunk morphology affect center of mass positioning across sloped surfaces, showing that Neandertals may have possessed biomechanical advantages in inclined environments. Chapter 5 addressed the methodological foundation of these analyses, validating the use of external anatomical landmarks for estimating skeletal lengths, while highlighting the limitations of using such proxies in ratio-based metrics like CI.

Taken together, these findings support the view that Neandertal morphology reflects a combination of climatic and biomechanical adaptations, and that interpreting their anatomy requires both functional and methodological nuances.

In this dissertation work, I was guided by three central research questions: (1) Do Neandertal limb proportions reflect cold-climate adaptations, biomechanical pressures, or both? (2) How do

these proportions influence center of mass (CoM) and biomechanical function, particularly in sloped terrain? (3) Can externally measured anatomical landmarks serve as reliable proxies for skeletal dimensions, especially when calculating indices like the crural index?

1. Neandertal limb proportions and cold climate versus biomechanical adaptation

Analysis of crural index (CI) values in Chapter 3 showed that Neandertals exhibit lower average CIs compared to pooled modern human populations, aligning with patterns observed in cold-adapted modern humans. This supports the long-standing hypothesis that Neandertal limb proportions were shaped in part by thermoregulatory pressures in glacial environments. However, while cold climate likely played a significant role, the mechanical implications of shorter distal limb segments—particularly for locomotion on uneven terrain—suggest that biomechanical demands may have also influenced Neandertal morphology. Rather than attributing limb proportions to a single selective factor, these results reinforce the need for multifactorial interpretations that consider both environmental temperature and terrain-based locomotor function.

2. Center of mass and functional implications of Neandertal morphology

Modeling results presented in Chapter 4 demonstrate that Neandertals exhibited a slightly lower and more posterior CoM compared to modern humans. These differences become more pronounced with increasing incline, suggesting that Neandertal body form may have offered biomechanical advantages in stability and energy efficiency on uneven terrain. Such adaptations would have been beneficial in the glacial and topographically complex environments Neandertals frequently inhabited. This work provides new quantitative support for terrain-based hypotheses on Neandertal locomotor adaptations.

3. Methodological evaluation of external measurement proxies

Chapter 5 assessed the accuracy of external anatomical landmarks in estimating skeletal segment lengths and crural index values. The study found high agreement between external and skeletal lengths for the femur and tibia, validating the use of external measurements in both anthropological and clinical contexts. However, when these lengths were combined into a ratio, moderate discrepancies emerged. This finding cautions against the uncritical use of externally derived CI values, particularly in fossil or forensic contexts where fine-scale differences are meaningful. Importantly, the validation of external measurements supports the broader interpretive framework of the dissertation by confirming the general reliability of comparative CI data, while also underscoring the need for methodological transparency.

Together, these results contribute to a more nuanced understanding of Neandertal adaptation and functional morphology, demonstrating that their anatomy cannot be fully explained by climate alone. By combining comparative data, biomechanical modeling, and measurement validation, this dissertation offers an integrative approach that enhances both theoretical interpretations and research methodology in paleoanthropology.

The findings presented in this dissertation have broader implications for how paleoanthropologists interpret postcranial morphology, especially in relation to behavioral and environmental contexts. By highlighting the interplay between climate, locomotion, and skeletal structure, this research reinforces the value of multifactorial models in understanding hominin anatomy. Neandertals were not simply cold-adapted hominins with compact limbs; they may well have been biomechanically tuned to the topographically diverse and demanding landscapes they inhabited. This perspective complicates overly simplistic narratives of adaptation and

encourages researchers to consider how multiple selective pressures may shape similar morphological traits.

From a methodological standpoint, this dissertation underscores the importance of validating the tools and assumptions that underlie evolutionary interpretation. The comparative modeling of center of mass provides a concrete framework for connecting limb proportions with locomotor function, while the evaluation of external landmark reliability offers a cautionary yet practical guide for data collection in both fossil and modern contexts. These contributions are especially relevant as paleoanthropology increasingly integrates digital modeling, clinical imaging, and large-scaled datasets into its analytical toolkit.

At the same time, several limitations must be acknowledged. The small sample size of Neandertal individuals with complete lower limb data constrains the statistical power and generalizability of some analyses. Although this reflects the realities of the fossil record, it remains a barrier to fully capturing population-level variation. Similarly, reconstructions of body mass and CoM rely on assumptions drawn from modern human segment parameters and scaling relationships. While necessary for comparative purposes, these assumptions may not fully capture species-specific differences in soft tissue distribution or spinal curvature. Finally, although the CT validation study provides strong evidence for the reliability of external measurements, the moderate variation in crural index values between external and skeletal sources highlights the need for caution when interpreting small intergroup differences based on ration-based metrics.

Despite these limitations, the interdisciplinary approach taken here strengthens the interpretative value of each individual analysis. The triangulation of fossil data, modern comparative datasets, and biomechanical modeling helps mitigate the impact of any single

limitation and allows for more robust conclusions about Neandertal morphology and its functional implications.

Looking forward, several avenues of research could expand on the findings presented here. Increasing the number of well-preserved Neandertal postcranial specimens, whether through new discoveries or improved reconstruction techniques, would help refine estimates of population-level variation in limb proportions and mass distribution. In parallel, incorporating highland or terrain-adapted modern human populations into center of mass modeling could provide a stronger comparative framework for evaluating functional adaptation to rugged landscapes. The use of dynamic simulation tools, such as OpenSim or AnyBody, may also offer a more detailed understanding of joint loading and muscle recruitment patterns under varied locomotor scenarios.

Methodologically, continued validation of external measurements across diverse populations and body types would strengthen the reliability of anthropometric proxies in both fossil and clinical settings. Efforts to standardize landmark placement and incorporate soft tissue variability into measurement models would improve the accuracy of ration-based metrics like the crural index. Such refinements are particularly important as digital imaging and biomechanical modeling become increasingly central to paleoanthropological research.

Ultimately, this dissertation contributes to a growing recognition that the study of hominin anatomy must go beyond descriptive morphology. By combining functional models with rigorous methodological validation, it offers a more holistic view of Neandertal adaptation —one that bridges anatomy, behavior, and environment. Neandertals emerge not just as cold-adapted hominins, but as biomechanically capable beings whose morphology supported survival in complex and demanding landscapes.

In clarifying both the adaptive significance and interpretive limits of postcranial traits, this work lays a foundation for more integrative approaches to understating human evolution. It demonstrates that even fragmentary remains, when paired with careful modeling and methodological scrutiny, can yield meaningful insights into how our ancestors lived, moved, and thrived.

Appendix A: Center of Mass Calculations – Neandertals

This appendix includes representative spreadsheets illustrating the center of mass (CoM) calculation process for Neandertal individuals. Each Spreadsheet includes limb segment lengths, segment masses, segment CoM positions, and the calculated total body CoM for standardized terrain incline of 30°. Additional slope conditions are available on request. The original spreadsheets used for these calculations were created by Dr. Patricia A. Kramer. They have been adapted here to include slope-specific values and representative outputs for each individual.

Figure A1. Amud 1 – Center of Mass Calculation Spreadsheet (30° slope)

				Deg	Radians Sin	Radians Cos			
stature =	1.77	m	**Slope Ang**	30	0.5	0.866025404			
total mass =	75.3	kg	**Trunk Ang**	15	0.2588	0.9659			
ref y =	0	m	**Thigh Ang**	64.653369	0.9037	0.4281			
ref z =	0	m							
			Step	**X**	**Z**				
				0.4356	0.2515				
shoulder ht=	1.760	m	**Shoulder**	**X**	**Z**				
hip height =	0.968	m		1.1736	1.7354				

member	member mass	member length	x location	z location	dif x	dif z	moment x	moment z	
left upper arm	2.794	0.318	1.126	1.558	1.126	1.558	3.146	4.353	
left forearm	0.467	0.253	0.987	1.379	0.987	1.379	0.461	0.644	
left hand	0.459	0.193	1.334	1.314	1.334	1.314	0.613	0.603	
left thigh	11.415	0.482	0.179	0.883	0.179	0.883	2.039	10.084	
left calf	2.507	0.386	0.436	0.592	0.436	0.592	1.092	1.485	
left foot	1.032	0.262	0.436	0.378	0.436	0.378	0.449	0.390	
right upper arm	2.794	0.318	1.126	1.558	1.126	1.558	3.146	4.353	
right forearm	0.467	0.253	0.987	1.379	0.987	1.379	0.461	0.644	
right hand	0.459	0.193	1.334	1.314	1.334	1.314	0.613	0.603	
right thigh	11.415	0.482	0.000	0.770	0.000	0.770	0.000	8.794	
right calf	2.507	0.386	0.000	0.341	0.000	0.341	0.000	0.855	
right foot	1.032	0.262	0.000	0.127	0.000	0.127	0.000	0.131	
head	5.949	0.247	0.231	1.831	0.231	1.831	1.376	10.894	
trunk	32.003	0.795	0.113	1.391	0.113	1.391	3.626	44.511	
sum	75.3						17.02	88.35	
					cg coordinates		0.23	1.17	m

Figure A2. La Chapelle 1 – Center of Mass Calculation Spreadsheet (30° slope)

				Deg	Radians Sin	Radians Cos			
stature =	1.6805	m	**Slope Ang**	30	0.5	0.866025404			
total mass =	77.3	kg	**Trunk Ang**	15	0.2588	0.9659			
ref y =	0	m	**Thigh Ang**	65.569706	0.9105	0.4136			
ref z =	0	m							
			Step	**X**	**Z**				
				0.3915	0.2260				
shoulder ht=	1.605	m	**Shoulder**	**X**	**Z**				
hip height =	0.870	m		1.0602	1.5800				

member	member mass	nember length	x location	z location	dif x	dif z	moment x	moment z	
left upper arm	2.868	0.318	1.013	1.403	1.013	1.403	2.905	4.023	
left forearm	0.479	0.253	0.873	1.225	0.873	1.225	0.418	0.587	
left hand	0.472	0.183	1.215	1.165	1.215	1.165	0.573	0.550	
left thigh	11.719	0.430	0.161	0.797	0.161	0.797	1.881	9.341	
left calf	2.574	0.340	0.392	0.541	0.392	0.541	1.008	1.394	
left foot	1.059	0.249	0.392	0.353	0.392	0.353	0.415	0.374	
right upper arm	2.868	0.318	1.013	1.403	1.013	1.403	2.905	4.023	
right forearm	0.479	0.253	0.873	1.225	0.873	1.225	0.418	0.587	
right hand	0.472	0.183	1.215	1.165	1.215	1.165	0.573	0.550	
right thigh	11.719	0.430	0.000	0.694	0.000	0.694	0.000	8.129	
right calf	2.574	0.340	0.000	0.315	0.000	0.315	0.000	0.812	
right foot	1.059	0.249	0.000	0.127	0.000	0.127	0.000	0.134	
head	6.107	0.235	0.215	1.671	0.215	1.671	1.311	10.205	
trunk	32.853	0.735	0.105	1.261	0.105	1.261	3.444	41.433	
sum	77.3						15.85	82.14	
					cg coordinates		0.21	1.06	m

Figure A3. La Ferrassie 1 – Center of Mass Calculation Spreadsheet (30° slope)

				Deg	Radians Sin	Radians Cos			
stature =	1.7228	m	**Slope Ang**	30	0.5	0.866025404			
total mass =	85	kg	**Trunk Ang**	15	0.2588	0.9659			
ref y =	0	m	**Thigh Ang**	65.753955	0.9118	0.4107			
ref z =	0	m							
			Step	**X**	**Z**				
				0.4176	0.2411				
shoulder ht=	1.690	m	**Shoulder**	**X**	**Z**				
hip height =	0.928	m		1.1251	1.6636				

member	member mass	member length	x location	z location	dif x	dif z	moment x	moment z	
left upper arm	3.154	0.318	1.078	1.486	1.078	1.486	3.398	4.688	
left forearm	0.527	0.253	0.938	1.309	0.938	1.309	0.494	0.690	
left hand	0.519	0.188	1.284	1.248	1.284	1.248	0.666	0.647	
left thigh	12.886	0.458	0.171	0.851	0.171	0.851	2.206	10.965	
left calf	2.831	0.370	0.418	0.573	0.418	0.573	1.182	1.622	
left foot	1.165	0.255	0.418	0.368	0.418	0.368	0.486	0.429	
right upper arm	3.154	0.318	1.078	1.486	1.078	1.486	3.398	4.688	
right forearm	0.527	0.253	0.938	1.309	0.938	1.309	0.494	0.690	
right hand	0.519	0.188	1.284	1.248	1.284	1.248	0.666	0.647	
right thigh	12.886	0.458	0.000	0.740	0.000	0.740	0.000	9.538	
right calf	2.831	0.370	0.000	0.332	0.000	0.332	0.000	0.940	
right foot	1.165	0.255	0.000	0.127	0.000	0.127	0.000	0.148	
head	6.715	0.240	0.222	1.757	0.222	1.757	1.491	11.798	
trunk	36.125	0.762	0.109	1.333	0.109	1.333	3.923	48.165	
sum	85						18.41	95.65	
					cg coordinates		0.22	1.13	m

Figure A4. La Ferrassie 2 – Center of Mass Calculation Spreadsheet (30° slope)

				Deg	Radians Sin	Radians Cos			
stature =	1.7063	m	**Slope Ang**	30	0.5	0.866025404			
total mass =	67	kg	**Trunk Ang**	15	0.2588	0.9659			
ref y =	0	m	**Thigh Ang**	63.024181	0.8912	0.4536			
ref z =	0	m							
			Step	**X**	**Z**				
				0.3645	0.2104				
shoulder ht=	1.610	m	**Shoulder**	**X**	**Z**				
hip height =	0.810	m		1.0156	1.5774				

member	member mass	nember length	x location	z location	dif x	dif z	moment x	moment z	
left upper arm	2.486	0.318	0.968	1.400	0.968	1.400	2.407	3.481	
left forearm	0.415	0.253	0.831	1.218	0.831	1.218	0.345	0.506	
left hand	0.409	0.186	1.167	1.151	1.167	1.151	0.477	0.471	
left thigh	10.157	0.409	0.149	0.734	0.149	0.734	1.518	7.455	
left calf	2.231	0.306	0.365	0.507	0.365	0.507	0.813	1.131	
left foot	0.918	0.253	0.365	0.337	0.365	0.337	0.335	0.310	
right upper arm	2.486	0.318	0.968	1.400	0.968	1.400	2.407	3.481	
right forearm	0.415	0.253	0.831	1.218	0.831	1.218	0.345	0.506	
right hand	0.409	0.186	1.167	1.151	1.167	1.151	0.477	0.471	
right thigh	10.157	0.409	0.000	0.642	0.000	0.642	0.000	6.524	
right calf	2.231	0.306	0.000	0.297	0.000	0.297	0.000	0.662	
right foot	0.918	0.253	0.000	0.127	0.000	0.127	0.000	0.117	
head	5.293	0.238	0.230	1.670	0.230	1.670	1.220	8.839	
trunk	28.475	0.795	0.113	1.233	0.113	1.233	3.226	35.105	
sum	67						13.57	69.06	
					cg coordinates		0.20	1.03	m

Figure A5. Shanidar 1 – Center of Mass Calculation Spreadsheet (30° slope)

				Deg	Radians Sin	Radians Cos			
stature =	1.7114	m	**Slope Ang**	30	0.5	0.866025404		**CG**	
total mass =	80.5	kg	**Trunk Ang**	15	0.2588	0.9659			
ref y =	0	m	**Thigh Ang**	63.584705	0.8956	0.4449			
ref z =	0	m							
			Step	**X**	**Z**				
				0.411525	0.2376				
shoulder ht=	1.691	m	**Shoulder**	**X**	**Z**				
hip height =	0.915	m		1.1155	1.6645				

member	member mass	nember length	x location	z location	dif x	dif z	moment x	moment z	
left upper arm	2.987	0.318	1.068	1.487	1.068	1.487	3.190	4.442	
left forearm	0.499	0.253	0.930	1.306	0.930	1.306	0.464	0.652	
left hand	0.491	0.187	1.269	1.241	1.269	1.241	0.623	0.609	
left thigh	12.204	0.460	0.169	0.831	0.169	0.831	2.059	10.138	
left calf	2.681	0.355	0.412	0.561	0.412	0.561	1.103	1.505	
left foot	1.103	0.254	0.412	0.365	0.412	0.365	0.454	0.402	
right upper arm	2.987	0.318	1.068	1.487	1.068	1.487	3.190	4.442	
right forearm	0.499	0.253	0.930	1.306	0.930	1.306	0.464	0.652	
right hand	0.491	0.187	1.269	1.241	1.269	1.241	0.623	0.609	
right thigh	12.204	0.460	0.000	0.726	0.000	0.726	0.000	8.861	
right calf	2.681	0.355	0.000	0.324	0.000	0.324	0.000	0.868	
right foot	1.103	0.254	0.000	0.127	0.000	0.127	0.000	0.140	
head	6.360	0.239	0.226	1.757	0.226	1.757	1.436	11.176	
trunk	34.213	0.777	0.111	1.328	0.111	1.328	3.789	45.426	
sum	80.5						17.39	89.92	
					cg coordinates		0.22	1.12	m

Figure A6. Shanidar 5 – Center of Mass Calculation Spreadsheet (30° slope)

				Deg	Radians Sin	Radians Cos			
stature =	1.6495	m	**Slope Ang**	30	0.5	0.866025404			
total mass =	68.5	kg	**Trunk Ang**	15	0.2588	0.9659			
ref y =	0	m	**Thigh Ang**	66.652884	0.9181	0.3963			
ref z =	0	m							
			Step	**X**	**Z**				
				0.4104	0.2369				
shoulder ht=	1.656	m	**Shoulder**	**X**	**Z**				
hip height =	0.912	m		1.1046	1.6306				

member	member mass	nember length	x location	z location	dif x	dif z	moment x	moment z	
left upper arm	2.541	0.318	1.057	1.454	1.057	1.454	2.687	3.694	
left forearm	0.425	0.253	0.916	1.278	0.916	1.278	0.389	0.543	
left hand	0.418	0.180	1.259	1.222	1.259	1.222	0.526	0.510	
left thigh	10.385	0.447	0.168	0.839	0.168	0.839	1.747	8.717	
left calf	2.281	0.365	0.410	0.566	0.410	0.566	0.936	1.291	
left foot	0.938	0.244	0.410	0.364	0.410	0.364	0.385	0.342	
right upper arm	2.541	0.318	1.057	1.454	1.057	1.454	2.687	3.694	
right forearm	0.425	0.253	0.916	1.278	0.916	1.278	0.389	0.543	
right hand	0.418	0.180	1.259	1.222	1.259	1.222	0.526	0.510	
right thigh	10.385	0.447	0.000	0.729	0.000	0.729	0.000	7.568	
right calf	2.281	0.365	0.000	0.329	0.000	0.329	0.000	0.751	
right foot	0.938	0.244	0.000	0.127	0.000	0.127	0.000	0.119	
head	5.412	0.230	0.217	1.720	0.217	1.720	1.172	9.308	
trunk	29.113	0.744	0.106	1.308	0.106	1.308	3.089	38.078	
sum	68.5						14.53	75.67	
					cg coordinates		0.21	1.10	m

Figure A7. Spy 2 – Center of Mass Calculation Spreadsheet (30° slope)

				Deg	Radians Sin	Radians Cos			
stature =	1.599	m	**Slope Ang**	30	0.5	0.866025404			
total mass =	83.6	kg	**Trunk Ang**	15	0.2588	0.9659			
ref y =	0	m	**Thigh Ang**	63.640056	0.8960	0.4440			
ref z =	0	m							
			Step	**X**	**Z**				
				0.3801375	0.2195				
shoulder ht=	1.572	m	**Shoulder**	**X**	**Z**				
hip height =	0.845	m		1.0330	1.5472				

member	**member mass**	**member length**	**x location**	**z location**	**dif x**	**dif z**	**moment x**	**moment z**	
left upper arm	3.102	0.318	0.986	1.370	0.986	1.370	3.057	4.250	
left forearm	0.518	0.253	0.847	1.189	0.847	1.189	0.439	0.616	
left hand	0.510	0.175	1.178	1.128	1.178	1.128	0.601	0.575	
left thigh	12.674	0.424	0.156	0.768	0.156	0.768	1.975	9.727	
left calf	2.784	0.032	0.380	0.364	0.380	0.364	1.058	1.014	
left foot	1.145	0.237	0.380	0.346	0.380	0.346	0.435	0.397	
right upper arm	3.102	0.318	0.986	1.370	0.986	1.370	3.057	4.250	
right forearm	0.518	0.253	0.847	1.189	0.847	1.189	0.439	0.616	
right hand	0.510	0.175	1.178	1.128	1.178	1.128	0.601	0.575	
right thigh	12.674	0.424	0.000	0.671	0.000	0.671	0.000	8.502	
right calf	2.784	0.321	0.000	0.305	0.000	0.305	0.000	0.848	
right foot	1.145	0.237	0.000	0.127	0.000	0.127	0.000	0.145	
head	6.604	0.223	0.211	1.634	0.211	1.634	1.396	10.791	
trunk	35.530	0.727	0.104	1.232	0.104	1.232	3.685	43.766	
sum	83.6						16.74	86.07	
					cg coordinates		0.20	1.03	m

Figure A8. Tabun 1 – Center of Mass Calculation Spreadsheet (30° slope)

				Deg	Radians Sin	Radians Cos			
stature =	1.543	m	**Slope Ang**	30	0.5	0.866025404			
total mass =	63.2	kg	**Trunk Ang**	15	0.2588	0.9659			
ref y =	0	m	**Thigh Ang**	64.737002	0.9044	0.4268			
ref z =	0	m							
			Step	**X**	**Z**				
				0.3735	0.2156				
shoulder ht=	1.607	m	**Shoulder**	**X**	**Z**				
hip height =	0.830	m		1.0310	1.5800				

member	member mass	nember length	x location	z location	dif x	dif z	moment x	moment z	
left upper arm	2.345	0.318	0.984	1.403	0.984	1.403	2.306	3.290	
left forearm	0.392	0.253	0.844	1.224	0.844	1.224	0.331	0.480	
left hand	0.386	0.168	1.173	1.167	1.173	1.167	0.452	0.450	
left thigh	9.581	0.413	0.153	0.758	0.153	0.758	1.467	7.260	
left calf	2.105	0.317	0.374	0.518	0.374	0.518	0.786	1.091	
left foot	0.866	0.229	0.374	0.343	0.374	0.343	0.323	0.297	
right upper arm	2.345	0.318	0.984	1.403	0.984	1.403	2.306	3.290	
right forearm	0.392	0.253	0.844	1.224	0.844	1.224	0.331	0.480	
right hand	0.386	0.168	1.173	1.167	1.173	1.167	0.452	0.450	
right thigh	9.581	0.413	0.000	0.661	0.000	0.661	0.000	6.330	
right calf	2.105	0.317	0.000	0.303	0.000	0.303	0.000	0.637	
right foot	0.866	0.229	0.000	0.127	0.000	0.127	0.000	0.110	
head	4.993	0.215	0.223	1.664	0.223	1.664	1.115	8.306	
trunk	26.860	0.777	0.111	1.243	0.111	1.243	2.974	33.394	
sum	63.2						12.84	65.86	
					cg coordinates		0.20	1.04	m

Appendix B: Center of Mass Calculations – Modern Human Populations

This appendix presents representative CoM calculation spreadsheets for five modern human population models. Calculations were performed using a standardized terrain incline of 30°. These examples reflect population averages where complete skeletal data were available. Additional populations and slope conditions are available upon request

Figure B1. Arikara – Center of Mass Calculation Spreadsheet (30° slope)

				Deg	Radians Sin	Radians Cos			
stature =	1.681445	m	**Slope Ang**	30	0.5	0.8660			
total mass =	62.33	kg	**Tr. Angle**	15	0.2588	0.9659			
ref y =	0	m	**Th. Angle**	61.71	0.8806	0.4739			
ref z =	0	m							
% Step length	0.45		**Step**	**X**	**Z**				
				0.4422305	0.2553				
shoulder ht=	1.447	m	**Shoulder**	**X**	**Z**				
hip height =	0.983	m		1.1600	1.6441				

member	**member mass**	**member length**	**x location**	**z location**	**dif x**	**dif z**	**moment x**	**moment z**	
left upper arm	1.689	0.237	1.125	1.512	1.125	1.512	1.900	2.554	
left forearm	1.010	0.242	1.001	1.363	1.001	1.363	1.011	1.376	
left hand	0.380	0.184	1.324	1.294	1.324	1.294	0.503	0.492	
left thigh	8.826	0.502	0.181	0.885	0.181	0.885	1.600	7.812	
left calf	2.699	0.381	0.442	0.566	0.442	0.566	1.194	1.528	
left foot	0.854	0.249	0.442	0.355	0.442	0.355	0.378	0.303	
right upper arm	1.689	0.237	1.125	1.512	1.125	1.512	1.900	2.554	
right forearm	1.010	0.242	1.001	1.363	1.001	1.363	1.011	1.376	
right hand	0.380	0.184	1.324	1.294	1.324	1.294	0.503	0.492	
right thigh	8.826	0.502	0.000	0.777	0.000	0.777	0.000	6.856	
right calf	2.699	0.381	0.000	0.311	0.000	0.311	0.000	0.839	
right foot	0.854	0.249	0.000	0.100	0.000	0.100	0.000	0.085	
head	4.301	0.235	0.202	1.735	0.202	1.735	0.867	7.463	
trunk	27.114	0.685	0.098	1.347	0.098	1.347	2.648	36.527	
sum	62.33						13.51	70.26	
					cg coordinates		0.22	1.13	m

Figure B2. Forensic – Center of Mass Calculation Spreadsheet (30° slope)

				Deg	Radians Sin	Radians Cos			
stature =	1.732374	m	**Slope Ang**	30	0.5	0.8660			
total mass =	66.20862	kg	**Tr. Angle**	15	0.2588	0.9659			
ref y =	0	m	**Th. Angle**	61.39	0.8779	0.4788			
ref z =	0	m							
% Step length	0.45		**Step**	**X**	**Z**				
				0.4542622	0.2623				
shoulder ht=	1.491	m	**Shoulder**	**X**	**Z**				
hip height =	1.009	m		1.1921	1.6909				

member	member mass	member length	x location	z location	dif x	dif z	moment x	moment z	
left upper arm	1.794	0.244	1.156	1.555	1.156	1.555	2.074	2.790	
left forearm	1.073	0.250	1.029	1.401	1.029	1.401	1.103	1.502	
left hand	0.404	0.189	1.360	1.329	1.360	1.329	0.549	0.537	
left thigh	9.375	0.517	0.186	0.908	0.186	0.908	1.746	8.512	
left calf	2.867	0.392	0.454	0.579	0.454	0.579	1.302	1.661	
left foot	0.907	0.257	0.454	0.362	0.454	0.362	0.412	0.329	
right upper arm	1.794	0.244	1.156	1.555	1.156	1.555	2.074	2.790	
right forearm	1.073	0.250	1.029	1.401	1.029	1.401	1.103	1.502	
right hand	0.404	0.189	1.360	1.329	1.360	1.329	0.549	0.537	
right thigh	9.375	0.517	0.000	0.797	0.000	0.797	0.000	7.475	
right calf	2.867	0.392	0.000	0.317	0.000	0.317	0.000	0.909	
right foot	0.907	0.257	0.000	0.100	0.000	0.100	0.000	0.091	
head	4.568	0.242	0.208	1.785	0.208	1.785	0.949	8.154	
trunk	28.801	0.705	0.101	1.385	0.101	1.385	2.898	39.888	
sum	66.20862						14.76	76.68	
					cg coordinates		0.22	1.16	m

Figure B3. Poundbury – Center of Mass Calculation Spreadsheet (30° slope)

				Deg	Radians Sin	Radians Cos			
stature =	1.664889	m	**Slope Ang**	30	0.5	0.8660			
total mass =	63.74598	kg	**Tr. Angle**	15	0.2588	0.9659			
ref y =	0	m	**Th. Angle**	61.82	0.8815	0.4723			
ref z =	0	m							
% Step length	0.45		**Step**	**X**	**Z**				
				0.4383193	0.2531				
shoulder ht=	1.433	m	**Shoulder**	**X**	**Z**				
hip height =	0.974	m		1.1495	1.6289				

member	**member mass**	**member length**	**x location**	**z location**	**dif x**	**dif z**	**moment x**	**moment z**	
left upper arm	1.728	0.234	1.115	1.498	1.115	1.498	1.925	2.588	
left forearm	1.033	0.240	0.992	1.351	0.992	1.351	1.025	1.395	
left hand	0.389	0.182	1.312	1.283	1.312	1.283	0.510	0.499	
left thigh	9.026	0.497	0.180	0.878	0.180	0.878	1.622	7.923	
left calf	2.760	0.377	0.438	0.562	0.438	0.562	1.210	1.551	
left foot	0.873	0.247	0.438	0.353	0.438	0.353	0.383	0.308	
right upper arm	1.728	0.234	1.115	1.498	1.115	1.498	1.925	2.588	
right forearm	1.033	0.240	0.992	1.351	0.992	1.351	1.025	1.395	
right hand	0.389	0.182	1.312	1.283	1.312	1.283	0.510	0.499	
right thigh	9.026	0.497	0.000	0.770	0.000	0.770	0.000	6.952	
right calf	2.760	0.377	0.000	0.309	0.000	0.309	0.000	0.852	
right foot	0.873	0.247	0.000	0.100	0.000	0.100	0.000	0.087	
head	4.398	0.232	0.200	1.719	0.200	1.719	0.878	7.562	
trunk	27.730	0.678	0.097	1.335	0.097	1.335	2.681	37.016	
sum	63.74598						13.69	71.22	
					cg coordinates		0.21	1.12	m

Figure B4. Southern Chinese – Center of Mass Calculation Spreadsheet (30° slope)

				Deg	Radians Sin	Radians Cos			
stature =	1.662999	m	**Slope Ang**	45	0.707106781	0.7071			
total mass =	58.58862	kg	**Tr. Angle**	22.5	0.3827	0.9239			
ref y =	0	m	**Th. Angle**	61.83	0.8816	0.4721			
ref z =	0	m							
% Step length	0.45		**Step**	**X**	**Z**				
				0.4378728	0.2528				
shoulder ht=	1.431	m	**Shoulder**	**X**	**Z**				
hip height =	0.973	m		1.2322	1.5987				

member	**member mass**	**member length**	**x location**	**z location**	**dif x**	**dif z**	**moment x**	**moment z**	
left upper arm	1.588	0.234	1.181	1.474	1.181	1.474	1.874	2.340	
left forearm	0.949	0.240	1.046	1.331	1.046	1.331	0.993	1.263	
left hand	0.357	0.181	1.366	1.263	1.366	1.263	0.488	0.451	
left thigh	8.296	0.497	0.180	0.877	0.180	0.877	1.489	7.275	
left calf	2.537	0.376	0.438	0.561	0.438	0.561	1.111	1.424	
left foot	0.803	0.246	0.438	0.353	0.438	0.353	0.351	0.283	
right upper arm	1.588	0.234	1.181	1.474	1.181	1.474	1.874	2.340	
right forearm	0.949	0.240	1.046	1.331	1.046	1.331	0.993	1.263	
right hand	0.357	0.181	1.366	1.263	1.366	1.263	0.488	0.451	
right thigh	8.296	0.497	0.000	0.769	0.000	0.769	0.000	6.383	
right calf	2.537	0.376	0.000	0.308	0.000	0.308	0.000	0.783	
right foot	0.803	0.246	0.000	0.100	0.000	0.100	0.000	0.080	
head	4.043	0.232	0.295	1.685	0.295	1.685	1.192	6.812	
trunk	25.486	0.677	0.143	1.318	0.143	1.318	3.639	33.586	
sum	58.58862						14.49	64.73	
					cg coordinates		0.25	1.10	m

Figure B5. Spitalfields – Center of Mass Calculation Spreadsheet (30° slope)

				Deg	Radians Sin	Radians Cos			
stature =	1.635808	m	**Slope Ang**	30	0.5	0.8660			
total mass =	57.91	kg	**Tr. Angle**	15	0.2588	0.9659			
ref y =	0	m	**Th. Angle**	62.01	0.8831	0.4693			
ref z =	0	m							
% Step length	0.45		**Step**	**X**	**Z**				
				0.4314491	0.2491				
shoulder ht=	1.407	m	**Shoulder**	**X**	**Z**				
hip height =	0.959	m		1.1312	1.6022				

member	member mass	nember length	x location	z location	dif x	dif z	moment x	moment z	
left upper arm	1.569	0.230	1.097	1.474	1.097	1.474	1.721	2.313	
left forearm	0.938	0.236	0.976	1.329	0.976	1.329	0.916	1.247	
left hand	0.353	0.179	1.291	1.263	1.291	1.263	0.456	0.446	
left thigh	8.200	0.489	0.177	0.865	0.177	0.865	1.451	7.091	
left calf	2.508	0.370	0.431	0.554	0.431	0.554	1.082	1.390	
left foot	0.793	0.242	0.431	0.349	0.431	0.349	0.342	0.277	
right upper arm	1.569	0.230	1.097	1.474	1.097	1.474	1.721	2.313	
right forearm	0.938	0.236	0.976	1.329	0.976	1.329	0.916	1.247	
right hand	0.353	0.179	1.291	1.263	1.291	1.263	0.456	0.446	
right thigh	8.200	0.489	0.000	0.758	0.000	0.758	0.000	6.219	
right calf	2.508	0.370	0.000	0.305	0.000	0.305	0.000	0.765	
right foot	0.793	0.242	0.000	0.100	0.000	0.100	0.000	0.079	
head	3.996	0.228	0.196	1.691	0.196	1.691	0.784	6.756	
trunk	25.191	0.666	0.095	1.313	0.095	1.313	2.393	33.084	
sum	57.91						12.24	63.67	
					cg coordinates		0.21	1.10	m